

Aus dem Institut für Medizinische Molekularbiologie
Der Universität zu Lübeck
Direktor: Prof. Dr. rer. nat. P. K. Müller

Host and viral factors involved in Hepatitis A virus RNA translation and replication

Inauguraldissertation
zur
Erlangung der Doktorwürde
der Universität zu Lübeck
-Aus der Technisch-Naturwissenschaftlichen Fakultät-

Vorgelegt von
Bo Zhang
Aus der Volksrepublik China

Lübeck 2005

1. Berichterstatterin: Prof. Dr. rer. nat. V. Gauss-Müller
2. Berichterstatter: Prof. Dr. rer. nat. Th. Peters

Tag der mündlichen Prüfung: 01.11.2005
Zum Druck genehmigt. Lübeck, den 01.11.2005

gez. Prof. Dr. rer. nat. Enno Hartmann
- Dekan der Technisch-Naturwissenschaftlichen Fakultät -

Acknowledgements

This study was carried out at the Institute of Medical Molecular Biology, University of Lübeck.

I like to express my sincere thanks to my supervisor, Prof. Dr. Verena Gauss-Müller, for giving me a chance to do my PhD thesis research work. Her expert knowledge about the project and her patience during my researching process encouraged me to finish my work in time.

I thank Dr. Yuri Kusov for advising me throughout my project and helping during my experiments.

I highly appreciated the technical assistance of Barbara Andresen and Barbara Kurowski and all other colleagues of the institute.

I would like to express my thanks to all the friends who accompanied me during my study in Luebeck.

Last, I am very grateful to my parents and my wife Ye, Hanqing for their permanent and self-giving support.

Contents

1. Abbreviations	6
2. Introduction	8
2.1 The structure of the HAV genome and proteins	9
2.2 Secondary structures of the HAV RNA	10
2.2.1 The 5'NTR	10
2.2.2 The 3'NTR	12
2.2.3 The intragenomic <i>cis</i> -acting replication element (CRE).....	13
2.3 Picornaviral replicons – a system to study genome replication	13
2.4 Conflict of translation and genome replication	14
2.5 Host proteins relevant for picornavirus translation and replication and their cleavage by viral proteinases.....	14
2.5.1 Poly (A) binding protein (PABP).....	15
2.5.2 eukaryotic initiation factor 4G (eIF4G)	15
2.5.3 Poly(C) binding protein PCBP ()	16
3. Aims of this study	17
4. Materials and methods	18
4.1 Materials.....	18
4.1.1 Chemicals and kits	18
4.1.2 Enzymes	20
4.1.3 Instruments and other equipment	20
4.1.4 Marker for protein and nucleic acids.....	20
4.1.5 Oligonucleotide for hammerhead ribozyme cloning.....	21
4.1.6 <i>E.coli</i> strains	21
4.1.7 Virus strains.....	21
4.1.8 Cell lines.....	22
4.1.9 Plasmids	22
4.1.10 Antibodies, their characterization	24
4.1.11 Buffers and stock solutions	24
4.2 Methods.....	28
4.2.1 Nucleic acid methods	28
4.2.2 Protein methods.....	32
4.2.3 Cell culture	34
4.2.4 HAV infection	34
4.2.5 ELISA detection of HAV particles	34
4.2.6 Recombinant protein expression in mammalian cells with vaccinia virus-T734	
4.2.7 RNA transfection.....	35
4.2.8 Luciferase assay	35
4.2.9 Proteolytic cleavage assay.....	35
4.2.10 Preparation of the S10 cell extract	35
4.2.11 Preparation of the S200 P200 fraction	36
4.2.12 In vitro translation in Huh-7 cell extracts.....	36
5. Results	37
5.1 HAV infection in Huh-7 and Huh-T7 cells.....	37
5.2 HAV replicon replication	38
5.2.1 Replication of the HAV replicon in Huh-T7 cells	38
5.2.2 Inhibition of replicon replication by guanidine hydrochloride (Gu-HCl).....	39

5.2.3	Comparison of replicon replication in Huh-7 and Huh-T7 cells.....	40
5.2.4	Analysis of the putative HAV CRE by studying replication of the mutated replicon	41
5.2.5	Analysis HAV replicon expression during cell passage	42
5.2.6	Insertion of a <i>cis</i> -active hammerhead ribozyme into the HAV cDNA at the 5'end of the viral genome.....	43
5.2.7	Replication of ribozyme-containing HAV transcripts	43
5.3	HAV replicon translation in Huh-7 S10 extract in vitro	46
5.3.1	HAV replicon translation in Huh-7 S10 extracts	46
5.4	Protein-RNA interaction determined by electrophoretic mobility shift assay (EMSA) .	47
5.4.1	PABP binding to the HAV 3'NTR is dependent of the poly (A) tail.....	48
5.4.2	PCBP2 directly binds to the HAV 5'CL	49
5.4.3	Complex formation of PABP and PCBP at the HAV 5'CL.....	50
5.4.4	HAV 3C enhances the interaction of PCBP with the 5'CL interaction	52
5.5	Host protein cleavage	52
5.5.1	PABP cleavage by HAV 3C.....	52
5.5.2	PCBP2 cleavage by HAV 3C in vivo and in vitro	59
5.5.3	eIF4G is not cleaved by HAV 3C in vivo and in vitro.....	63
6.	Discussion	67
6.1	Role of the host cell and template switching during HAV replication.	67
6.2	RNA secondary structures involved in HAV translation and replication – <i>cis</i> -acting elements in the HAV genome	68
6.2.1	The 5'CL and the role of the true 5'end for HAV replication	68
6.2.2	The HAV IRES	69
6.2.3	The putative HAV CRE	70
6.2.4	The HAV 3'NTR and poly (A) tail	71
6.3	Transacting host proteins	72
6.3.1	eIF4G.....	72
6.3.2	PABP and its function in host and viral translation	72
6.3.3	PCBP: RNA binding and function in translation	75
7.	Summary	77
8.	References	78
9.	Appendix	84

1. Abbreviations

AP.....	alkaline phosphatase
APS.....	ammonium persulphate
BCIP.....	5-bromo-4-chloro-3'-indolyl phosphate
BSA.....	bovine serum albumin
CL.....	cloverleaf
CPE.....	cytopathic effect
CRE.....	<i>cis</i> -acting replication element
CTD.....	carboxyl-terminal domain of PABP
CVB.....	coxsackievirus B3
DEPC.....	diethyl pyrocarbonate
DMF.....	dimethyl formamide
dNTP.....	deoxynucleotide 5'-triphosphate
DTT.....	dichlorodiphenyltrichloroethane
DMEM.....	Dulbecco minimal essential medium
DNA.....	deoxyribonucleic acid
EB.....	ethidium bromide
EDTA.....	ethylenediamine tetra-acetic acid
EMSA.....	electrophoresis mobility shift assay
eIF4G.....	eukaryotic initiation factor 4G
FCS.....	fetal calf serum
FMDV.....	foot and mouth disease virus
GAPDH.....	glyceraldehyde-3-phosphate dehydrogenase
HAV.....	hepatitis A virus
HEPES.....	N-2-hydroxyethylpiperazine-N'-ethansulfonic acid
HRV.....	human rhinovirus
IPTG.....	isopropyl- β -D-thiogalactopyranoside
IRES.....	internal ribosome entry site
kb.....	kilo base
kDa.....	kilodalton
LB.....	Luria-Bertani broth

Met	methionine
MOI.....	multiplicity of infection
MOPS.....	3-[N-morpholino]-propanesulfonic acid
MW.....	molecular weight
NBT.....	nitro-blue tetrazolium chloride
NTR.....	non-translated region
OD.....	optical density
ORF.....	open reading frame
PABP.....	poly (A) binding protein
PAGE.....	polyacrylamide gel electrophoresis
PBS.....	phosphate-buffered saline
PBS-T.....	PBS + 0.05 % (v/v) Tween20
PCBP.....	poly(C) binding protein
pi.....	post infection
PIPES.....	piperazine-N,N'-bis[2-ethanesulfonic acid]
PMSF.....	phenylmethylsulfonyl fluoride
POD.....	peroxidase
pt.....	post transfection
PTB.....	polypyrimidine tract-binding protein
PV.....	poliovirus
RC.....	replication complex
RRM.....	RNA recognition motif
RSW.....	ribosomal salt wash fraction
RIBO.....	ribosome-enriched fraction
RT.....	room temperature
SDS.....	sodium dodecyl sulfate
TAE.....	Tris-acetate-EDTA buffer
TBE.....	Tris-boric acid-EDTA buffer
TBS.....	Tris buffered saline
TBS-T.....	TBS + 0.05 % Tween 20
TCA.....	trichloroacetic acid
TMB.....	tetramethyl benzidine
TMEV.....	Theiler's murine encephalomyelitis virus

2. Introduction

Hepatitis A virus (HAV) is a small, nonenveloped, positive-strand RNA virus belonging to the family *Picornaviridae* (genus *Hepatovirus*). This family is subdivided into six genera: *Enterovirus*, including polioviruses (PV), coxsackieviruses, and echoviruses; *Rhinovirus*; *Hepatovirus*; *Parechovirus*; *Cardiovirus* and *Aphthovirus*. HAV is transmitted via the fecal-oral route and causes acute viral hepatitis. HAV is the most common cause of acute viral hepatitis (**Fig. 1**) - probably about half of all cases are due to this virus. Persons infected with HAV may not have symptoms of the disease. Older persons are more likely to have symptoms than children. If symptoms are present, they usually occur abruptly and may include fever, tiredness, loss of appetite, nausea, abdominal discomfort, dark urine, and jaundice (yellowing of the skin and eyes).

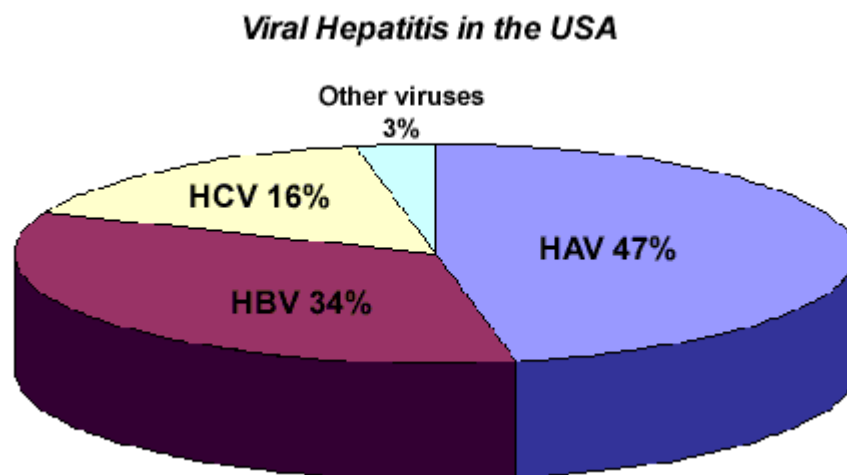


Fig. 1. The proportion of HAV infection among all viral hepatitis cases

A variety of primate cell types have been shown to be permissive for HAV, but most wild-type virus isolates replicate very slowly in cell culture (Binn et al., 1984; Daemer et al., 1981); (Flehmig, 1980). Fetal rhesus monkey kidney (Frhk-4), African green monkey kidney (BS-C-1), diploid human lung fibroblast (MRC-5), and human hepatocellular carcinoma (Huh-7) cells have been used to propagate the virus. Although more rapid replication and higher final yields are achieved with virus that has been adapted to growth in cell culture, even highly cell culture adapted HAV variants replicate slowly and less efficiently than PV. In almost all cases, wild-type or low-passage virus does not induce visible cytopathic effects, and there is no evidence that HAV interferes with host cell macromolecular synthesis (Gauss-Muller and Deinhardt, 1984). In

vitro infection generally results in the establishment of persistent infection (Vallbracht et al., 1984).

Although the reasons for its inefficient replication are not agreed upon, it is supposed to include inefficient uncoating (Wheeler et al., 1986), ineffective polyprotein processing (Gauss-Muller et al., 1984), highly efficient sequestration of virion RNA into virions (Anderson, Ross, and Locarnini, 1988), inefficient translation (Whetter et al., 1994; Schultz et al., 1996; Funkhouser et al., 1999), asynchronous replication, and down regulation of viral RNA synthesis (Lemon et al., 1991; Brack et al., 2002).

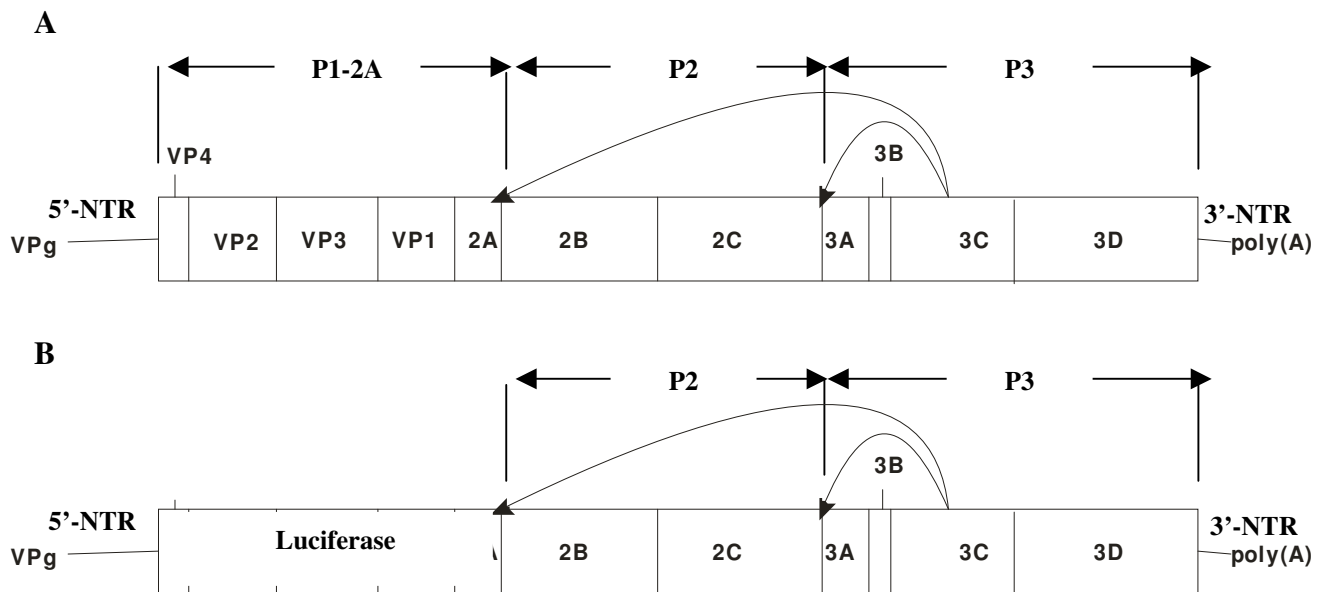


Fig. 2. Structure of the HAV genome (A) and the replicon (B). Primary cleavages by 3C are indicated by arrows.

2.1 The structure of the HAV genome and proteins

The viral genome is surrounded by an icosahedral capsid that is around 28 nm in diameter. The HAV genome consists of a single stranded RNA with a small viral protein (3B = VPg) covalently linked to its 5' end and a poly (A) tail at its 3' end. The HAV genome is about 7.5 kb in length and functions directly as mRNA in infected cells. Its single open reading frame is translated into a polyprotein that is processed proteolytically to release both structural and functional viral proteins. All cleavages are carried out by the viral proteinase 3C. HAV is unique among the human picornaviruses with respect to its tropism for liver cells and its capacity to induce an acute hepatocellular injury. Like other picornaviruses, HAV genome contains a lengthy 5' nontranslated region (5'NTR, 734 nucleotides), a single large open reading frame

(ORF, 6681 nucleotides), and a short 3'NTR (63 nucleotides) followed by a poly (A) tail. The HAV polyprotein can be divided into three regions, designated P1-2A, P2, and P3.

As **Fig. 2** A shows the P1-2A segment of the polyprotein encodes the capsid proteins: VP4 (6 kDa, not yet detected in infectious virus particles), VP2, VP3, and VP1-2A. The P2 and P3 regions encode the non-structural proteins that are all involved in replication of the viral RNA. P2 encodes proteins 2B, and 2C. Although their exact function is not defined, 2C has a nucleotide triphosphatase motif; while 2B acting alone or together with 2C, may be involved in membrane rearrangements essential for RNA replication. The P3 segment encodes four proteins: 3A, 3B, 3C, and 3D. 3B (VPg) is covalently linked to the 5' end of genomic and anti-genomic RNA, while 3C is the only virus-encoded proteinase and is responsible for most cleavages during polyprotein processing. Unlike other picornaviruses, HAV 3C carries out both the primary cleavages, with the initial cleavages occurring between the proteins P1-2A and P2 and between P2 and P3 (see **Fig. 2**), and all subsequent secondary cleavages. HAV 3C is a cysteine proteinase with a fold similar to chymotrypsin. Finally, 3D contains sequence motifs suggesting that it is the RNA-dependent RNA polymerase, which is responsible for genome replication.

After polyprotein translation, release of the mature viral proteins by proteolytic processing and formation of the viral replication complex (RC), the plus strand genome is transcribed into a negative strand by the RC. Since an infectious cDNA clone and a system to synthesize viral RNA in vitro by DNA-dependent RNA polymerases was developed, it was found that the authentic genome's 5' terminus was required for efficient and successful replication (Herold and Andino, 2000). Additional or missing sequences at the 5' end had deleterious effects on viral genome replication (Boyer and Haenni, 1994).

2.2 Secondary structures of the HAV RNA

2.2.1 The 5'NTR

Computer-assisted folding predictions and biochemical probing showed that the HAV 5'NTR (**Fig. 3**) forms extensive higher-order structures which include six predicted stem-loop domains. Domains I and II (bases 1 to 95) contain a 5'-terminal hairpin and two stem-loops followed by a single-stranded and highly variable pyrimidine-rich tract (pY1, bases 96 to 154). The remainder of the 5'NTR (domains III to VI, bases 155 to 734) contains several complex stem-loops, one of which may form a pseudoknot, and terminates in a highly conserved region containing an oligopyrimidine tract preceding the putative start codon by 13 bases (Brown et al., 1991).

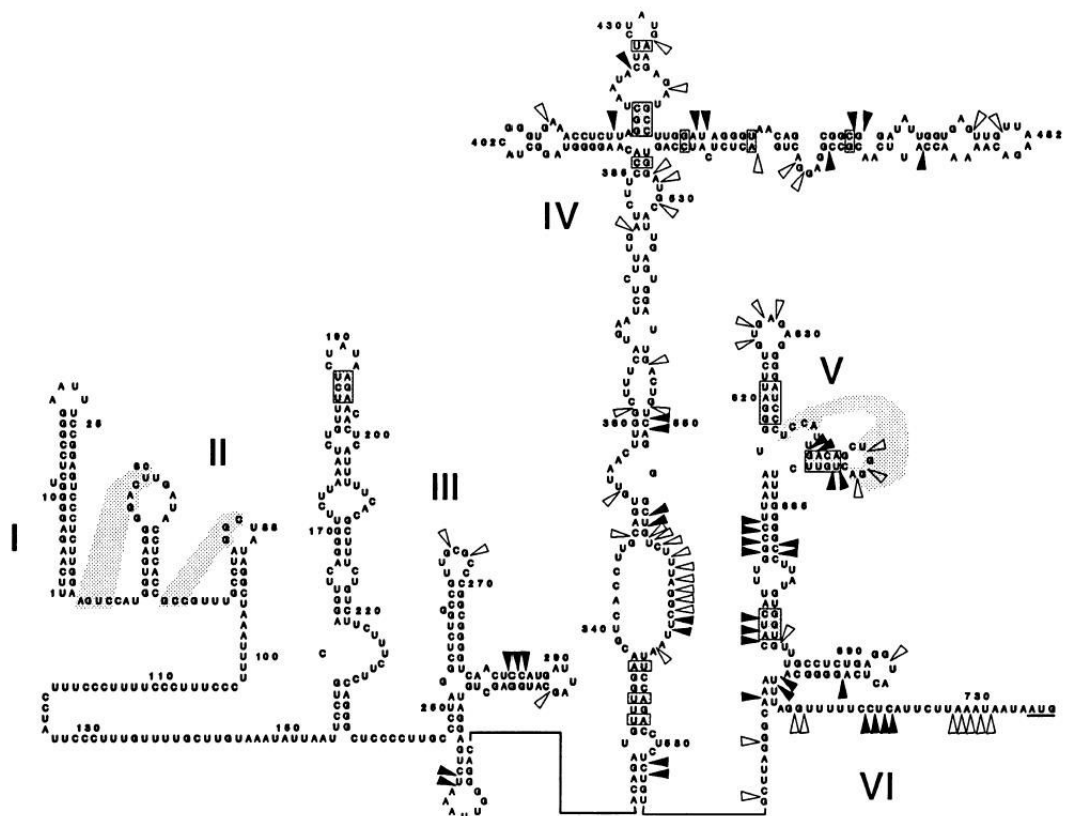


Fig. 3. Proposed secondary structure of the HAV HM175/wt 5'NTR (taken from (Brown et al., 1991)). This model is based on a combination of phylogenetic comparisons, thermodynamic predictions, and nuclease digestions of synthetic RNA between nucleotide 300 and 735. Major structural domains are labeled I through VI. The HAV IRES is included in domains III to VI. Possible pseudoknots are indicated by shaded areas. The single-stranded pyrimidine-rich tract is between domains II and III.

Like other picornaviruses, the HAV 5'NTR can be divided into two functional domains, the larger of which is an internal ribosome entry site (IRES), reported to include sequences from nucleotides (nt) 152 to 735 (Glass et al., 1993); (Brown et al.,1994) The IRES is required for cap-independent translation, but is not as efficient as that of other picornaviruses (Brown et al., 1994; Whetter et al., 1994). IRES elements have been formally identified in the genomes of all picornaviruses. They exhibit considerable structural and functional divergence. On the basis of sequence and structural features and the requirements for optimal activity, three types of picornavirus IRES have been distinguished: type I enterovirus and rhinovirus IRESs, the type II cardiovirus and aphthovirus IRESs, and the type III HAV IRES. There is very little sequence similarity between the IRES of HAV and other picornavirus, and in many respects the HAV IRES is unique in the conditions required for optimal activity *in vitro*. Most interestingly, it is the only picornavirus IRES whose activity is severely inhibited *in vitro* and *in cell culture* in the

presence of the enterovirus and rhinovirus 2A and the aphthovirus Lb proteinase (Borman et al., 1995; Borman and Kean, 1997; Whetter et al., 1994).

Binding of the ribosomal initiation complex to the IRES element is presumably facilitated by one or more cellular trans-acting protein factors distinct from the canonical initiation factors. These factors may vary with respect to their distribution in different cells and requirement by different picornaviruses (Graff et al., 1998). The HAV IRES interacts with a number of host proteins, such as the polypyrimidine tract-binding protein (PTB) (Chang et al., 1993), glyceraldehydes-3-phosphate dehydrogenase (GAPDH) which interacts with stem-loop IIIa (nt 155 to 235) (Yi, et al., 2000); (Schultz et al., 1996), and eukaryotic initiation factor 4GI (eIF4GI) (Borman and Kean, 1997; Borman et al., 2001; Ali et al., 2001). Interestingly and in spite of its higher-order structure, it was recently shown that some domains of the HAV IRES are targets for RNA interference (Kanda et al., 2005). siRNA-mediated suppression might be a new way to specifically inhibit HAV infection in patients with severe cases of hepatitis A.

Unlike the enterovirus and rhinoviruses 5' termini that fold into a cloverleaf (CL) structure, the 5' terminal end of the HAV 5'NTR, consisting of 150 bases comprises three stem-loops and a poly-pyrimidine tract (pY1) (Brown et al., 1991); (Le et al., 1993; Yi et al., 2000). Genetic analysis suggested that this structure might be functionally similar to the PV CL which is a *cis*-acting replication element for viral RNA replication. It was demonstrated that the poly(C) binding protein 2 (PCBP2) interacts with the HAV 5'end suggesting its role in HAV replication (Graff et al., 1998)

2.2.2 The 3'NTR

The HAV 3'NTR and/or sequences of the 3D polymerase-coding region presumably folds into a pseudoknot and interacts specifically with GAPDH (Dollenmaier and Weitz, 2003; Kusov et al., 1996) and with hnRNP A1 (Huang and Lai, 2001) which may be essential for viral genome replication. The poly (A) tail stimulates picornaviral IRES translation, and this effect is mediated through the eIF4G-PABP interaction (Bergamini et al., 2000; Michel et al., 2000; Michel et al., 2001; Svitkin et al., 2001). At the same time, the 3' poly (A) tail of the PV genomic RNA is an important *cis*-acting element for negative strand RNA synthesis *in vitro* and *in vivo*. A minimum length of 8 to 12 adenylate residues is sufficient to support efficient initiation of RNA synthesis (Herold and Andino, 2001). The removal or shortening of the poly (A) tail results in a defect of RNA replication (Barton et al., 1996; Iizuka and Sarnow, 1997). Since all cellular mRNAs contain a 3' poly (A) tail, this cannot be the primary *cis*-acting element that specifies replication

of the viral RNA (Herold and Andino, 2001). It was demonstrated that the 3'NTR preceding the poly (A) determined PV RNA template specificity for replication (Pilipenko et al., 1996). On the other hand, some experiments showed that a recombinant PV with deleted 3'NTR was viable, although it replicated more slowly than the wild-type virus (Todd et al., 1997). 3'NTR plays a regulatory role rather than acting as the origin of replication for negative strand RNA synthesis (Herold and Andino, 2001).

2.2.3 The intragenomic *cis*-acting replication element (CRE)

The 5' and 3'NTR are *cis*-acting replication elements in the non-coding sequences. An intragenomic *cis*-acting replication element (CRE) located within the coding sequences of a picornavirus RNA was first discovered in HRV14 (McKnight and Lemon, 1996). This RNA segment consists of a hairpin structure in the capsid protein VP1. Similar *cis*-acting elements were recently described by Goodfellow et al in the PV protein 2C [CRE (2C)] (Goodfellow et al., 2003). Although the PV1 and HRV14 *cis*-replicating elements differ in sequence and structure, they have a similar function in vivo. Both elements are required in the context of the plus-strand RNA and are position-independent. A CRE was also identified in VP2 of TMEV (Lobert et al., 1999) and in 2A of HRV2 (Gerber et al., 2001) and in the 5' NTR of FMDV (Mason et al., 2002). An internal or terminal loop with three unpaired adenosine residues seems to be a common CRE structure. It is assumed that HAV also has an intragenomic CRE that needs to be identified and characterized (see below).

2.3 Picornaviral replicons – a system to study genome replication

In order to study *cis*- and *trans*-acting factors essential for picornavirus genome replication, several subgenomic RNA replicons were developed by replacing the capsid coding sequence with a reporter gene (e.g. firefly luciferase, see **Fig. 2 B**) (Andino et al., 1993; Yi and Lemon, 2002; Goodfellow et al., 2000). The RNA sequence encoding the capsid proteins is not required for RNA replication as long as it does not contain a CRE (Percy et al., 1992). The subgenomic replicon RNA is translated into a polyprotein containing the reporter gene product at its N-terminus (see **Fig. 2 B**). The appropriate proteolytic cleavages can release the active reporter and the viral functional proteins that can subsequently catalyse viral RNA replication from the polyprotein. After expression of an active (replication-competent) replicon, the expression rate of the reporter gene is proportional to the amount of viral RNA present in the cells, and therefore is a measure of viral RNA synthesis (Andino et al., 1993). After expression of an inactive

(replication-incompetent) replicon, the reporter gene activity detected is a product of translation of input RNA.

2.4 Conflict of translation and genome replication

The picornaviral RNA genome serves as a template for both translation and replication. This dual function of the viral RNA creates a conflict: while the ribosomes are moving along the viral RNA in the 5' to 3' direction, the viral polymerase initiates replication at the 3' end of the same RNA and moves in the opposite direction, as it synthesizes the complementary negative strand. These biosynthetic processes, which proceed in opposite directions are mutually exclusive on one molecule and presumably temporally and/or spatially regulated. In order to solve the conflict, the virus has evolved mechanisms to down-regulate translation in order to begin RNA synthesis. The detailed molecular mechanisms involved in these conflicting processes are the subject of ongoing studies (Gamarnik and Andino, 1998; Barton et al., 1999).

2.5 Host proteins relevant for picornavirus translation and replication and their cleavage by viral proteinases

To ensure optimal replication, viruses have evolved mechanisms to divert host cell metabolism for their need. During picornaviruses infection, viral proteins have been shown to rearrange cell membranes and viral proteinases affect the structure and localization of host cell proteins. In the PV polyprotein, there are three kinds of proteinases, 2A, 3C, and 3CD that are all active on host proteins. It is well known that cleavage of translation initiation factor eIF4G by PV proteinase 2A or FMDV proteinase Lb results in shutting off the cap-dependent translation of host mRNAs (Liebig et al., 1993; Ziegler et al., 1995). A similar observation was made in feline calicivirus (FCV) infected cells (Willcocks et al., 2004). Cleavage of poly (A) binding protein (PABP) that is a non-canonical initiation factor by PV proteinase 2A and 3C has also been demonstrated (Joachims et al., 1999; Kerekatte et al., 1999). PABP cleavage by PV 3C has shown to inhibit cellular translation (Kuyumcu-Martinez et al., 2004). Moreover, PV 3C induced morphological changes in host cells by cleaving microtubule-associated protein (MAP-4) (Joachims et al., 1995). In addition, PV 3C inhibits the transcription of host mRNAs through cleavage of transcription factors (Clark et al., 1993; Das and Dasgupta, 1993; Yalamanchili et al., 1997; Yalamanchili et al., 1997). The cleavage of La autoantigen by PV 3C seems to result in the enhanced translation of viral mRNAs (Shiroki et al., 1999), whereas cleavage of polypyrimidine tract-binding proteins (PTB) by PV 3C inhibited translation of PV mRNA (Back et al., 2002).

2.5.1 Poly (A) binding protein (PABP)

PABP, a 70-kDa protein, is highly abundant in eukaryotic cells and binds to poly (A) stretches (Gorlach et al., 1994; Nietfeld et al., 1990). The N-terminal part of PABP consists of four highly conserved RNA recognition motifs (RRMs) that are composed of approximately 90 amino acids, with a hydrophobic core (Nagai et al., 1995). The C-terminal domain (CTD) is highly conserved and mediates PABP homodimerization on RNA and the creation of higher-order PABP-poly (A) structures. PABP is multifunctional and active in mRNA stabilization, deadenylation, inhibition of mRNA decapping and maturation (Brown and Sachs, 1998; Dehlin et al., 2000; Gao et al., 2000; Wormington et al., 1996). PABP/poly (A)-dependent translation stimulation was demonstrated most effectively using nuclease-treated yeast or HeLa translation extracts, and after PABP depletion of these extracts (Bergamini et al., 2000; Tarun et al., 1997). PABP binding was proposed to induce cooperative conformational changes in eIF4E and eIF4G that enhance the stability of initiation complexes on capped mRNAs (Wei et al., 1998) and to act in joining of the 40S ribosomal subunit to the mRNA (Tarun and Sachs, 1995) and in the recruitment of the 60S ribosomal subunit (Sachs and Davis, 1989).

2.5.2 eukaryotic initiation factor 4G (eIF4G)

The translation initiation factor eIF4G (also named p220 or eIF4- γ) is a large polypeptide with a molecular weight of 220 kDa. eIF4G acts as a scaffold connecting eIF4E (cap-binding protein) and eIF4A (an RNA helicase) (Lamphear et al., 1995; Ziegler et al., 1995) to form the initiation factor complex eIF4F (Morley et al., 1997). eIF4G is believed to mediate nonspecific RNA binding of the eIF4F complex. During translation initiation, the eIF4F complex recruits ribosomes to the mRNA-initiation factor pre-complex via an interaction with 40S ribosome-associated eIF3 (Morley et al., 1997; Sachs et al., 1997). In PV or FMDV infected cells, cleavage of eIF4G roughly correlates with the loss of cellular cap-dependent protein synthesis (Liebig et al., 1993; Ziegler et al., 1995). Cleavage of eIF4G separates the eIF4E and eIF3 binding domains on eIF4G and thus contributes to host cell shut-off. The C-terminal eIF4G cleavage product can stimulate IRES-dependent translation of enterovirus and rhinovirus RNA and thus favor viral over host protein biosynthesis (Borman et al., 1997; Ohlmann et al., 1997; Ohlmann et al., 1996).

2.5.3 Poly(C) binding protein (PCBP)

PCBP1 and PCBP2 are poly (rC) binding proteins (also known as hnRNP E or α -CP) (Parsley et al., 1997; Gamarnik and Andino, 1997). They contain three internal peptide repeats corresponding to K-homologous (KH) domains, originally identified in heterogeneous nuclear ribonucleoprotein K. PCBP regulates the stability and expression of several cellular mRNAs (Ostareck-Lederer et al., 1998) and participates in translational control of cellular mRNAs (Holcik and Liebhaber, 1997). PCBP is a component of an RNP complex that forms at the 3'NTR of the human α -globin mRNA and determines its stability (Kiledjian et al., 1995). PCBP is a positive regulator of PV translation by binding to the PV CL (Gamarnik and Andino, 1998; Parsley et al., 1997).

3. Aims of this study

Unlike other picornaviruses, yet similar to the hepatitis viruses HBV and HCV, hepatitis A virus (HAV) persistently infects liver cells in culture without shutting-off host cell translation.

Although various steps in the viral life cycle have been proposed to limit viral replication, the molecular mechanisms of viral persistence still remain enigmatic. In particular, little is known on both the host and viral factors that enables the virus to withstand the host's antiviral system and to compete with the host's unaffected metabolism.

The specific aims of this study are summarized as follows:

1. Establishment of an optimized in vivo and in vitro system to study HAV genome replication using the HAV replicon
2. Identification of the HAV intragenomic *cis*-acting replication element (CRE)
3. Insertion of a *cis*-acting ribozyme to assess the role of the authentic 5' end of the viral RNA
4. Identification of translation factors that can be potentially modified during HAV infection (eIF4G, PABP, PCBP) and characterization of the cleavage product of the viral proteinase 3C
5. Characterization of the interaction of host proteins PABP and PCBP with the viral 5' and 3' terminal RNA structures.

4. Materials and methods

4.1 Materials

4.1.1 Chemicals and kits

Acetic acid.....	Merck (Darmstadt)
Acetone.....	Merck (Darmstadt)
Acrylamide(30%)/Bisacrylamid (0.8%)	Roth (Karlsruhe)
Agarose.....	Invitrogen (Paisley)
Ampicillin.....	Sigma (Aldrich)
Ammonium bicarbonate	Merck (Darmstadt)
Ammonium persulfate	Merck (Darmstadt)
Calcium chloride	Sigma (St. Louis)
Chloramphenicol	Serva (Heidelberg)
Coomassie brilliant blue R250	Merck (Darmstadt)
DMEM	Gibco (Paisley)
DMRIE-C	Invitrogen (Paisley)
EDTA	Merck (Darmstadt)
Ethanol	Roth (Karlsruhe)
Fetal calf serum	Biochrom AG (Berlin)
Glycine	Biomol (Hamburg)
G418 sulfate	Merck (Darmstadt)
Guanidium HCl	Biomol (Hamburg)
HEPES.....	Carl Roth (Karlsruhe)
Imidazole.....	Merck (Darmstadt)
Kanamycin	Sigma (Aldrich)
Magnesium Chloride	Merck (Darmstadt)
Methanol	Merck (Darmstadt)
MetaPhor® Agarose.....	Cambrex (Rockland)
Milk powder (non-fat).....	Töpfer (Dietmannsried)
OptiMEM	Gibco NY
Ovalbumin.....	Sigma (Aldrich)

Ponceau-S.....	Serva (Heidelberg)
Potassium Chloride	Merck (Darmstadt)
Penicillin/Streptomycin.....	Biochrom KG (Berlin)
Phenylmethylsulfonyl fluoride.....	Fluka (Buchs)
QIAGEN Plasmid Maxi Kit	Qiagen (Hilden)
QIAquick Gel Extraction Kit	Qiagen (Hilden)
Sodium bicarbonate.....	Merck (Darmstadt)
Sodium chloride	Merck (Darmstadt)
SDS.....	Fluka (Buchs)
Sodium hydroxide	Fluka (Buchs)
TEMED	Roth (Karlsruhe)
Tris-Cl	Biomol (Hamburg)
Trizol Reagent.....	Invitrogen (Paisley)
Triton X-100.....	Fluka (Buchs)
tRNA from E.coli MRE 600	Roche (Mannheim)
Trypsin	Biochrom KG (Berlin)
Tween-20.....	Serva (Heidelberg)
NucleoSpin Plasmid Kit	Macherey-Nagel (Düren)
NucleoBond PC 100 Kit.....	Macherey-Nagel (Düren)
NucleoSpin Extract 2 in 1	Macherey-Nagel (Düren)
QIAquick Gel Extraction Kit	QIAGEN (Hilden)
S.N.A.P. UV-Free Gel Purification Kit.....	Invitrogen (Paisley)
Centricon YM 10.....	Millipore (Bedford)
Centricon YM 30.....	Millipore (Bedford)
Rapid DNA Ligation Kit.....	MBI
RiboMAX™ Large Scale RNA Production System-T7	Promega (Madison)
RiboMAX™ Large Scale RNA Production System-SP6	Promega (Madison)
MaxIscrip™ In Vitro Transcription Kit.....	Ambion (Austion)
Luciferase Assay System	Promega (Madison)
TMB Liquid Substrate System.....	Sigma
Micro BCA Protein Assay Reagent Kit	Pierce (Rockford)

4.1.2 Enzymes

Restriction enzymes and buffers	New England Biolabs or MBI
T4 DNA ligase	New England Biolabs
Mung bean nuclease	MBI
Calf intestine alkaline phosphatase (CIAP)	MBI
Micrococcal nuclease S7	Roche

4.1.3 Instruments and other Equipment

Eppendorf centrifuge 5415D	Eppendorf (Hamburg)
FPLC	Amersham Bioscience (Uppsala)
J 2-21 M/E centrifuge.....	Beckman (Fullerton)
L88-55 Ultracentrifuge.....	Beckman (Fullerton)
Cell incubator Nu-440-400E	NuAire (Plymouth)
PCR amplifier PTC-200	Biozym (Oldendorf)
Spectrophotometer Ultrospec 3000.....	Amersham Bioscience (Uppsala)
Luminometer Lucy-3.....	Anthos (Krefeld)
Thermoblock 100-6106	Liebisch (Bielefeld)
HiTrap Chelating HP column (1ml).....	Amersham Biosciences (Uppsala)
Semi-Dry-Blotter PEGASUS	Phase (Luebeck)
Nitrocellulose transfer membrane (0.2 µm)	Schleicher&Schuell (Dassel)

4.1.4 Marker for protein and nucleic acids

RNA marker:

RNA Ladder, High Range, ready-to-use.....	MBI
RNA Ladder, Low Range, ready-to-use.....	MBI

DNA marker:

SmartLadder	Eurogentec
1 Kb ladder	Gibco
GeneRuler™ 50bp DNA ladder	MBI

Protein marker:

MultiMark Multi-Colored Standard.....	Invitrogen
---------------------------------------	------------

4.1.5 Oligonucleotide for hammerhead ribozyme cloning

- PrimerI AAAACTGCAGTAATACGACTCACTATAGGGCTCTTGAAGCTGA
- PrimerII GCCTCATCAGTTCAAGAGCCCTATAGTGAGTCGTATTACTGCAGTTTT
- PrimerIII TGAGGCCGAAAGGCCGAAAACCCGGTATCCCGGGTT□TTCAAGAGGGG
- PrimerIV CGGAGACCCCTCTTGAA□GAACCCGGGATAACCGGGTTTTTCGGCCTTTTCG
- PrimerV TGAGGCCGAAAGGCCGAAAACCCGGTATCCCGGGTT□TTCAAGAGGGG
- PrimerVI CGGAGACCCCTCTTGAA□GAACCCGGGATAACCGGGTTTTTCGGCCTTTTCG
- PrimerVII TCTCCGGGAATTTCCGGAGTCCCTCTTGGAAGTCCATGGTGAGCTCCGG
- PrimerVIII CCGGAGCTCACCATGGACTTCCAAGAGGGACTCCGAAATTCC

All oligonucleotide were phosphorylated and produced by AGOWA, Berlin. The nucleotide at the active and inactive cleavage sites are indicated by boxes in primers III and IV and primers V and VI. The introduced cloning sites of *Pst*I (primer I and II) and *Sac*I (primer VII and VIII) are underlined.

4.1.6 E.coli strains

- XL2 Genotype: *recA1 endA1 gyrA96 thi-1 hsdR17 supE44 relA1 lac* [F' *proAB lacI^qZΔM15 Tn10 (Tet^r) Amy Cam^r*]^a
- BL21 (DE3) Genotype: *F- ompT hsdSB (rb- mB-) gal dcm (DE3)*
The (DE3) cells carry a chromosomal copy of the T7 RNA polymerase gene under control of the lacUV5 promoter. This strain is used for protein expression of pET vectors.
- BL21 (DE3) pLysS Genotype: *F- ompT hsdSB (rb- mB-) gal dcm (DE3) pLysS (Cm^R)*
Same as above but contains an additional vector that produces small amounts of T7 lysozyme that suppresses basal expression of T7 RNA polymerase prior to induction and thus reduces leaky expression.
- JM109 transformed with pQE9-PCBP2

4.1.7 Virus strains

- vTF7-3 (Fuerst et al., 1986)

The recombinant vaccinia virus expresses T7 RNA polymerase.

- HAV strain HM175/18f, sequence in gene bank M59808 (Lemon et al., 1991)
HM175/18f is highly adapted to growth in BS-C-1 and Huh-7 cells.

4.1.8 Cell lines

- BS-C-1 ATCC CCL-26 green monkey kidney cell
- COS-7 cells ATCC CRL-651
- HeLa S3 cells ATCC CCL-2.2
- Huh-7 cells are derived from a human hepatocellular carcinoma (Nakabayashi et al., 1982).
- Huh-T7 cells are a derivative of Huh-7 that stably express the T7 RNA polymerase (Schultz et al., 1996).

4.1.9 Plasmids

- pT7-18f contains a cDNA copy of the complete sequence of the rapidly replicating variant of HAV (HM175/18f) under the control of the T7 promoter (Kusov and Gauss-Muller, 1999; Zhang et al., 1995). It has a poly (A) tail of 26 residues.
- pT7-18f-A60, same as pT7-18f, but with 60 adenosine residues.
- pT7-18f-A60-mut, same as pT7-18f-A60, but with a frame-shift mutation in the RNA polymerase (3D^{pol}).
- pT7-18f-Luc-A60 (Gauss-Muller and Kusov, 2002) encodes the HAV replicon.
- pT7-18f-Luc-A60-mut (Gauss-Muller and Kusov, 2002) encodes the replication deficient HAV replicon with a frame-shift mutation in the RNA polymerase (3D^{pol}).
- pT7-18f-Luc-A60-cre (constructed by Dr. V. Gauss-Müller) encodes the replication deficient HAV replicon with mutations (8 nt) in the putative CRE sequence.
- pT7-18f-(Δ P1-P3) A0rbz (constructed by Dr. Y. Kusov) was used for the preparation of radio-labeled HAV RNA 3'NTR-A0.
- pT7-18f-(Δ P1-P3) A14 (constructed by Dr. Y. Kusov) was used for preparation of radio-labeled HAV RNA 3'NTR-A14.
- pT7-18f-(Δ P1-P3) A20 (constructed by Dr. Y. Kusov) was used for the preparation of radio-labeled HAV RNA 3'NTR-A20.
- pT7-18f-(Δ P1-P3) A60 (constructed by Dr. Y. Kusov) was used for the preparation of radio-labeled HAV RNA 3'NTR-A60.
- pET15b-3ABCwt (Kusov et al., 1997) encodes the proteinase 3C precursor 3ABC with an N-terminal His-tag and is controlled by the T7 promoter.
- pET15b-3ABCmut6 (constructed by Andre Güllmer) carries mutations at both the 3A/B and 3B/C cleavage sites that are described in (Kusov and Gauss-Muller, 1999).

- pET15b-3ABC μ (Kusov et al., 1997) carries an Ala residues in place of the active site Cys residues in 3C.
- pEXT7-LA-3C-C172A encodes the inactive proteinase 3C of HAV strain LA with an Ala instead of the active site Cys (see PhD thesis of Christian Probst, 1997).
- pEXT7-LA-3C encodes the active HAV proteinase 3C. (Probst et al., 1997).
- pEXT7-Xgal (see PhD thesis of Monika Jecht, 1998)
- pcDNA3.1 (Invitrogen)
- pET28-PABP (kindly provided by Dr. Roland Zell) is a subclone of PABP described by Gorlach (Gorlach et al., 1994).
- pET28-PABP1234 (kindly provided by Goodall,GJ (Sladic et al., 2004)) encodes the N-terminal four RNA binding motifs of PABP.
- pET28-PABPCT (kindly provided by Kiledjian, M, (Wang and Kiledjian, 2000)) encodes the PABP CTD.
- pGEM2 (Promega)
- pQE9-PCBP2 (kindly provided by Dr. Roland Zell) is a subclone of pQE30-PCBP2 described by Garmanik (Gamarnik and Andino, 1997)).
- pGEM2-PCBP2 (constructed in this work) encodes PCBP under the T7 promoter.
- pGEM2- Δ PH (constructed in this work) was constructed by deleting the T7 promoter fragment between *PvuII* and *HindIII* site.
- pGEM2-rib(+) (constructed in this work) contains the HAV-specific active hammerhead ribozyme under the T7 promoter.
- pGEM2-rib(-) (constructed in this work) contains the HAV-specific inactive hammerhead ribozyme under the T7 promoter.
- pGEM2-rib(+)-18f-Luc-A60 (constructed in this work) contains the active HAV replicon preceded by the active hammerhead ribozyme and the T7 promoter.
- pGEM2-rib(-)-18f-Luc-A60 (constructed in this work) contains the active HAV replicon preceded by the active hammerhead ribozyme and the T7 promoter.
- pGEM2-rib(+)-18f-A60 (constructed in this work) contains the HAV genome preceded by the active hammerhead ribozyme and the T7 promoter.
- pGEM2-rib(-)-18f-A60 (constructed in this work) contains the HAV genome preceded by the active hammerhead ribozyme and the T7 promoter.
- pRluc31 (kindly provided by Andino) encodes the replication-competent PV replicon (Andino et al., 1993)

- pRluc181 encodes the replication-deficient PV replicon (kindly provided by Andino) (Andino et al., 1993) that carries a mutation in 3C active site.
- prib(+)-RLuc encodes the PV replicon pRluc31 with the active hammerhead ribozyme (kindly provided by Andino) (Herold and Andino, 2000).
- prib(-)-RLuc encodes the PV replicon pRluc31 with the inactive hammerhead inactive ribozyme (kindly provided by Andino) (Herold and Andino, 2000).

4.1.10 Antibodies, their characterization

- Anti-His tag: mouse monoclonal antibody (Novagen) (used at 1:2500 dilution)
- Anti-PABP: rabbit polyclonal antibody (Kuyumcu-Martinez et al., 2004) was raised against a synthetic peptide sequence (GIDDERLRKEFSPFGTC) in the RRM4 of PABP (used at 1:2000 dilution).
- Anti-PCBP2: rabbit polyclonal antibody (Blyn et al., 1997) (used at 1:4000 dilution)
- Anti-eIF4G: rabbit polyclonal antibody ZP1 is directed against peptide 7 (KKEAVGDLLDAFKEVN, position 523-538) of the N-terminus of eIF4G (Baugh and Pilipenko, 2004) (used at 1:1000 dilution).
- Anti-HAV 3C: rabbit polyclonal antibody (Schultheiss et al., 1995) (used at a dilution 1:2000)
- Anti-HAV (7E7): mouse monoclonal anti-HAV, IgG class (Mediagnost, Tübingen) (used in 1:15,000 dilution)
- POD-conjugated anti-HAV (7E7) IgG (Mediagnost, Tübingen) (used in 1:15,000 dilution)
- Alkaline phosphatase-conjugated swine anti-rabbit immunoglobulin (Dako Denmark) (used in 1:2,500 dilution)
- Alkaline phosphatase-conjugated rabbit anti-mouse immunoglobulin (Dako Denmark) (used in 1:2,500 dilution)

4.1.11 Buffers and stock solutions

Oligonucleotide annealing buffer:

10 mM Tris-HCl (pH 7.5), 50 mM NaCl

3 M sodium acetate (pH 5.5)

TE buffer

10 mM Tris-HCl (pH 7.5), 1 mM EDTA

50 X TAE (per litre)

242 g Tris base, 57.1 g glacial acetic acid, 100 ml 0.5 M EDTA pH 8.0

10 X TBE (per litre)

108 g Tris base, 55 g boric acid, 40 ml 0.5 M EDTA, pH 8.0

6 X gel loading buffer for DNA

0.25% bromophenol blue, 0.25% xylene cyanol, 15% ficoll type 4000, 120 mM EDTA

CaCl₂ solution (250 ml) for preparation of competent cells

60 mM CaCl₂, 10 mM PIPES, 15% glycerol

10 X MOPS buffer:

0.2 M MOPS, 50 mM sodium acetate, 5 mM EDTA (pH 7.0)

1 X RNA denaturing sample buffer for agarose-formaldehyde electrophoresis:

10 µl 10x MOPS

6.54 µl 37% formaldehyde

50 µl formamid

33 µl DEPC-water

4 µl EB (1 mg/ml, diluted in DEPC-water)

20 µl Blue-juice (1 mM EDTA, 0.25% bromophenolblue, 0.25% xylene cyanol, 50% glycerol)

Running buffer for nondenaturing polyacrylamide gel (to 2 liters)

13.45 ml 1 M Tris-acetate (pH 7.9)

6.6 ml 1 M sodium acetate

4.0 ml 0.5 M EDTA

Ethidium bromide (10 mg/ml) in water

EMSA binding buffer

5 mM HEPES, pH 7.9, 25 mM KCl, 2 mM MgCl₂, 6 mM DTT, 0.05 mM PMSF, 166 µg/ml of *E. coli* tRNA, 5% glycerol

EMSA sample loading buffer

1 mM EDTA, 0.25% bromophenol blue, 0.25% xylene cyanol, 50% glycerol

Buffer A for His-tag protein purification

50 mM Tris-HCl (pH 8.0), 300 mM NaCl, 10 mM imidazol

Buffer B for His-tag protein purification

50 mM Tris-HCl (pH 8.0), 300 mM NaCl, 250 mM imidazol

Exchange buffer for protein buffer exchange

50 mM Tris-HCl (pH 8.0), 50 mM NaCl, 15% glycerol

0.1 M NiCl₂

0.5 M EDTA (pH 8.0)

1.5 M Tris (pH 8.8) for preparation of the separating gel

1 M Tris-HCl (pH 6.8) for preparation of the stacking gel

10 % SDS in water

5 X SDS-PAGE running buffer

0.125 M Tris-HCl, 0.960 M glycine, 0.5% SDS

Protein 5 X sample buffer

10% w/v SDS, 10 mM DTT, 20% v/v glycerol, 0.2 M Tris-HCl (pH 6.8), 0.4% bromophenol blue

Preparation of separating gel (for 15ml)

Final concentration	10%	12%
dd H ₂ O	5.9 ml	4.9 ml
Acrylamide (30%)/bisacrylamide (0.8%)	5 ml	6.0 ml
1.5 M Tris (pH 8.8)	3.8 ml	3.8 ml
10% SDS	0.15 ml	0.15 ml
10% APS	0.15 ml	0.15 ml
TEMED	0.006 ml	0.006 ml

Preparation of stacking gel (5% ,5 ml)

dd H ₂ O	3.4 ml
Acrylamide (30%)/bisacrylamide (0.8%)	0.83 ml
1 M Tris (pH 6.8)	0.63 ml
10% SDS	0.05 ml
10% APS	0.05 ml
TEMED	0.005 ml

Ponceau S staining solution for immunoblot

0.05 % Ponceau S in 3 % trichloroacetic acid

Blotting buffer

25 mM Tris base, 193 mM glycine, 20% methanol

10 X TBS-T for immunoblot

87.6 g NaCl, 12.1 g Tris base, 5 ml Tween 20 to 1 L with H₂O (pH 8)

Alkaline phosphatase (AP) buffer for immunoblot

100 mM Tris (pH 9.5), 100 mM NaCl, 5 mM MgCl₂

NBT/BCIP stock solution for immunoblot

225 volumes NBT (75 mg/ml in 70 % (v/v) dimethyl formamide (DMF)) and 175 volumes BCIP (50 mg/ml in 70 % DMF)

NBT/BCIP staining solution:

0.8 ml of stock + 100 ml AP buffer

3C cleavage buffer

100 mM NaCl, 5 mM MgCl₂, 10 mM HEPES-KOH (pH 7.4)

10 X HNG buffer (250 ml) for preparation of S10 cell extract

21.3 g NaCl, 4.95 g D-glucose, 87.5 ml HEPES (1M)

Hypotonic buffer (50 ml) for preparation of the S10 cell extract

0.625 ml KCl (4 M)

1.25 ml HEPES (1 M)

15.3 µl MgCl₂ (4.9 M)

50 µl DTT (1 M)

10 X concentrated buffer for preparation of the S10 cell extract

25 mM HEPES, pH 7.5

1 M KAc

30 mM MgCl₂

30 mM DTT

0.075 M CaCl₂

0.1 M EGTA

Translation mix for in vitro translation (10 X)

0.125 M HEPES (pH 7.3)

10 mM ATP

2 mM GTP

2 mM CTP

2 mM UTP

100 mM creatine phosphate

0.2 mM 19 amino acid mix minus Met

1 mg/ml creatine phosphokinase

Salt Mix for in vitro translation (10 X)

1 M	K-acetate
30 mM	MgCl ₂
2.5 mM	spermidine

4.2 Methods

4.2.1 Nucleic acid methods

4.2.1.1 Plasmid purification

Mini preparations (10 µg DNA) were performed according to the user manual of NucleoSpin Plasmid Kit. Midi preparations (1 mg DNA) were performed according to the user manual of NucleoBond PC 100 Kit.

4.2.1.2 DNA restriction digestion

Restriction enzyme digestions were performed by incubating double-stranded DNA molecules with an appropriate amount of restriction enzyme, in its respective buffer as recommended by the supplier, and at the optimal temperature for that specific enzyme. The reactions were incubated for 1 - 3 h to insure complete digestion.

4.2.1.3 DNA precipitation

1/10 volume 3 M sodium acetate (pH 5.5) and 2.5 - 3 volumes ethanol were added to the DNA sample and incubated in an ice-water bath for at least 10 min. The mixture was centrifuged at 12,000 g in a microcentrifuge for 15 min at 4 °C. The supernatant was discarded, and 75% ethanol (corresponding to about two volumes of the original sample) was added to the pellet, incubated at RT for 5-10 min and centrifuged again for 5 min, and the DNA pellet were dried for about 5-10 min RT. Dried DNA was dissolved in TE buffer.

4.2.1.4 DNA agarose gel electrophoresis

1 g agarose was dissolved in 100 ml of 1X TAE or TBE buffer (gives a 1% gel) in the microwave oven. Dissolved agarose containing 0.5 µg/ml ethidium bromide was put on the plate with the comb in place; 6 X gel loading buffer and sample were mixed and loaded into the wells. The gel was run in 1 X TAE or TBE for 30-60 min at 100~150 V.

4.2.1.5 DNA extraction from agarose gel

DNA fragments were extracted from agarose gel according to the user manual of NucleoSpin Extract 2 in 1 or QIAquick Gel Extraction Kit or S.N.A.P. UV-Free Gel Purification Kit.

4.2.1.6 Determination of DNA and RNA concentration

The concentration of DNA and RNA was determined by reading OD_{260nm} in a spectrophotometer.

4.2.1.7 DNA ligation

Purified DNA fragments (vector and insert) were ligated by rapid DNA ligation kit according to the manual supplied with the kit. The molar ratio of vector to insert was 1:3 at a total concentration around 200 ng in 20 μ l reaction. 5 μ l of the ligation mixture was directly used for transformation.

4.2.1.8 Preparation of competent E. coli

5 μ l glycerol culture of XL2 or BL21 (DE3) was added to 5 ml LB and incubated overnight at 37 $^{\circ}$ C. 2 ml overnight culture was added to 200 ml LB and incubated at 37 $^{\circ}$ C until the OD_{600nm} reached 0.5. The culture was cooled on ice for 10 min and collected by centrifugation at low speed (7 min, 3,000 g, 4 $^{\circ}$ C). The supernatant was discarded and the pellet suspended in 10 ml CaCl₂ solution and collected by centrifugation at low speed (5 min, 2500 g, 4 $^{\circ}$ C). The cells were resuspended in 10 ml CaCl₂ solution for second time and incubated on ice for 30 min. The cells were collected by centrifugation at low speed (5 min, 2500 g, 4 $^{\circ}$ C) and resuspended in 2 ml CaCl₂ solution. 50 μ l aliquots were stored at -70 $^{\circ}$ C.

4.2.1.9 Transformation of E.coli

An aliquot of plasmid (10 ng) or a ligation mixture (5 μ l or less) was mixed with 50 μ l competent cells. The mixture was incubated on ice for 30 min, at 42 $^{\circ}$ C for 30 sec, and on ice for another 2 min. 500 μ l LB was added to the mixture and shaken at 37 $^{\circ}$ C for 60 min. 50 μ l and 250 μ l aliquots were plated on LB-agar plates containing the appropriate antibiotic and incubated at 37 $^{\circ}$ C overnight.

4.2.1.10 Insertion of the hammerhead ribozyme at the 5'end of the HAV full-length genome and replicon

➤ Annealing and ligation of hammerhead and T7 promoter containing oligonucleotide pairs
Equimolar amounts of oligonucleotide pairs I/II, III/IV, V/VI, and VII/VIII (100 pmol) were combined separately in 20 μ l oligonucleotide annealing buffer and heated to 94 $^{\circ}$ C, then cooled to 25 $^{\circ}$ C in 30 min in the PCR machine. 1 μ l (10 pmol) of each pair I/II, III/IV, and VII/VIII (representing the T7 RNA polymerase promoter, the hammerhead ribozyme and the 5'-terminal first 53 nucleotides of the HAV (HM175/18f) genome, respectively) or I/II, V/VI, and VII/VIII (like the other pairs, but containing a mutated hammerhead ribozyme) were ligated in 20 μ l ligation mixture according to the manual of the rapid DNA ligation kit. The ligation product was 139 bp.

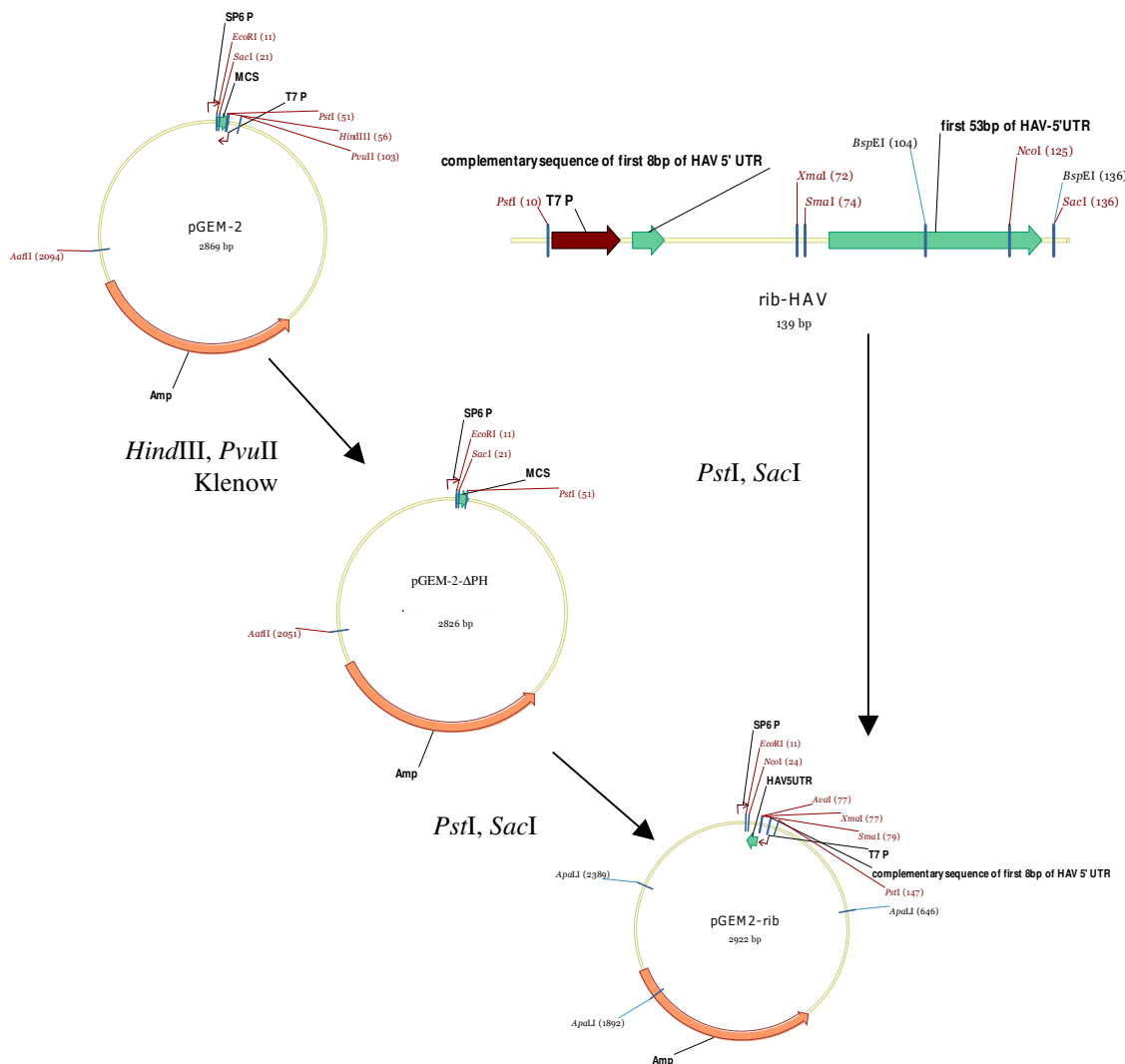


Fig. 4. The flow chart of the hammerhead ribozyme cloning.

➤ PCR amplification of the oligonucleotide ligation products

In order to enlarge the amount of the oligonucleotide ligation product for the subsequent cloning step, oligonucleotide I (10 pmol) and VIII (10 pmol) and 1 μ l of the ligation product were amplified in a 50 μ l PCR mixture. PCR conditions were 95 $^{\circ}$ C, 20 sec; 55 $^{\circ}$ C, 20 sec; 72 $^{\circ}$ C, 10 sec; for 30 cycles. The 139 bp PCR product was purified after separation on a 4 % Metaphor agarose gel.

➤ Cloning of the active and inactive ribozyme containing cDNA fragment into pGEM2

Both fragments presenting the active and inactive ribozyme were separately cloned into the *Pst*I and *Sac*I sites of pGEM2- Δ PH (which was derived from pGEM-2 after removal of the T7 promoter by deleting the *Pvu*II and *Hind*III fragment and religation) and resulted in pGEM2-rib(+), and pGEM2-rib(-) respectively. The flow chart of the cloning is shown in **Fig. 4**.

➤ Insertion of the HAV full-length genome and replicon into pGEM2-rib

The inserts of the HAV replicon were prepared from pT7-18f-Luc-A60 and pT7-18f-Luc-A60-mut by cutting with *NcoI* and *AatII* and cloned into pGEM2-rib(+) and pGEM2-rib(-) at the same position. The resulting constructs are named pGEM2-rib(+)-replicon, pGEM2-rib(-)-replicon, pGEM2-rib(+)-replicon-mut. The inserts of the HAV full genome were prepared from pT7-18f-A60 and pT7-18f-A60-mut by cutting with *BspEI* and *AatII* and cloned into pGEM2-rib(+) and pGEM2-rib(-) at the same position. The resulting constructs are named pGEM2-rib(+)-18f-A60, pGEM2-rib(-)-18f-A60, and pGEM2-rib(+)-18f-A60-mut.

4.2.1.11 Large scale RNA preparation

RNA was prepared in large scale according to the user manual of the RiboMAX Large Scale RNA production System. Normally, 150 µg RNA was obtained from 2 µg linearized DNA as template. The HAV full-length genome and the replicon cDNAs with and without ribozyme were linearized with *AgeI*, and the genome and replicon RNAs were prepared by T7 polymerase. The PV replicon cDNA was linearized with *MluI*, and the replicon RNA was prepared by T7 RNA polymerase.

4.2.1.12 Radio-labeled RNA preparation

Radio-labeled RNA was prepared as described in the manual of the MaxIscript™ in vitro transcription kit with 3 µl α-³³P-UTP (10 µCi/µl) and additional 2 µl UTP (0.05 mM) in a 20 µl volume. Radio-labeled RNA was purified by phenol, and dissolved in 50 µl DEPC-H₂O.

pT7-18f-(ΔP1-P3) A0rbz cDNA was linearized with *RsrII* for HAV 3'NTR-A0 transcript. pT7-18f-(ΔP1-P3) A14, pT7-18f-(ΔP1-P3) A20, pT7-18f-(ΔP1-P3) A60 were linearized with *AgeI* for HAV 3NTR-A14, -A20, -A60 transcript. pT7-18f was linearized with *SspI* for HAV 5'NTR-148 transcript.

4.2.1.13 Denaturing polyacrylamide gel electrophoresis for RNA (5%, 15ml)

7.2 g urea, 1.5 ml 10 X TBE, 2.5 ml 30% acrylamide/bis, and DEPC-H₂O were mixed to 15 ml. The mixture was stirred at RT until the urea was completely dissolved. Then 120 µl 10% APS and 16 µl TEMED were added. The gel was pre-run for 5~10 min, the wells were rinsed with buffer before the samples were loaded on the gel. The gel was run for approximately 1 h at 250 V in 0.5 X TBE buffer.

4.2.1.14 Agarose-formaldehyde electrophoresis

➤ Agarose gel preparation (40 ml, 0.8% - 1.5%):

0.32 – 0.6 g SeaKem GTG agarose in 31.2 ml DEPC water was heated and then cooled to 60°C. 4 ml 10 X MOPS, 4.4 ml 37% formaldehyde were added and then poured the gel into the chamber with the comb.

➤ RNA sample preparation and gel running

0.5 - 1 µg RNA in 1 - 2 µl was mixed with 12 µl 1 X RNA denaturing sample buffer and heated at 55 °C for 15 min. The mixture was immediately put on ice for 2 - 5 min. The samples were loaded on the gel and run at 110 V in 1 X MOPS (diluted with DEPC-water) for 30 min.

4.2.1.15 DEPC treated dd-H₂O preparation

5 ml DEPC was added into 5 liters dd-H₂O, the mixture was stirred at RT overnight. The DEPC treated H₂O was autoclaved 2 times. All solutions used for RNA were prepared in DEPC water.

4.2.1.16 RNA electrophoresis mobility shift assay (EMSA) (Kusov and Gaus-Muller, 1997)

➤ Nondenaturing polyacrylamide gel (5 %) preparation for EMSA

	335 µl	1 M Tris-acetate, pH 7.9
	100 µl	0.5 M EDTA
	165 µl	1 M sodium acetate
	8.5 ml	30% acrylamide
	2.5 ml	50% glycerol
	39 ml	DEPC treated water
Total	50 ml	
	0.25 ml	10% APS
	25 µl	TEMED

The gel was pre-run at 4°C and 80 V for 60 min

- For protein and RNA interaction, a 15 µl reaction mixture containing radio-labeled RNA (0.5 - 1 × 10⁵ cpm) and different amounts of protein in binding buffer was incubated for 20 min at 30°C. 5 µl sample loading buffer was added to the mixture, and analyzed on a 5% nondenaturing polyacrylamide gel that had been pre-run for 60 min at 4°C and 80 V. Electrophoresis was conducted at 200 V at 4°C until the bromophenol blue marker had migrated to a position of 1/2 - 2/3 of the gel length, depending on the size of the RNA probe. The gels were dried or subjected directly to photoimaging.

4.2.2 Protein methods

4.2.2.1 Purification of recombinant proteins from E.coli

➤ Induction of protein expression

JM109 (pQE9-PCBP2) or BL21 (DE3) pLysS (pET28-hPABP) were inoculated in 50 ml LB containing the appropriate antibiotic and cultured overnight at 37°C. 50 ml overnight culture was put into 1 L LB containing the appropriate antibiotic. The mixture was shaken at 37°C until OD_{600nm} reached 0.6 - 0.8. 0.5 ml 1 M IPTG was added to the culture and incubated for an

additional 4 h. The cells were centrifuged at 5,000 g for 20 min and the pellet was kept for crude protein extraction.

➤ Crude protein extraction

The pellet of the induced cells was suspended in Buffer A (5 ml per gram wet weight) and the cells were destroyed by 3 times freezing/thawing. DNA was destroyed by sonication on ice and the lysate was centrifuged at 13,000 g for 20 min at 4 °C. The supernatant was stored at 4 °C for purification.

➤ Affinity chromatography

The HiTrap chelating HP column was rinsed with 10 volumes of water at a rate of 1 ml/min. The column was loaded with 10 volumes of 0.1 M NiCl₂ and rinsed with 10 volumes of water at a rate of 1 ml/min. The column was equilibrated with 10 volumes of Buffer A. The crude protein extract was loaded at a rate of 0.5 ml/min. The column was rinsed with Buffer A until the absorbance reached the baseline (5 volumes) at a rate of 1 ml/min. The bound protein was eluted with an imidazole gradient of 10 to 250 mM in 30 min at a rate of 1 ml/min. 1 ml fractions were collected. For regeneration, the column was stripped with 0.5 M EDTA, rinsed with water, reloaded with 0.1 M NiCl₂, rinsed with water and equilibrated with Buffer A for further use.

➤ Concentration and buffer exchange

PABP (Centricon YM 30) and PCBP2 (Centricon YM 10) were concentrated according to the manual of Centricon by using the exchange buffer.

Briefly, Centricon YM was washed with 1ml exchange buffer by centrifuging at 5,000 g, (8,000 rpm, Beckman JA20); 2 ml protein sample was added to the Centricon YM container, then centrifuged for 30 min so that approximately 0.4 ml was left. 2 ml exchange buffer was added, and centrifuged at 8,000 rpm 30 min two times.

4.2.2.2 SDS-PAGE

The separating and stacking gel was prepared with the buffers described above. Protein samples were prepared by mixing protein solution with 4 x sample buffer, heated at 95 °C for 5 min, cooled on ice for a few min and centrifuged briefly. The samples were electrophoresed at constant 110 V until the dye reached the bottom of the separating gel.

4.2.2.3 Immunoblot analysis

After separation of the protein samples by SDS-PAGE, the protein samples were transferred to a nitrocellulose membrane in blotting buffer with a semi dry blotter at 30 V for 90 min. The transferred membrane was stained with Ponceau S staining solution for 5 - 10 min and destained with 10% acetate solution for photocopy. After completely destaining, the membrane was blocked with 5% (w/v) milk in TBS-T. The membrane was incubated with a dilution of the first

antibody in TBS-T with 1% ovalbumin overnight at 4°C. After three washes with TBS-T, the blot was incubated with a dilution of the second antibody conjugated to AP in TBS-T at RT for 2 h. The membrane was washed two times with TBS-T and one time with AP buffer; the membrane was incubated in NBT/BCIP staining solution in the dark. The color reaction was stopped by washing with H₂O and TBS-T.

4.2.3 Cell culture

- Huh-7 cells, BS-C-1 and Hela cells were grown in Dulbecco's modified Eagle's medium (DMEM) supplemented with 10% fetal calf serum (FCS), penicillin (100 U/ml), streptomycin sulfate (100 µg/ml).
- Huh-T7 cells were grown in DMEM supplemented with 10% FCS, penicillin (100 U/ml), streptomycin sulfate (100 µg/ml), and Geneticin (G-418, 400 µg/µl).

4.2.4 HAV infection

70% ~ 80% confluent Huh-7 cells were washed with PBS, then inoculated for 3 h at 37°C with the soluble extract of HAV-infected cells at a multiplicity of infection (MOI) of 1 in OptiMEM (Gibco BRL, Grand Island, NY). Infected cells were incubated in DMEM containing 5 % or 10 % FCS at 37°C.

4.2.5 ELISA detection of HAV particles

Micotiter plates (Nunc-Maxisorb) were coated with 100 µl of the 7E7 antibody (diluted in carbonate buffer pH 9.6) over night at RT. The plate was washed three times with 250 µl PBS-T. The plates were blocked with PBS-T containing 1% BSA (200µl per well) by incubation for 1 h at RT. After washing with PBS-T, 100 µl antigen containing solution was added to each well and incubated for 1 h at 37°C by rocking. The sample was removed by suction and washed 3 times with PBS-T. 100 µl freshly prepared conjugate dilution (horse radish peroxides conjugated 7E7-POD-diluted 1: 20,000 in PBS-T containing 1% BSA) was added to each well and incubated for 1 h at 37 °C by rocking. The plate was washed 3 times with PBS-T and 100 µl TMB as substrate was added to each well. The plate was incubated at 37 °C for 5 - 20 min dependent on the color development of the positive control. 100 µl 1 M H₂SO₄ was added to each well to stop the color reaction and the OD was read at 450 nm.

4.2.6 Recombinant protein expression in mammalian cells with vaccinia virus-T7

The transfection mixture containing 1 µg of cDNA and 8 µl Lipofectamin (Invitrogen) in 200 µl OptiMEM was pre-incubated for 30 min at RT, diluted with OptiMEM to 1 ml and transferred to cells (5×10^5) grown in one well of a 6-well plate. After incubation for 3 h at 37°C, transfected cells were further infected with vTF7-3 diluted in 1 ml OptiMEM. After 1 h at 37°C, the inoculum was replaced by DMEM containing 10% FCS. After 24 - 48 h incubation the samples

were reclaimed in 250 μ l PBS-T. After three cycles of freeze-thawing, the clarified supernatant was used for immunoblot analysis.

4.2.7 RNA transfection

1 μ g RNA (for one well of a 6-well plate) was mixed with 3 μ l DMRIE-C in 1 ml OptiMEM and immediately added onto the cells that were washed by PBS. After incubation for 4 h, complete medium containing 10% FCS was added.

4.2.8 Luciferase assay

Firefly luciferase activity was assayed with the Luciferase Assay System (Promega). Briefly, cells were washed with PBS, and 100 μ l of Passive Lysis Buffer was added to each well of a 12-well plate (250 μ l for each well of a 6-well plate). The culture plates were placed at RT for 15 min prior to collection of the lysate. 20 μ l of each lysate was monitored for a luminescent signal in the luminometer Lucy-3 equipped with a dual injector according to the protocols supplied by the manufacturer.

4.2.9 Proteolytic cleavage assay

1 μ g purified recombinant PABP or PCBP2 and various amounts of HAV or CBV proteinases 3C (final concentration, 33.5 to 335 μ g/ml) were incubated at 37°C for 6 to 24 h in cleavage buffer (Kuyumcu-Martinez et al., 2002). The reaction was stopped by the addition of SDS-PAGE sample buffer and the products were analyzed on a 12% acrylamide gel by SDS-PAGE, followed by immunoblot with anti-3C, anti-PCBP2, anti-PABP, or anti-His antibody.

4.2.10 Preparation of the S10 cell extract

The extracts were prepared similarly as described before (Barton et al., 1996; Svitkin and Sonenberg, 2003). The cells in 18 flasks of 175 cm² at 90% confluence were each washed with 10 ml PBS and treated with 5 ml trypsin. Trypsinization was stopped by adding 10 ml DMEM-10% FCS, and the cell suspension was transferred to a 250 ml CORNING conical centrifuge tube.

1. The cells were harvested by centrifugation at 800 g, 4°C, 6 min.
2. The cells were washed 4 times by suspending them first in DMEM containing 20%FCS, two times in HNG buffer at 800 g, 6 min, last time with HNG buffer at 600 g, 8 min.
3. Cells were resuspended in 2 volumes of hypotonic buffer. The suspension was allowed to swell on ice for 15 min, before they were lysed with 15 strokes of a 7 ml Wheaton Douncer (for HeLa and BS-C-1 cells, 30 strokes). Then 1/9 volume of 10 x concentrated buffer was added.
4. The debris was spun at 11,000 g, for 20 min at 4°C. The supernatant was collected avoiding the lipid layer. The extract concentration should be > 25 A₂₆₀ U/ml for good translation.

5. 150 μ l aliquots were frozen quickly in liquid nitrogen or in dry ice and stored at -70°C .

4.2.11 Preparation of the S200 and P200 fraction

For fractionation of cells into further compartments, the S10 lysate was centrifuged at 200,000 g for 1 h with a SW 65K rotor in a Beckman ultracentrifuge. The supernatant was retained as the non-ribosome-associated fraction (S200). The pellet (P200) was resuspended in the same volume of lysis buffer. P200 contained ribosome-associated proteins and can be used to prepare the crude translation initiation factor extract (RSW) and the ribosome-enriched fraction (RIBO) as described in (Kuyumcu-Martinez et al., 2002).

4.2.12 In vitro translation in Huh-7 cell extracts

1.5 μ l micrococcal nuclease S7 (15 U/ μ l, prepared in 50 mM glycine, 5 mM calcium acetate pH 9.2) and 1.5 μ l 0.07 M CaCl_2 were added to 150 μ l S10 extract. The mixture was incubated at 20°C for 20 min and 3 μ l 0.1 M EGTA was added to the mixture to stop the S7 nuclease activity. The 50 μ l translation mixture contained 25 μ l nuclease S7 treated Huh-7 S10, 5 μ l 10 x translation mix, 5 μ l salt mix, 1 μ l 1 mM methionine, 40 U RNase inhibitor, and 1 μ g RNA. The mixture was incubated at 30°C . Aliquots were taken at different time points, and luciferase activity was tested.

In some experiment, the S10 cell extract was not treated by S7 nuclease.

5. Results

5.1 HAV infection in Huh-7 and Huh-T7 cells.

Replication of HAV in cell culture is slow and persistent and often depends on the type and origin of the host cell and its state in the cell cycle. To test whether two variants of a human liver cell line differ in their permissiveness for HAV, Huh-7 and Huh-T7 cells grown in 6-well plates were infected with the same HAV inoculum. Infection was followed by analyzing viral particles with an ELISA over a 12 day time period. In addition, infected cells were also treated with 5 mM guanidine hydrochloride (Gu-HCl) to test the inhibitory potential of this compound.

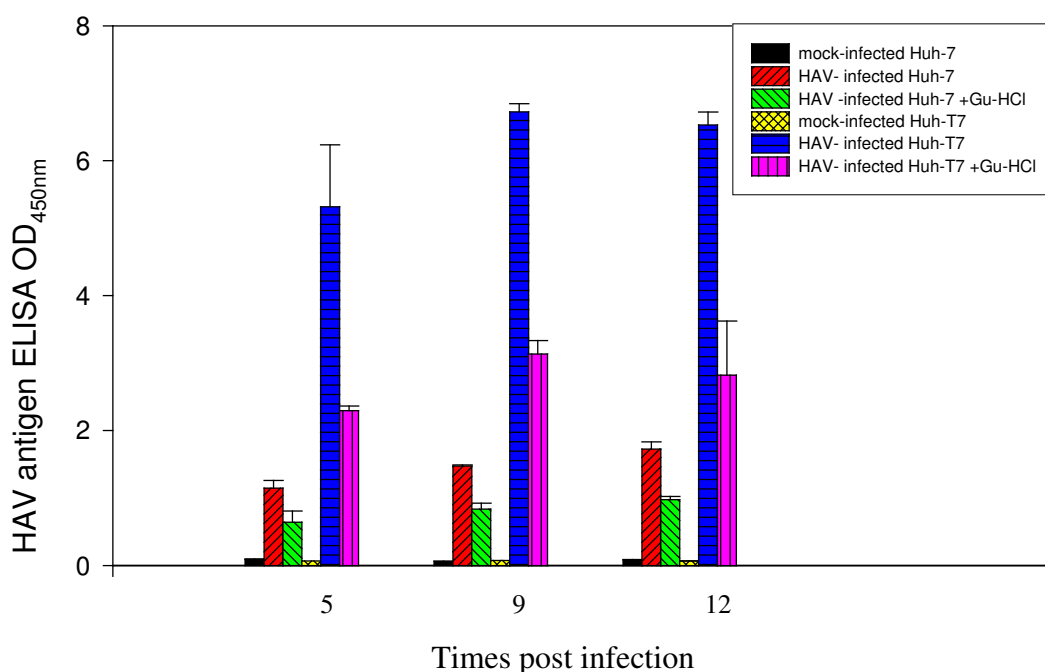


Fig. 5. HAV particle formation in infected Huh-7 and Huh-T7 cells. Mock-infected and HAV-infected Huh-7 and Huh-T7 cells were incubated in duplicate for various lengths of time in the presence and absence of Gu-HCl (5mM) and HAV antigen was measured in cell lysates.

Fig. 5 shows that HAV antigenicity accumulated over a 12 day period. It is obvious that HAV replicated much faster in Huh-T7 cells than in Huh-7 cells and produced approximately 6 times more viral antigen already 5 days post infection (pi). During the course of the asynchronous HAV replication, viral antigenicity remained always higher in Huh-T7 than in Huh-7 cell. These results suggest that either Huh-T7 cells contain factors which actively support HAV replication or that the antiviral system is more active in Huh-7 cells.

To test for the antiviral activity in both cell lines, IFN- β gene expression was determined by RT-PCR. Neither in HAV-infected nor in mock-infected cells, the IFN- β amplification products was detectable. As control, GAPDH was successfully amplified in both cell lines. These data (not shown) suggest that the HAV replication efficiency in Huh-7 and Huh-T7 cells was not affected by the antiviral activity as described by Brack (Brack et al., 2002). In both cell lines, Gu-HCl reduced viral antigenicity by approximate 50% (**Fig. 5**). However, this effect was connected with the toxic effect of Gu-HCl on the cells, rather than with specific inhibition of HAV genome replication by Gu-HCl. The protein concentration in the extracts of Gu-HCl treated cells was 2 times lower than that of untreated cells.

To find out whether the enhanced HAV growth in Huh-T7 cells is directly connected with the replication of the viral genome, the subgenomic replicons that allow to discriminate genome synthesis from the other steps of the virus life cycle were constructed and used for expression in vivo and in vitro.

5.2 HAV replicon replication

5.2.1 Replication of the HAV replicon in Huh-T7 cells

Subgenomic RNA replicons have been constructed from the genomes of several picornaviruses (such as PV, HRV and FMDV) and the hepatitis C virus (HCV) by replacing parts or all of the capsid-coding sequence with a reporter gene. The replication of the replicon was determined by quantifying the reporter gene activity over time (Yi and Lemon, 2002; Andino et al., 1993; Goodfellow et al., 2000). Following the same strategy, a similar subgenomic replicon of HAV (18f-Luc-A60) was constructed by replacing the P1 capsid sequences with the firefly luciferase gene ((Yi and Lemon, 2002; Gauss-Muller and Kusov, 2002). As a negative control, a replication-defective replicon with a frame shift mutation in the RNA polymerase (3D^{pol}) was used.

HAV replicon RNA was prepared in vitro after *Age*I-linearization of the cDNA. The replication of the HAV replicon was demonstrated by assaying the luciferase activity in Huh-T7 cells transfected with replicon RNA. As shown in **Fig. 6**, expression of both the replication-competent replicon (18f-Luc-A60, black circle) and the replication-deficient replicon (18f-Luc-A60-mut, black triangle) yielded the same curve of luciferase activity within the first 48 h post transfection (pt); luciferase activity reached a peak between 12 and 24 h pt. The 18f-Luc-A60 replicon demonstrated additional luciferase activity starting around 48h pt. In contrast, the 18f-Luc-A60-mut replicon demonstrated a steady decrease of luciferase activity after it had reached its peak

around 12 and 24 h pt. Because there was no difference of the luciferase activities produced by the replication-competent and replication-deficient replicon up to 48 h pt, this activity must be produced by translation of the input RNAs. In contrast, the increase of luciferase activity produced 48 h pt by the replication-competent replicon RNA reflected the newly synthesized RNA. The increase of luciferase activity associated with the replication-competent replicon took place much later than for the PV replicon (Herold and Andino, 2000) and with a long initial delay period (around 48 h). In contrast to PV, the HAV replicon RNA was exclusively translated within the first 24 h pt. After 24 h, translation of input RNA seemed to completely decrease, before the translation products of the newly synthesized RNA appeared. The drop in the apparent luciferase about 48 h pt, indirectly points to a complete stop of translation prior to the switch and the initiation of RNA synthesis.

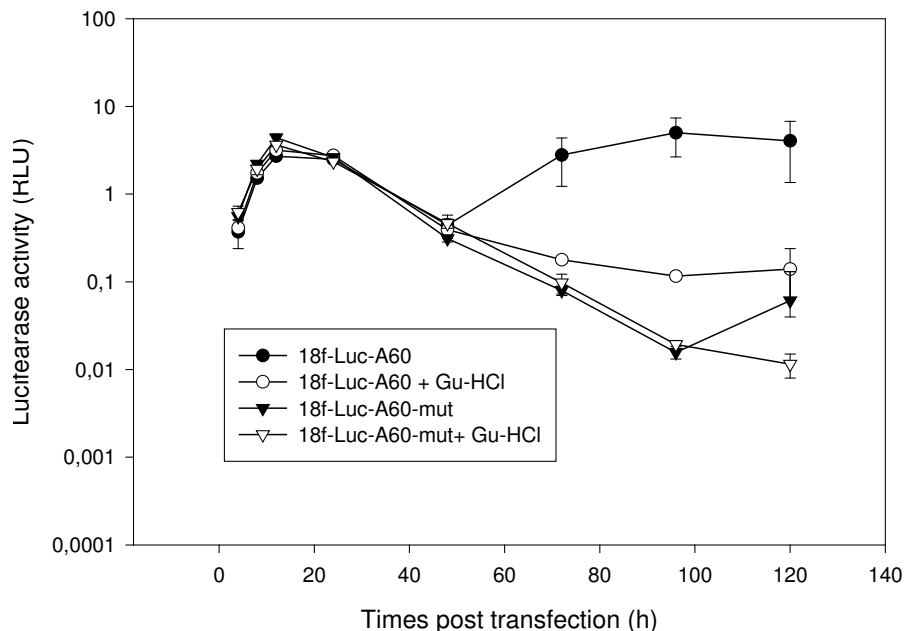


Fig. 6. HAV replicon expression in Huh-T7 cells with and without Gu-HCl (5 mM). The replication competent and incompetent HAV replicons are indicated. Replicon RNA (0.25 μ g/well) was transfected into cells in triplicate in a 24 well-plate. Cell extracts were obtained 4, 8, 12, 24, 48, 72, 96, 120 h after transfection and luciferase activity was determined.

5.2.2 Inhibition of replicon replication by guanidine hydrochloride (Gu-HCl)

Gu-HCl specifically inhibits genome replication of many picornaviruses, including HAV, but does not affect viral translation. To clearly distinguish between viral translation and genome replication, the expression of replication-competent and replication-deficient replicon RNA was performed in the presence of 5 mM Gu-HCl. As shown in **Fig. 6**, Gu-HCl specifically inhibited HAV replicon replication without affecting translation that occurred within the first 24 h pt.

Inhibition by Gu-HCl was not complete as the luciferase activity 70 to 120 h pt of the replication-competent replicon (white circles) was higher than that of the replication-deficient replicon (white triangles).

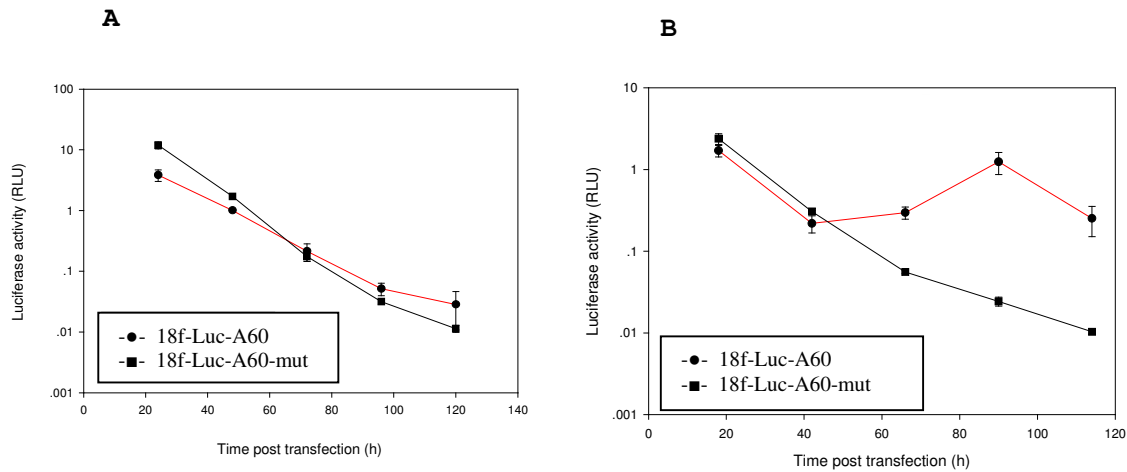


Fig. 7. Comparison of replicon replication in Huh-7 (A) and Huh-T7 cells (B). Replicon RNAs were transfected into cells and luciferase activity was determined 24, 48, 72, 96, 120 h pt.

5.2.3 Comparison of replicon replication in Huh-7 and Huh-T7 cells

Although Huh-7 and Huh-T7 have the same origin, they differ in their growth rate. Cell replication has been described to affect HAV replication (Kusov et al., 2005) and HAV infection was found to be enhanced in Huh-T7 cells (see **Fig. 5**). To test whether HAV genome replication was specifically enhanced in Huh-T7 cells, Huh-7 and Huh-T7 cells were compared for their ability to support replication of the HAV replicon. The same amounts of the active and inactive replicon RNA were transfected into Huh-7 and Huh-T7 cells and luciferase activity was determined at different time points pt (**Fig. 7 A and B**). In both cells, translation of input RNA as determined by luciferase activity was maximal 24 h pt with a subsequent decrease for the inactive replicon. Whereas in Huh-7 all the luciferase activity was steadily decreasing after 24 h pt (**Fig. 7 A**), the reporter gene activity of the replication-competent replicon reached a second maximum 90 h pt in Huh-T7 cells (**Fig. 7 B**). The data indicate that replication of the HAV replicon was more efficient in Huh-T7 as compared to Huh-7 cells. The dependence of the HAV replicon on the cell culture system was reported before (Yi and Lemon, 2002). Although RNA replication as determined by the reporter gene activity seemed to be very low in Huh-7 cells, replication competence of the active HAV replicon in Huh-7 cells was clearly shown earlier by genetic recombinant in vivo (Gauss-Muller and Kusov, 2002; Kusov 2005). It can be assumed

that due to their more active metabolism, Huh-T7 cells more efficiently support HAV replication (see below).

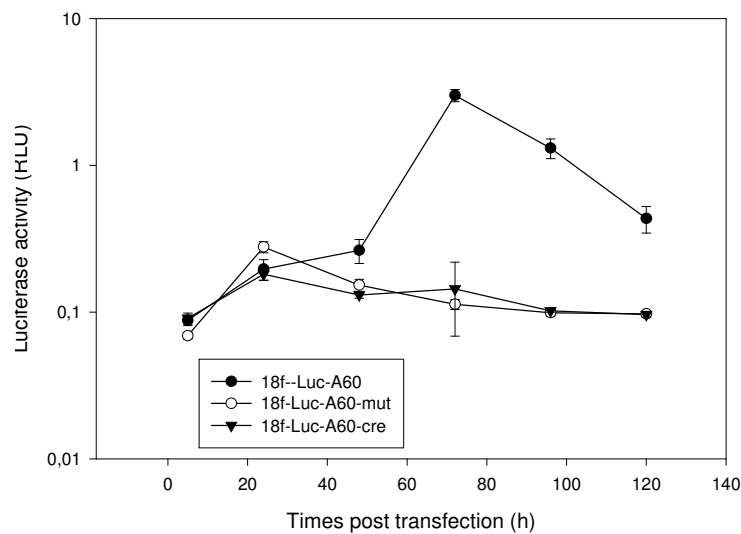


Fig. 8. Luciferase activity of the HAV replicon carrying mutations in the putative CRE. Huh-T7 cells were transfected with synthetic RNA of the wild-type and *CRE*-mutated replicons and luciferase activity was determined 5, 24, 48, 72, 96, 120 h pt.

5.2.4 Analysis of the putative HAV CRE by studying replication of the mutated replicon

After demonstration that the HAV genome is self-replicating in the absence of the P1 sequences, we concluded that a intragenomic *cis*-acting replication element (CRE) is not present within P1 region. Based on sequence alignments and comparison with CRE's of other picornaviruses, a putative element was spotted at nucleotide position around 6,000 (Dr. D. Evans, personal communication). The picornaviral CRE is a small RNA hairpin structure with widely different nucleotide sequences except for a conserved AAACA motif in the loop. The putative HAV CRE was mutated in the replicon by introducing eight silent mutations that disrupted the RNA secondary structure but retained the amino acid sequence. Replication competence of the wild type and CRE-mutated replicon was determined by transfection RNA transcripts into Huh-T7 cells. Cell extracts were obtained at various time points pt and luciferase activity was determined. As clearly shown in **Fig. 8**, the mutation of the CRE demolished the replication ability of the HAV replicon. The expression kinetic of the CRE mutant showed a similar luciferase profile as a replication-deficient replicon carrying a frame-shift mutation in 3D. Compared with **Fig. 7**, the luciferase kinetic of **Fig. 8** confirms that after a drop of activity 24 h pt, new luciferase expression was initiated from newly synthesized RNA 48 pt. This again indicates that after translation of input HAV RNA switching to RNA synthesis is delayed.

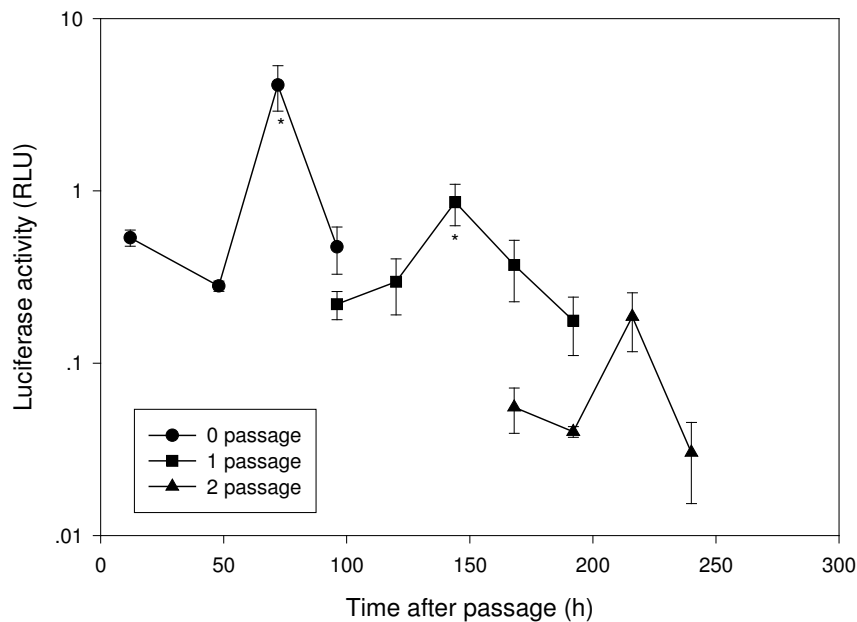


Fig. 9. Replicon replication in HuhT7 cells after cell passage. Cells transfected with the active HAV replicon were passaged at the time points indicated by asterisk.

5.2.5 Analysis HAV replicon expression during cell passage

Although belonging to different viral families, not only HAV, but also HCV and HBV initiate a persistent infection in cell culture. A HCV replicon carrying the neomycin resistance gene in place of the structural proteins was shown to be persistent in transfected Huh-7 cells under the appropriate selection pressure (Lohmann et al., 1999). To test whether also the HAV replicon can be persistent in Huh-T7 cells and autonomously replicate during cell passage, Huh-T7 cells in a 24-well plate were transfected with HAV replicon RNA and the cells were passaged in a 1:4 ratio. For this, replicon-transfected cells of 6 wells were suspended by trypsinization, combined, and distributed into new 24 wells 72 h after RNA transfection or cell passage. Cell extracts were prepared every 24 h after cell passage and luciferase activity was determined. As depicted in **Fig. 9**, luciferase activity produced from the transfected RNA reached the peak around 80 h pt (black circles). Transfected cells passaged at this time point (marked by asterisk) and continued to grow until 200 h expressed lower amounts of luciferase (black squares). However, after this first passage the luciferase activity peaked around 150 h pt and 70 h after cell passage indicating that the replicon RNA had been amplified. After a second passage of the transfected cells harvested 140 h pt, a peak of luciferase activity was detected 220 h pt and 70 h after passage. Although overall luciferase activity levels decreased during the two cell passages, luciferase activity peaked approximately 70 h after each cell passage indicating that the replicon RNA was retained

in the transfected cells and was actively replicating with a concomitant increase of luciferase activity. No increase of luciferase activity was observed when replication-deficient replicon RNA was used for transfection and cell passage in the same way (data not shown). It is reasonable to assume that the reduction in luciferase level is due to preferential growth of replicon RNA-free cells as compared to transfected cells

5.2.6 Insertion of a *cis*-active hammerhead ribozyme into the HAV cDNA at the 5'end of the viral genome

A typical feature of the 5'end of the picornaviral RNA genome are two uridine residues and the ability of the first 100 nucleotides to form a stable CL structure that is required as a *cis*-acting replication element for both plus and minus strand RNA synthesis. It has been assumed that nonviral nucleotides at the 5'end added during *in vitro* transcription might destabilize this structure and thus decrease replication efficiency of the synthetic transcripts. For the PV replicon, it was shown that the correct 5'end produced by a ribozyme is necessary for efficient genome replication (Herold and Andino, 2000). In order to test the importance of a precise 5'end for efficient HAV replication, the sequence of a *cis*-active hammerhead ribozyme was cloned between the T7 RNA polymerase promoter and the first HAV nucleotide at the 5'-terminus of the viral genome following the strategy described by (Herold and Andino, 2000). The oligonucleotide and the cloning procedure are described in Material and Methods. Both the full-length HAV cDNA (pT7-18f) and the luciferase-expressing HAV replicon cDNA (pT7-18f-Luc-A60) was supplemented with the ribozyme resulting in the plasmids pGEM-rib (+)-18f-A60, respectively and pGEM-rib(+)-18f-Luc-A60. As control, constructs were prepared encoding an inactive ribozyme by replacing the essential cytosine at position -1 of the hammerhead ribozyme by a guanosine residue. **Fig. 10 A** shows the ribozyme structure at the 5'end of the HAV genome. The first 8 viral nucleotides (depicted in blue) anneal with the nucleotides of the ribozyme structure marked in red. Annealing of the HAV 5'nucleotides with the ribozyme nucleotides thus competes with hybridization in the 5'CL (see **Fig. 3**). **Fig. 10, B** depicts the replicon RNA transcribed from pGEM-rib(+/-)-18f-Luc-A60 and pGEM-rib(+/-)-18f- A60.

5.2.7 Replication of ribozyme-containing HAV transcripts

To assess the role of the correct HAV 5'end, synthetic transcripts of the full-length viral genome were produced using the *Age*I-linearized plasmids pT7-18f-A60, pGEM2-rib(+)-18f-A60, and pGEM2-rib(-)-18f-A60. Equal amounts of transcripts were transfected into Huh-T7 cells and cell extracts prepared after various time periods. Viral replication was determined with the particle-

specific 7E7-ELISA. As shown in **Fig. 11**, RNA 18f-A60 (containing 14 nonviral nucleotides downstream of two guanines at its 5'end), RNA rib(-)-18f-A60 (containing 52 additional nucleotides at its 5'end) and RNA rib(+)-18f-A60 (containing a correct 5'end starting with UUCAAGAGG...), replicated at approximately the same rate, with RNA 18f-A60 being the most rapid. This result suggests that the overall infectivity of synthetic RNA is not significantly affected by nonviral nucleotides at the 5'end.

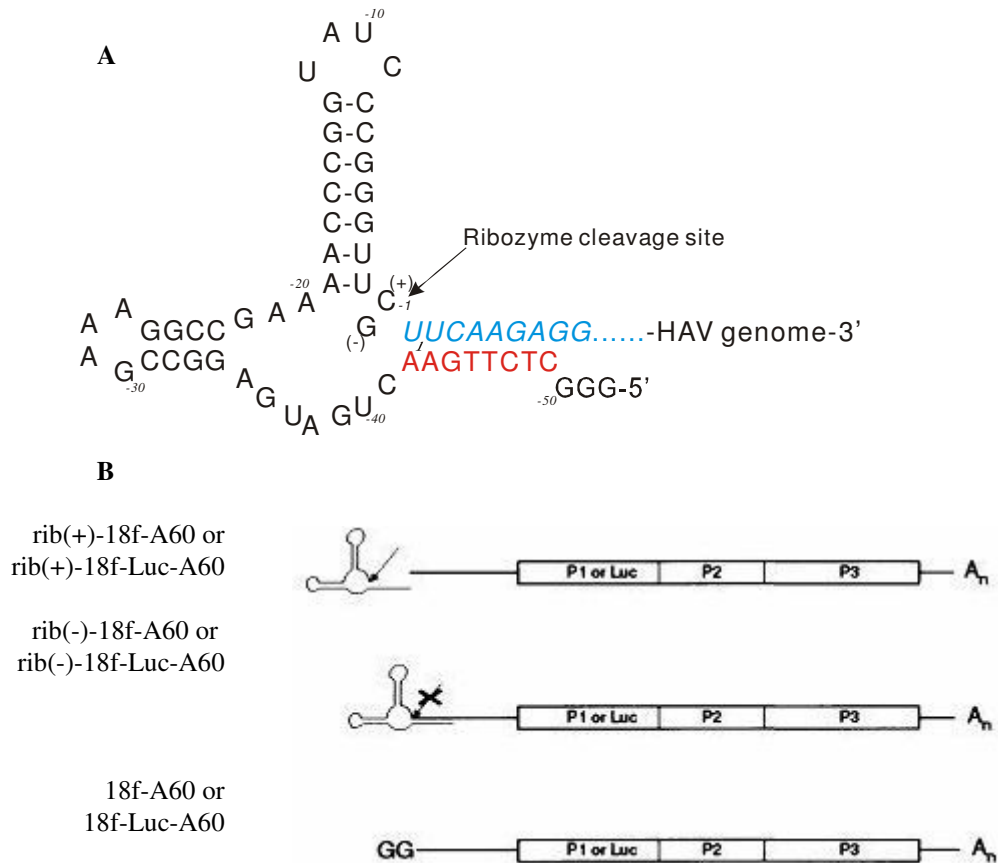


Fig. 10. HAV-specific *cis*-acting hammerhead ribozyme at the 5'end of the genome. (A) Predicted secondary structure of the *cis*-active hammerhead ribozyme attached to the 5'end of the HAV genome and replicon. HAV sequences are in italic. The first nucleotide U of HAV is referred to as 1. The active ribozyme contains a cytosine at position -1; the inactive form has a guanosine. (B) Scheme of the HAV RNA genome and replicon with and without the ribozyme(+/-). Constructs containing an active ribozyme at the 5'end are referred to as rib (+) and inactive ribozyme are referred to as rib (-).

This result on RNA infectivity contrasts with observations obtained with ribozyme-containing PV replicon that had enhanced replication ability (Herold and Andino, 2000). To test whether the effect of precise 5'end can be better evidenced using the HAV replicon, ribozyme-containing HAV replicon RNA was transfected into Huh-T7 cells and the luciferase activity was determined over 100 h. As shown in **Fig. 12**, only RNAs 18f-Luc-A60 and rib(+)-18f-Luc-A60 produced a

second peak of luciferase activity approx. >70h pt, whereas the luciferase activity of RNA rib(-)-18f-Luc-A60 decrease starting 24 h pt. The luciferase profile of RNA rib(-)-18f-Luc-A60 was similar to the replication-deficient replicon shown in **Fig. 6** and **Fig. 8**. Based on these data, it seems that the 5' ribozyme has little or no effect on the HAV replication efficiency. Possible secondary structures formed at the 5' end of the synthetic RNAs will be discussed below.

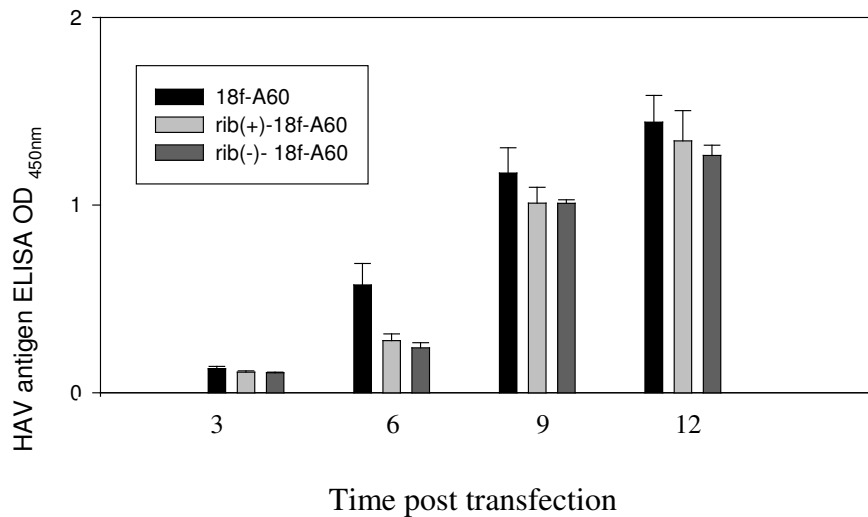


Fig. 11. Particle formation of HAV full-length RNA transcripts with and without a 5'terminal ribozyme. Synthetic RNAs 18f-A60, rib(+)-18f-A60 and rib(-)-18f-A60 were transfected into Huh-T7 cells and viral particles were determined at the indicated time points with the 7E7 ELISA.

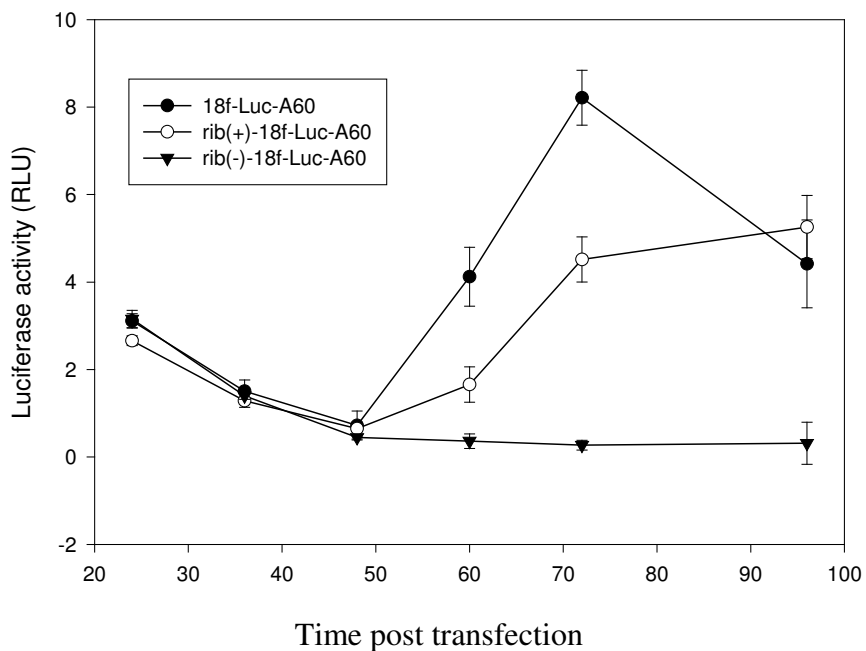


Fig. 12. Luciferase activity of the HAV replicon with and without the ribozyme. Huh-T7 cells were transfected with RNAs 18f-Luc-A60, rib(+)-18f-Luc-A60, and rib(-)-18f-Luc-A60 and luciferase activity was determined 24, 36, 48, 60, 72, 96 h pt.

5.3 HAV replicon translation in Huh-7 S10 extract in vitro

5.3.1 HAV replicon translation in Huh-7 S10 extracts

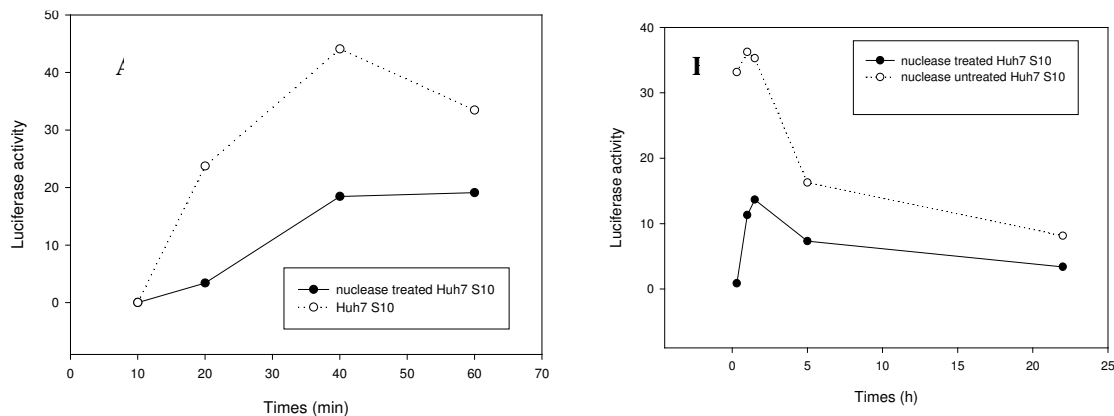


Fig. 13. HAV replicon expression in a Huh-7 S10 extract in short time (A) and long time (B) kinetics. Nuclease treated and untreated Huh-7 S10 extracts are compared. 1 μ g HAV RNA was used in a 50 μ l translation/replication mixture. The luciferase activity was measured at the indicated time points.

In recent years cell-free systems have been employed to understand in detail the role of host and viral factors on viral protein and RNA synthesis. After optimizing the preparation of cell extracts, it was possible to produce infectious PV starting from synthetic or viral RNA outside a living cell (Molla, 1991). In order to study the molecular mechanisms of HAV genome translation and replication and the role of host proteins, a cell-free mammalian expression system was established. For viral genome expression, translation and replication was compared by testing the reporter gene activity of the active and inactive HAV replicon in nuclease-treated and untreated extracts prepared from Huh-7 or Huh-T7 cells. S10 extracts were prepared following the protocol described by Svitkin for EMCV virus (Svitkin and Sonenberg, 2003). Synthetic HAV replicon RNA (1 μ g) derived from the linearized plasmid pT7-18f-Luc-A60 was incubated for various lengths of time in the S10 extract of Huh-7 cells and luciferase activity was determined (**Fig. 13**). The expression of the HAV replicon RNA reached its peak around 1 h, then the luciferase activity decreased steadily. The untreated extract supported HAV replicon expression more efficiently than the nuclease-treated extract (**Fig. 13**). The same result was obtained when the S10 extract of HeLa and Huh-T7 cells was used (not shown), confirming the earlier

observation that micrococcal nuclease treatment led to a profound loss of translation activity (Bergamini et al., 2000).

To differentiate between genome translation and replication, the expression kinetics of the active and inactive HAV and PV replicon in the cell-free extract was compared next. Synthetic RNAs prepared from linearized HAV and PV replicon plasmids (pT7-18-Luc-A60 and pRLuc31) were incubated with the S10 extract of Huh-T7 cells.

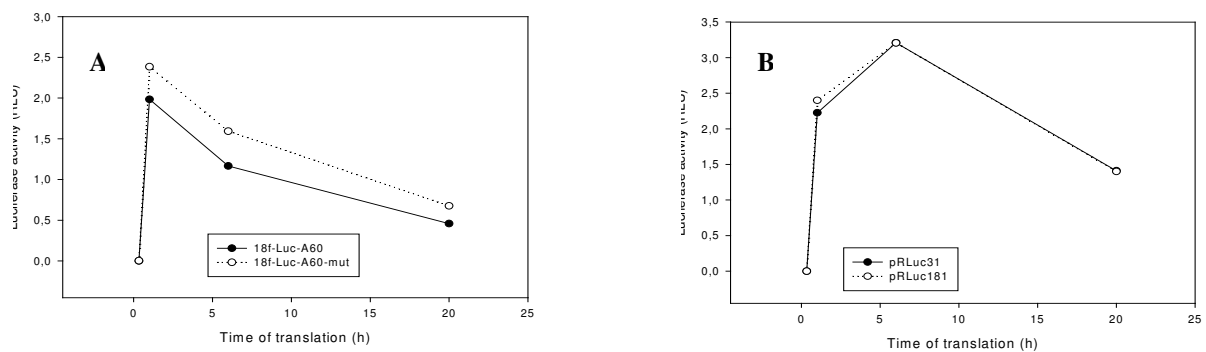


Fig. 14. Translation comparison of the HAV replicon (A) and the PV replicon RNA (B) in the Huh-T7 S10 extract. Luciferase activity was determined at 0, 1, 5 and 20 h pt.

As shown in **Fig. 14**, the luciferase activity produced by both the HAV and the PV RNAs reached similar levels suggesting that translation efficiency of the HAV and PV RNA was very similar in this system. Since also no difference between the expression pattern of the active and inactive PV and HAV replicons was detectable, it can be concluded that this cell extract was deficient in supporting RNA replication. Other extracts were tested for the ability to allow PV genome replication. However, none was found that showed higher levels of luciferase activity produced from the active PV replicon as compared to the inactive replicon. Collectively, the data suggest that neither PV nor HAV RNA replication was supported in S10 extracts of human liver cells under the conditions described here. Further experiments will be required to find conditions that allow HAV genome replication in vitro. Taken together the data described in 5.1 to 5.3, various in vivo systems clearly show the replication activity of the HAV genome, however in vitro replication could not be detected.

5.4 Protein-RNA interaction determined by electrophoretic mobility shift assay (EMSA)

5.4.1 PABP binding to the HAV 3'NTR is dependent of the poly (A) tail

For viral genome translation and replication, various host proteins are required, yet their detailed role has not been assessed. PABP binding to a homopolymeric poly (A) tail is dependent on its length with a minimal tail of 12 adenosine residues being required for efficient binding. In order to test whether PABP binding to the HAV 3'NTR is similarly dependent on the poly (A) tail length, RNA protein interaction was assessed by EMSA using the HAV 3'NTR followed by poly (A) tails of variable length. **Fig. 15** clearly shows that PABP bound to the HAV poly (A) tail, as the RNA mobility was shifted in the presence of PABP only when a poly (A) was present. PABP binding affinity increased with the length of the poly (A) tail. Whereas 50 nM PABP only shifted appropriate 50% of the RNA with 20 adenosine residues, almost 100% of the RNA with 60 residues was shifted (compare **Fig. 15**, lanes 6 and 11). PABP did not interact with the tailless 3'NTR (**Fig. 15**, lanes 2 to 4). Since PABP binding to the HAV poly (A) tail in vitro is similar to that of host cell mRNA, it is likely that PABP plays a similar role in HAV translation as it does in host mRNA translation. Furthermore based on studies of Kusov et al (2005) and Herold (Herold and Andino, 2001), it is assumed that the HAV poly (A) tail is a *cis*-acting element in viral RNA replication and particularly involved in minus-strand synthesis.

PABP has been shown to be involved in the circularization of host mRNA and of PV RNA (Herold and Andino, 2001), thus ensuring the cross-talk between the 5' and 3' ends of the RNA and efficient recycling of ribosomes. In order to test whether PABP directly interacted with the HAV 5' cloverleaf (CL), synthetic radio-labeled RNA representing the first 150 nucleotides was incubated with increasing amounts of PABP and RNA protein interaction was analyzed by EMSA. As **Fig. 16** shows, PABP did not directly bind to the HAV 5'CL at concentrations that otherwise (see **Fig. 15**) bound to the HAV poly (A) tail. Neither the amount of free RNA was reduced in the presence of PABP, nor was a RNA-protein complex with decreased mobility observed.

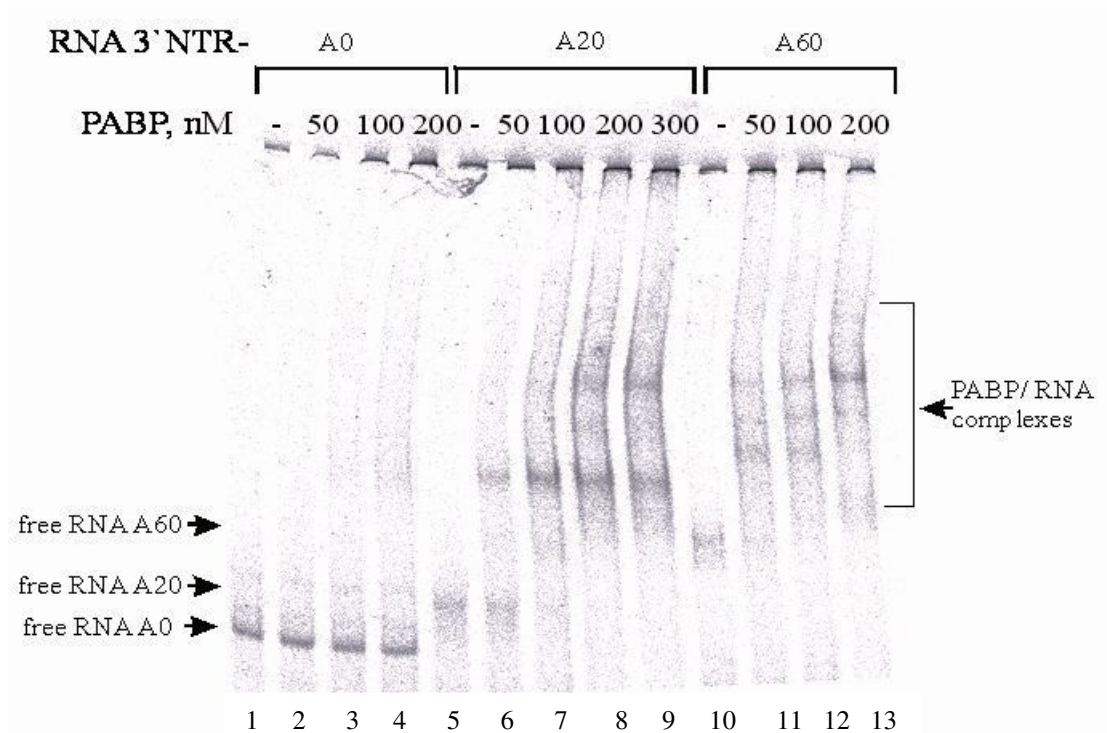


Fig. 15. PABP binds to the poly (A) tail of the HAV 3'NTR. Lanes 1, 5 and 10 show the mobility of free 3'-NTR with poly (A) tails of different lengths, their positions are indicated by arrows. The different concentrations of PABP are indicated on the top of the figure.

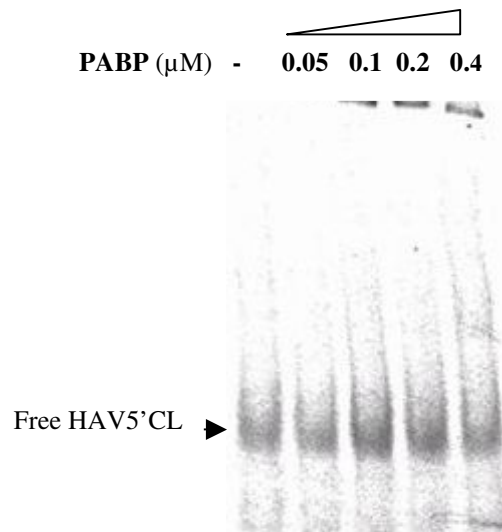


Fig. 16. PABP does not interact with the HAV 5'CL. Free RNA of the HAV 5'CL migrated as indicated by the arrow. The PABP concentration is shown at the top of the figure.

5.4.2 PCBP2 directly binds to the HAV 5'CL

Since PABP did not directly bind to the HAV 5'CL, the assumed HAV RNA circularization might involve other host or viral proteins. In PV, it was demonstrated that PCBP2 forms a

ternary complex with the 5'-terminal sequences of PV RNA and the viral 3CD. We first tested whether PCBP2 can interact with the HAV 5'CL by EMSA.

As obvious by the shift of mobility (**Fig. 17**, lanes 3 to 5), PCBP2 directly interacted with the HAV 5'CL in a concentration-dependent manner, thus confirming an earlier report (Graff et al., 1998).

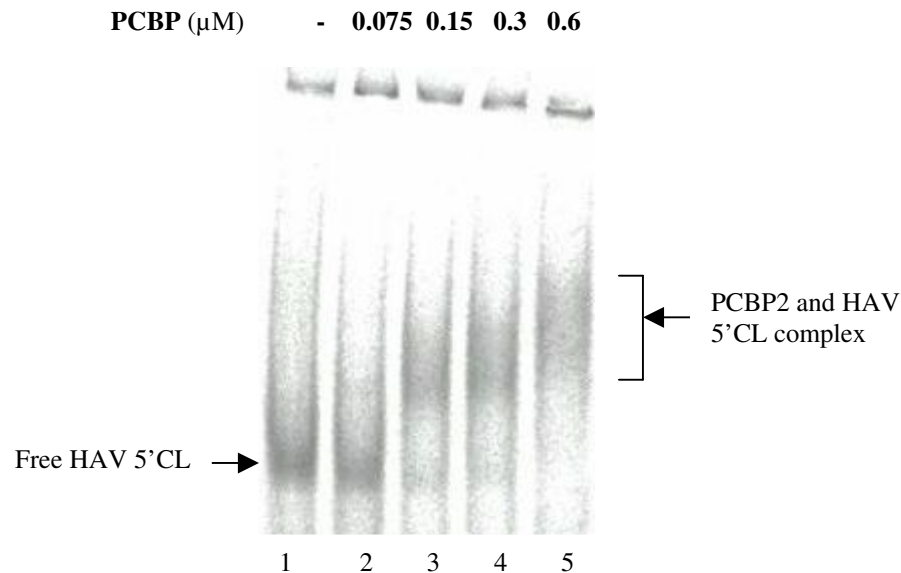


Fig. 17. PCBP2 directly interacts with the HAV 5'CL. The amount of PCBP2 is indicated on the top of the figure. The mobility of free HAV 5'CL and the RNA-protein complex is indicated by arrows.

5.4.3 Complex formation of PABP and PCBP at the HAV 5'CL

RNA circularization by a protein bridge was shown for host mRNA with a concomitant positive effect on translation (Wells et al., 1998). For PV RNA, genome circularization over a protein bridge that included PABP appeared to enhance viral RNA synthesis (Herold and Andino, 2001). In order to test whether the HAV RNA might also be circularized through a protein bridge, the interaction of the HAV 5'CL with PABP and PCBP was determined. Radio-labeled HAV 5'CL RNA was simultaneously incubated with PABP and limiting amounts of PCBP that were not sufficient by themselves to induce a complete shift of RNA mobility. As shown in **Fig. 18**, lane 3, PCBP induced an incomplete mobility shift and PABP alone did not interact with the RNA as no shift was observed (lane 4). However, the mobility of the PCBP-RNA complex was significantly enhanced, when PABP was added to the mixture (lane 2).

PABP(μ M)	-	0.23	-	0.23
PCBP(μ M)	-	0.1	0.1	-

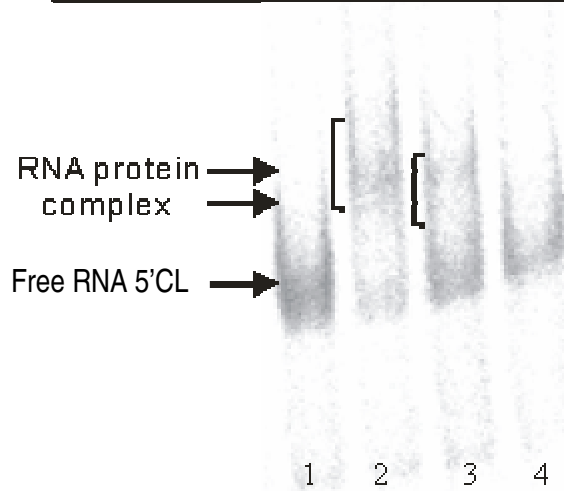


Fig. 18. PABP enhanced PCBP interaction with the HAV 5'CL. Radio-labeled RNA was incubated for 20 min with PCBP and PABP, before the mobility was analyzed on a 5 % gel.

The observation that PABP enhanced PCBP-RNA complex formation was confirmed by another experiment where increasing concentrations of PABP were incubated with the complex of the HAV 5'CL with PCBP (**Fig. 19**). In this experiment, again small amounts of PCBP were used for complex formation, in order to demonstrate changes.

PABP(μ M)	0.01	0.03	0.06	0.12	0.2	-
PCBP(μ M)	0.05	0.05	0.05	0.05	0.05	-

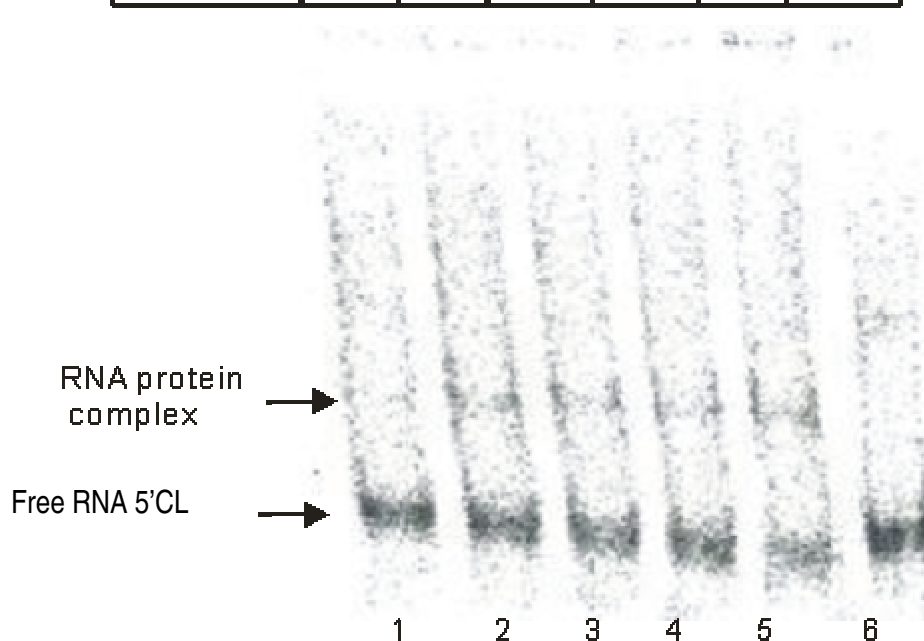


Fig. 19. PABP enhanced PCBP interaction with the HAV 5'CL. Increasing amounts of PABP were incubated with limiting amounts of PCBP and radio-labeled RNA. In the last lane no protein was added.

As obvious from the loss of free RNA and the increase of complexed RNA, PABP enhanced complex formation of PCBP with the HAV 5'CL.

5.4.4 HAV 3C enhances the interaction of PCBP with the 5'CL interaction

For HAV 3C specific, yet weak interaction with the HAV CL was reported ((Kusov and Gauss-Muller, 1997; Peters et al., 2005; Zell, unpublished observation). To test whether 3C might affect the PCBP-CL interaction, radio-labeled RNA was incubated with 3C and low amounts of PCBP which can not shift 5'CL, alone or in combination, as show in **Fig. 20**. None of the proteins alone induced a shift of the RNA mobility (lanes 2 and 4), however when incubated together significantly more RNA was shifted as obvious from the loss of free RNA (lanes 3). This suggests that either the RNA folding was altered in the presence of both proteins such that the RNA could interact, or that the proteins together had an altered conformation that improved their RNA interaction ability, although not shifted band was visible.

Taken together the data suggest that multiple protein binding at the HAV 5'CL might facilitate RNA circularization which might be essential for efficient translation and/or genome replication.

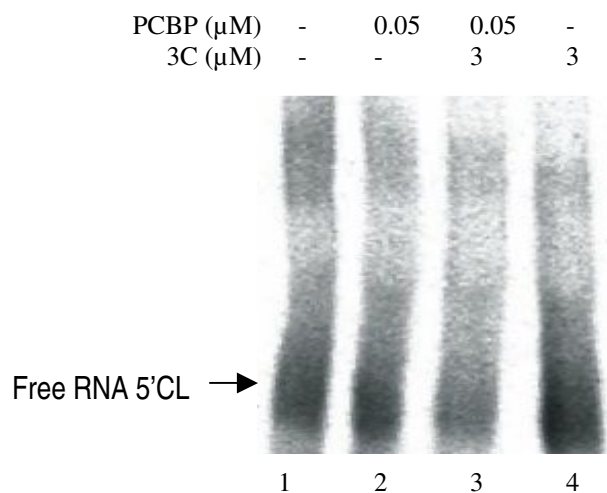


Fig. 20. The mobility of the HAV 5'CL is altered in the presence of PCBP together with 3C. Radio-labeled RNA was incubated for 20 min with PCBP (lanes 2 and 3) and with or without 3C (3 μ M).

5.5 Host protein cleavage

5.5.1 PABP cleavage by HAV 3C

5.5.1.1 PABP cleavage by viral proteinase 3C in vitro

PABP has been shown to be essential for translation of cellular mRNAs (Michel et al., 2001).

Experimental evidence has also accumulated that PABP cleavage by picornaviral 3C might inhibit host cell translation and therefore contribute to the host cell shut-off observed during picornaviral replication (Joachims et al., 1999; Kuyumcu-Martinez et al., 2002; Kuyumcu-Martinez et al., 2004). To assess the role of PABP during HAV infection, we investigated whether HAV 3C can cleave PABP in vitro and in vivo. First, the capability of HAV 3C to cleave PABP in vitro was tested.

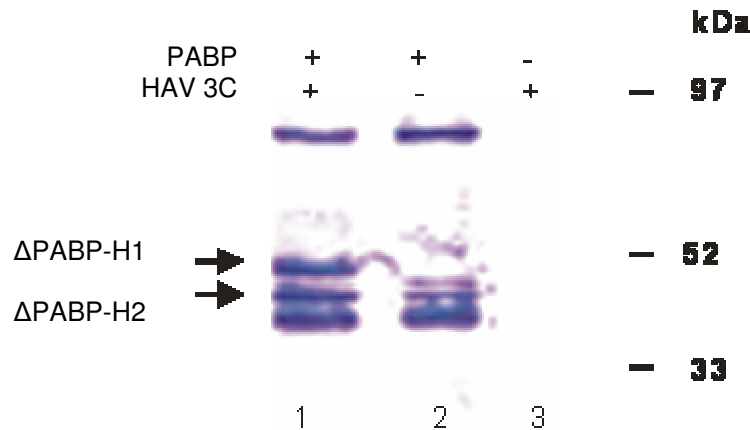


Fig. 21. Cleavage of purified recombinant PABP by HAV 3C. PABP and its two N-terminal cleavage products (Δ PABP-H1 and Δ PABP-H2) were detected by anti-His and indicated by arrows. Protein markers are indicated on the right.

In vitro cleavage assays were performed with purified recombinant PABP as substrate and purified recombinant HAV 3C as enzyme (1.34 μ g). After incubation at 37°C for 6 h, the products were analyzed by immunoblot with anti-His. As shown in **Fig. 21** lane 1, two His-tagged polypeptides (Δ PABP-H1, Δ PABP-H2) were produced by 3C. Lane 2 shows the polypeptide pattern of complete PABP (70 kDa) and some degradation products. Since the His-tag is located at the N-terminus of PABP, the cleavage products detected present the N-terminal domain. As no complete PABP cleavage by HAV 3C was achieved under the described condition above, PABP was next incubated for 24 h with increasing amounts of purified recombinant HAV 3C (**Fig. 22**). Clearly, at the highest 3C concentration, PABP was almost completely cleaved indicating that PABP cleavage was dependent on the HAV 3C concentration (**Fig. 22**, lane 2). Δ PABP-H1 seemed to be the preferred cleavage product because it was the prominent cleavage product at low concentrations of HAV 3C. Δ PABP-H1 and Δ PABP-H2 are collinear, as they are both recognized through their N-terminal His-tag. As determined in a kinetic experiment, long incubation periods were required for complete PABP cleavage (data not shown).

After having demonstrated that HAV 3C can cleave recombinant PABP in vitro, we tested whether HAV 3C can cleave endogenous PABP that is an abundant cytoplasmic protein. For this, the soluble fraction S10 of Huh-7 cells was prepared and used as 3C cleavage substrate. After in vitro incubation with 6.7 μg 3C in a 20 μl reaction mixture for 24 h, the cleavage products were analyzed by immunoblot with an anti-PABP polyclonal antibody. **Fig. 23** shows that $\Delta\text{PABP-H1}$ and $\Delta\text{PABP-H2}$ were the products of 3C in vitro cleavage.

For PV it was demonstrated that initiation factor- and ribosome-associated PABP (RSW, and RIBO) was specifically targeted by PV 3C in vitro, whereas non-ribosome-associated PABP (present in the S200 fraction) was resistant to PV 3C cleavage (Kuyumcu-Martinez et al., 2002). To test whether HAV 3C shows a preference for the various forms of PABP, the S200 and P200 fractions were incubated for 24 h with purified recombinant HAV 3C. As show in **Fig. 23**, PABP in the S200 (lane 3) and P200 (lane 5) fractions were both cleaved, suggesting that 3C can cleave ribosome-associated as well as non-ribosome associated PABP.

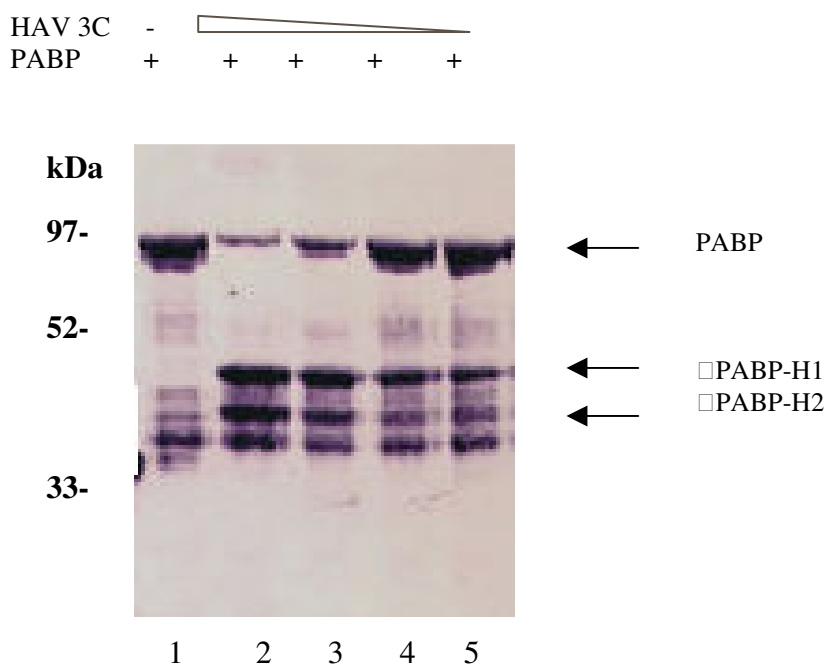


Fig. 22. Concentration dependence of PABP cleavage by HAV 3C. From lanes 2 to 5, the amount HAV 3C was 335, 167.5, 70, 33.5 $\mu\text{g}/\text{ml}$, respectively. The cleavage products were detected by anti-His and indicated by arrows. The molecular mass of protein standards are shown on the left.

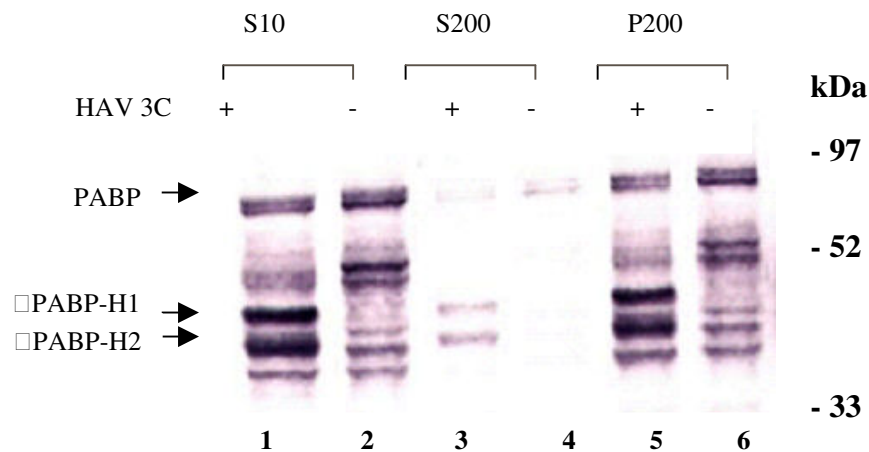


Fig. 23. Cleavage of endogenous PABP by HAV 3C in vitro. The indicated cell fractions were incubated with (+) and without (-) HAV 3C (160 $\mu\text{g/ml}$) for 6h. PABP and its cleavage products were detected by anti-PABP and are indicated by arrows. The molecular mass of protein standards are shown on the right.

5.5.1.2 PABP cleavage by viral proteinase 3C in vivo

After demonstration that PABP can be cleaved by HAV 3C in vitro, we next tested PABP cleavage in vivo. In order to produce large amounts of the viral proteinase and PABP in the same cell, both pGEM-3C and pET28-PABP were co-expressed in COS7 cells with the help of the recombinant vaccinia virus vTF7-3. In this transient expression system, the T7 RNA polymerase expressed by vaccinia virus transcribes the genes that are placed under the T7 promoter. Since the 3C precursor polypeptide 3ABC is also proteolytically active, yet with a different substrate specificity than mature 3C (Kusov and Gauss-Muller, 1999), this 3C precursor was also expressed in its active (pET15b-3ABC, pET15b-3ABCmut6) and inactive (pET15b-3ABC μ) form. As 3ABCwt is autoproteolytically active producing 3C and 3BC (Probst et al., 1998), its substrate specificity was compared with 3ABCmut6 that carries mutations at both the 3A/3B and 3B/3C cleavage sites and that has lost its autoproteolytic capacity. 3ABC μ carries a mutation (C172A) at the active site resulting in the loss of its proteolytic activity. All 3ABC constructs contain an N-terminal His-tag and were thus detectable along with PABP carrying an N-terminal His-tag in the same blot (**Fig. 24**, lanes 1 to 3, indicated by arrows).

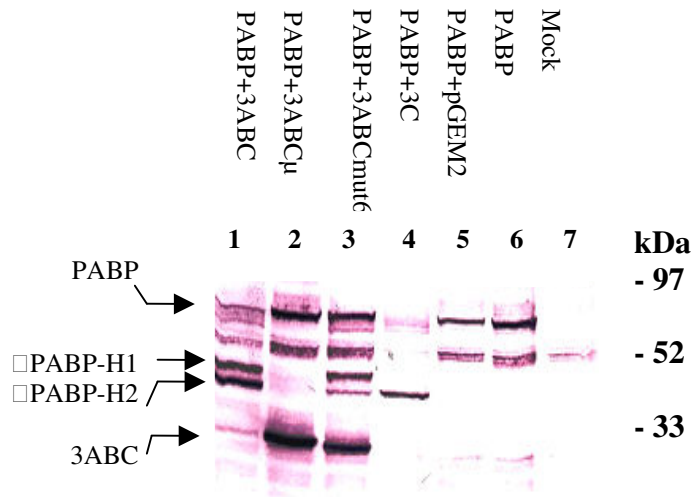


Fig. 24. Recombinant PABP cleavage by 3C and its precursors in vivo. As indicated above the lanes, PABP and various forms of HAV 3C were co-expressed for around 24 h with the help of vTF7-3. The cleavage products and 3ABC were detected by anti-His and are marked on the left.

Owing to its autoproteolytic activity, lower amounts of 3ABC were found than either 3ABC μ (lane 2) or 3ABCmut6 (lane 3). The autoproteolytic activity of 3ABCwt was obvious in an anti-3C immunoblot (**Fig. 29, C**). **Fig. 24** shows that under the experimental conditions used, 3C (lane 4) exclusively produced Δ PABP-H2, whereas 3ABCmut6 (lane 3) predominantly produced Δ PABP-H1. As expression of 3ABCwt (lane 1) resulted in a mixture of 3C, 3BC, 3ABC, co-expression with PABP showed the cleavage products specific for both 3ABCmut6 and 3C. Interestingly the cleavage pattern produced by 3ABCwt in vivo was similar to the pattern produced by 3C in vitro using purified PABP (see **Fig. 22**). PABP cleavage by 3C was more complete than that of 3ABCwt and 3ABCmut6. The observation that Δ PABP-H2 is the product of complete 3C cleavage suggests that Δ PABP-H1 and Δ PABP-H2 are a nested set of products with a collinear His-tagged N-terminus (see below **Fig. 36** for a model of the HAV 3C cleavage sites in PABP). As negative control, 3ABC μ was co-expressed with PABP resulting in no PABP cleavage (lane 2). In order to exclude that Δ PABP-H1 and Δ PABP-H2 were cleavage products of recombinant vaccinia virus, PABP was expressed alone and with vector pGEM2 with the help of vTF7-3. No cleavage products (lanes 5 and 6) were detected, clearly indicating that Δ PABP-H1 and Δ PABP-H2 are the specific products of 3C and 3ABC. Taken together, the data indicate that dependent on their activity two cleavage sites with PABP were the target of 3C and its precursor (see model below).

5.5.1.3 PABP cleavage in HAV-infected cells

After we had demonstrated that recombinant PABP can be cleaved by HAV 3C *in vivo* and *in vitro*, cleavage of endogenous PABP in HAV-infected cells was determined next. Huh-7 cells were infected with HAV and analyzed for viral particle formation by ELISA and for PABP cleavage by immunoblot with anti-PABP. HAV-infected and mock-infected Huh-7 cells were harvested at different time points post infection (pi). As clearly indicated by the increase in the ELISA signal, the inoculated virus was actively replicating in the cells (**Fig. 25 B**). No morphological alterations were obvious in the infected cells at any time point (data not shown). As shown in **Fig. 25 A** a PABP cleavage product of approx. 43 kDa (Δ PABP-H1) appeared 9 days after HAV infection. The amount of the PABP cleavage product (Δ PABP-H1) did not significantly increase after viral replication had almost reached saturation levels (here approximately 9 days pi) and comprised about 1 ~ 2% of the total content of PABP, indicating that only a small portion of PABP served as substrate of HAV 3C during infection. As a protein co-migrates at the same position of Δ PABP-H2 in the mock-infected cells, it remained uncertain whether Δ PABP-H2 was formed in HAV-infected cells. Taken together, the data show that PABP served as substrate for HAV 3C *in vivo* and *in vitro*.

5.5.1.4 PABP cleavage specificity of HAV and CVB 3C

In order to demonstrate that PABP cleavage by HAV 3C was specific, *in vitro* cleavage assays were performed with crude S10 extracts of BS-C-1, Huh-7 and Hela cells as substrate and HAV and coxsackievirus B3 (CVB) 3C as enzymes (using 1.34 μ g and 1 μ g 3C, respectively). After incubation at 37°C for 6 h, the products were analyzed by immunoblot with anti-PABP. As **Fig. 26**, lane 5 shows, a prominent product of around 60 kDa was formed after CVB 3C cleavage. No such product was found for HAV 3C demonstrating different cleavage specificity. However, both proteinases liberated similar small products of around 40 ~ 50 kDa (lanes 5 and 6). Next to Huh-T7 cells, the S10 extracts of BS-C-1 (lanes 1, 2, and 3) and Hela cells (lanes 4, 5 and 6) were also tested as substrate. The S10 extracts were incubated for 6 h and analyzed by anti-PABP immunoblot. Both proteinases were found to cleave endogenous PABP of these cells with the same specificity.

Collectively, the data show that HAV 3C can cleave PABP not only *in vitro*, but also *in vivo*, in HAV-infected cells, although the cleavage specificity differs from that of PV 3C and CVB 3C. This cleavage may prevent the viral genome circularization through a protein-protein bridge. Therefore, next we studied the cleavage specificity of PCBP which turned out to be a partner in this bridge.

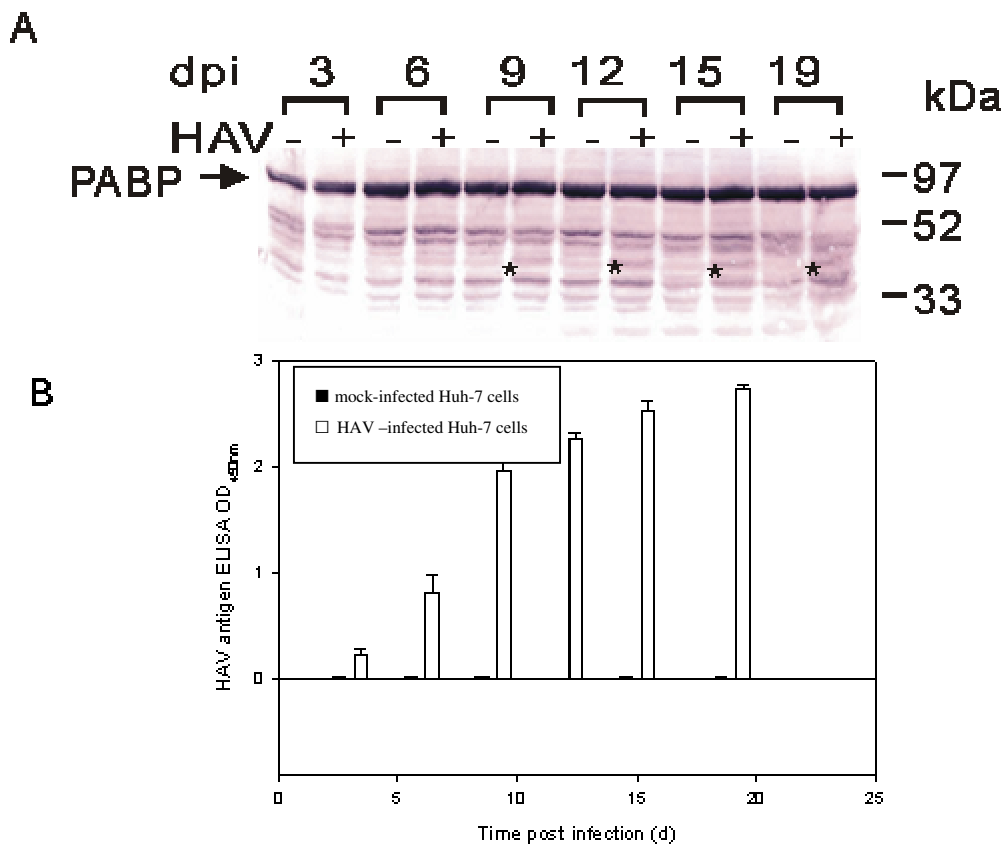


Fig. 25. PABP cleavage of HAV-infected Huh-7 cells. A, Cells harvested at the indicated time point pi were analyzed by immunoblot with anti-PABP. Δ PABP-H1 is indicated by asterisk. B, Analysis of viral replication by ELISA.

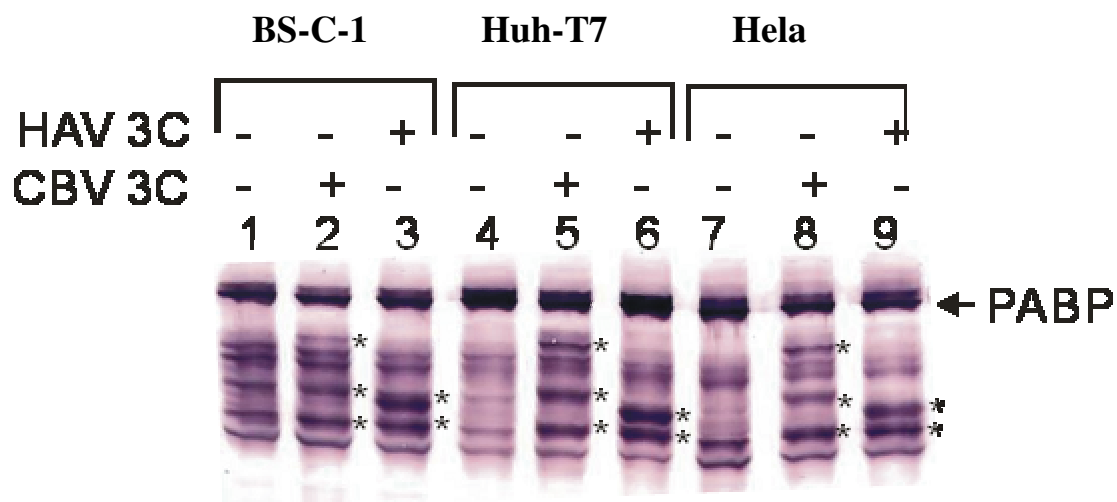


Fig. 26. Endogenous PABP cleavage by HAV and CVB 3C in various cell extracts. HAV and CVB 3C cleavage products are indicated by asterisk. The name cleavage product is same as Fig. 32 A indicating. Intact PABP is indicated by an arrow. Components in each cleavage mixture are indicated above the figure.

5.5.2 PCBP2 cleavage by HAV 3C in vivo and in vitro

5.5.2.1 PCBP2 cleavage by HAV 3C in vitro

PV RNA replication seems to require genome circularization through a protein-protein interaction, which involves PABP, PCBP2 and the PV protein 3CD (Herold and Andino, 2001). PCBP2 is a positive regulator of PV and HAV translation by binding to the PV and HAV 5'CL (Graff et al., 1998; Gamarnik and Andino, 1998; Parsley et al., 1997). For PV it was postulated that specific domains and multimerization of PCBP1 and 2 might have distinct roles in viral translation and RNA replication (Walter et al., 2002). After we (see **Fig. 17**) and others had shown that intact PCBP2 specifically interacted with the RNA domain connecting the HAV 5'CL with the IRES, we were interested to determine whether PCBP2 can be cleaved by HAV 3C and may thus play a regulatory role during HAV infection.

In order to determine whether PCBP2 can serve as substrate for HAV 3C, PCBP2 carrying a His-tag at its N-terminus was expressed in *E.coli* and purified by affinity chromatography (Ni-NTA). In vitro cleavage assays were performed with purified recombinant PCBP2 as substrate and HAV or CVB 3C (carrying a His-tag at its N-terminus) as enzymes. 1 µg of CVB and 1.34 µg HAV 3C were incubated with the 250 ng purified recombinant PCBP2 in 15 µl for 24 h at 37°C. The products were analyzed by immunoblot with anti-His. The mobility of the major HAV 3C cleavage product (Δ PCBP2-H) differed from that of the CVB 3C cleavage product (Δ PCBP2-C) (**Fig. 27**, lanes 1 and 3). The PCBP2 cleavage product of HAV 3C migrated with an apparent molecular mass of 30 kDa (Δ PCBP2-H), whereas the CVB 3C cleavage product had an apparent MW of 27 kDa (Δ PCBP2-C).

In order to test whether complete PCBP2 cleavage can be achieved, His-PCBP2 was incubated for 24 h with increasing amounts of purified recombinant HAV 3C (**Fig. 28**). Compared with the control (lane 1), increasing amounts of cleavage product (Δ -PCBP2-H) of approximately 30 kDa (indicated by an arrow) were found (lanes 2 to 5), indicating that PCBP2 was specifically cleaved in a concentration-dependent manner. Compared with the PABP cleavage by HAV 3C, PCBP2 cleavage was less complete (compare with **Fig. 22**).

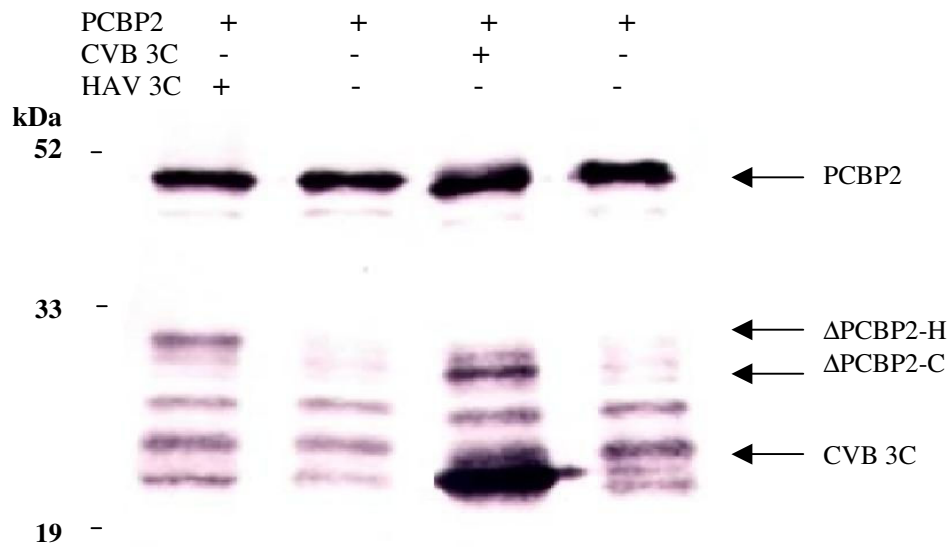


Fig. 27. PCBP2 cleavage by HAV and CVB 3C. The cleavage products were detected by anti-His and indicated by arrows. The molecular mass of protein standards are shown on the left.

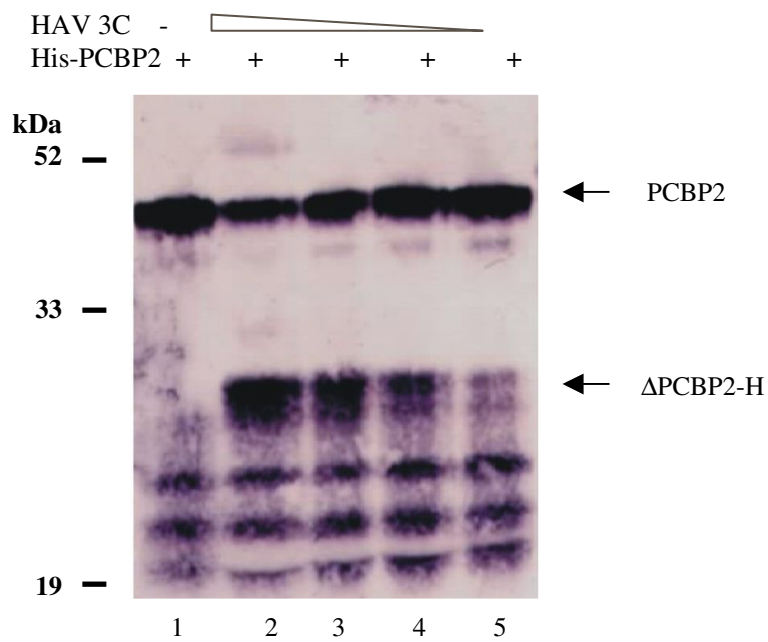


Fig. 28. Concentration dependence of PCBP2 cleavage by HAV 3C. The amounts HAV 3C was 335, 167.5, 70, and 33.5 $\mu\text{g/ml}$ in lanes 2 to 5, respectively. PCBP2 and its products were detected by anti-His. The 3C specific cleavage product is indicated by an arrow.

5.5.2.2 PCBP2 cleavage by 3C and its precursors in vivo

After we had demonstrated that recombinant purified PCBP2 can be cleaved by HAV 3C in vitro, we next tested PCBP2 cleavage in vivo. In order to produce large amounts of the viral proteinase and PCBP2, both were co-expressed in COS7 cells with the help of vTF7-3. Since the original

plasmid for expression of recombinant PCBP2 (in pQE9) did not contain the T7 promoter, PCBP2 was re-cloned by inserting the *EcoRI* and *PstI* fragment of PCBP2 into pGEM2. Two clones of pGEM2-PCBP2 (clone 1 and clone 2 in **Fig. 29**) were used for co-expression. The expression constructs of 3C and its precursors (3ABC, 3ABCmut and 3ABC μ) were the same as described for PABP cleavage (see description to **Fig. 24**).

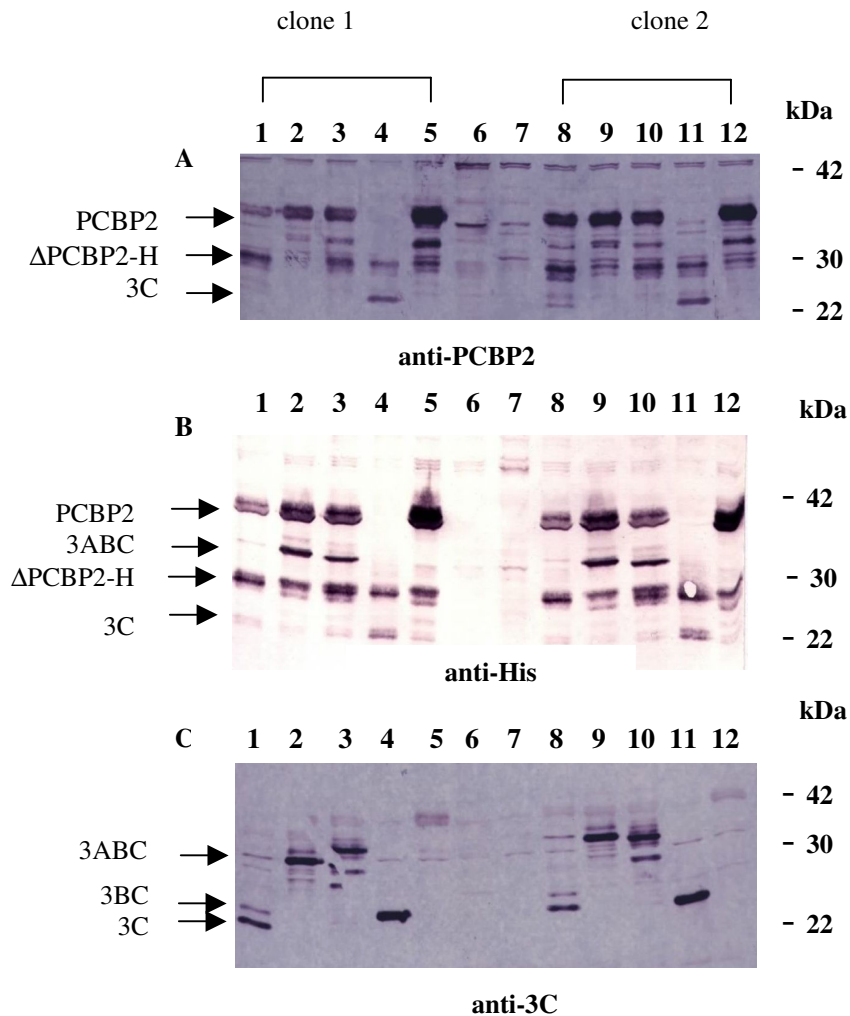


Fig. 29. PCBP2 cleavage by 3C and its precursors in vivo. His-PCBP2 and various forms of HAV 3C were co-expressed with the help of vTF7-3. **A.** The cleavage products were detected by anti-PCBP2. **B.** The cleavage products were detected by anti-His. **C.** 3C and its precursor were detected by anti-3C. Markers are indicated on the right. Lane 1, PCBP-cl1+3ABCwt; lane 2, PCBP-cl1+3ABC μ ; lane 3, PCBP-cl1+3ABCmut6; lane 4, PCBP-cl1+3C; lane 5, PCBP-cl1+pGEM2; lane 6, mock; lane 7, mock+vTF7-3; lane 8, PCBP-cl2+3ABCwt; lane 9, PCBP-cl2+3ABC μ ; lane 10, PCBP-cl2+3ABCmut6; lane 11, PCBP-cl2+3C; lane 12, PCBP-cl2+pGEM2.

Fig. 29 A (lanes 5 and 12) illustrates that recombinant PCBP2 was expressed in large amounts, clearly exceeding the constitutively produced protein (lanes 6 and 7). When co-expressed with 3C, PCBP2 was completely cleaved. This was obvious by the complete loss of the recombinant protein (A, lanes 4 and 11). PCBP2 cleavage by 3ABCwt and 3ABCmut6 was less efficient than by 3C (A and B, lanes 1, 3, 8, 10), even though 3ABCwt and 3ABCmut were expressed in high

amounts as can be seen in the anti-3C blot (C, lanes 1, 3, 8, and 10). Whereas active 3ABCmut6 remained autocatalytically uncleaved, the expression products of 3ABCwt comprised 3C, 3BC and 3ABC (C, lanes 1 und 8). Overall, **Fig. 29** A and B show that when co-expressed with 3C or one of its active precursors, PCBP2 was cleaved yielding a 30 kDa polypeptide Δ PCBP2-H. As co-expression with 3C and 3ABCwt reduced the amounts of complete PCBP2 more efficiently than 3ABCmut6, it can be concluded that the mature proteinase had higher substrate specificity and activity than its precursors.

5.5.2.3 PCBP2 cleavage in HAV-infected cells was not detectable

After having demonstrated that HAV 3C can cleave recombinant PCBP2 in vitro and in vivo, we tested whether HAV 3C can cleave endogenous PCBP2 that is an abundant cytoplasmic and nuclear protein (Makeyev and Liebhaver, 2002). For this, different fractions of a crude HAV-infected and mock-infected Huh-7 cell extract (S10, S200 and P200) were prepared (see also the PABP cleavage assay shown in **Fig. 23**). PCBP2 cleavage was determined by immunoblot with anti-PCBP2 that recognizes all forms of PCBP. Neither the loss of complete PCBP2 nor the appearance of PCBP2 cleavage products was detectable when the fractions of the infected cells were compared with the uninfected control extracts. **Fig. 30**, lanes 7 and 8, show the 3C cleavage products (Δ PCBP2-H) of recombinant His-tagged PCBP2 as comigration standard. As we failed to detect PCBP2 cleavage in the S10, S200 and P200 fraction of HAV infected Huh-7 cells, it can be assumed that native PCBP2 is complexed such that its 3C cleavage site is inaccessible, whereas recombinantly expressed and purified PCBP2 has a conformation that renders it susceptible to 3C cleavage. When the samples used for PCBP2 cleavage were assayed for PABP cleavage products, PABP cleavage products were detected indicating that 3C was active.

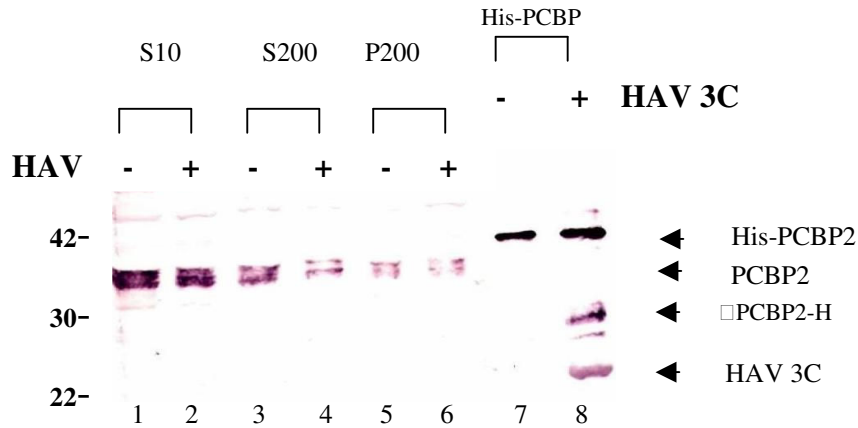


Fig. 30. Cleavage of endogenous PCBP in HAV-infected Huh-7 cells is not detectable. PCBP and its cleavage product were identified by anti-PCBP2. As control, purified recombinant PCBP incubating without and with HAV 3C were loaded into lanes 7 and 8.

5.5.2.4 Huh-T7 cells contain more PCBP than BS-C-1 and Hela cells

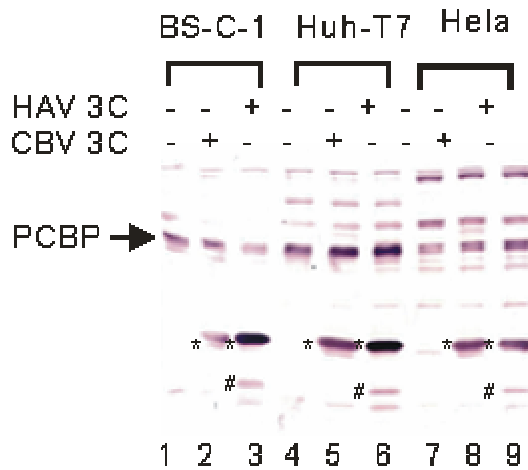


Fig. 31. Amounts and cleavage of constitutive PCBP in different cell lines. S10 extract of BS-C-1, Huh-T7 and Hela cells were incubated with HAV 3C (1.34 μ g) and CBV 3C (1 μ g) for 6 h and the products were detected by immunoblot with anti-PCBP. HAV and CVB 3C are indicated by asterisk. An additional polypeptide produced by HAV 3C (lanes 3, 6, 9) is indicated by #.

In order to assess the cytoplasmic abundance of PCBP in Hela, BSC and Huh-T7 cells, the same amounts of S10 extracts were incubated with HAV and CBV 3C and separated on a 12 % SDS-PAGE. Again no specific cleavage products were found. However, **Fig. 31** demonstrates that Huh-T7 cells (lane 4) contain more PCBP than BS-C-1 (lane 1) and Hela cells (lane 7). For unknown reason, the anti-PCBP antibody used reacted also with HAV and CBV 3C (indicated by asterisk in **Fig. 31**). Taken together the data indicate that PCBP cleavage in the HAV-infected cell is highly inefficient and not detectable under the conditions used.

PABP cleavage products), as shown before for cleavage of purified recombinant PABP by HAV and CVB 3C (see **Fig. 21**). The PABP cleavage products of CBV 3C were as expected and are described below in **Fig. 36**.

3ABC is a stable 3C precursor with proteinase activity. 3ABC and 3C (see **Fig. 29 C** lane1, 3 and 4) can cleave PABP in Huh-7 cells when over-expressed with the help of vaccinia virus. To test whether HAV 3ABC can cleave eIF4G *in vivo*, this and other forms of the proteinase were expressed in Huh-7 cells with the help of vTF7-3, similarly as described before (see **Fig. 24, Fig. 29**). As source of HAV 3C, plasmids pET15b-3ABC, pET15b-3ABCmut6, pET15b-3ABC μ , pGEM-3C, pET3b-3C μ were used. As shown in **Fig. 33**, 3ABCwt, 3ABCmut6 and 3C were able to cleave PABP (**Fig. 33 A**, lanes 1, 2 and 3; also see **Fig. 24**, lane 1, 2 and 3). However, none of them cleaved eIF4G under the same conditions (**Fig. 33 B**) confirming the resistance of eIF4G cleavage by HAV 3C in S10 extracts *in vitro* (see **Fig. 32**, lane2).

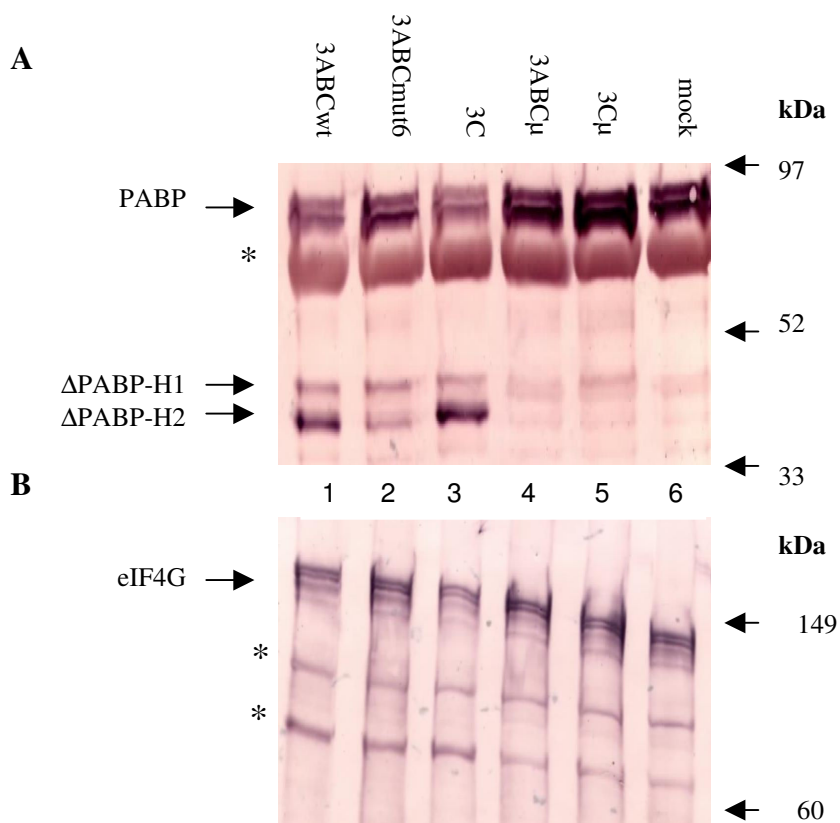


Fig. 33. PABP (A) and eIF4G (B) cleavage by recombinant HAV 3C and its precursors in vTF7-3 infected Huh-7 cells. PABP and PABP cleavage products were separated on a 12 % gel and detected by anti-PABP. eIF4G and its cleavage products were separated on a 8 % gel and detected by anti-eIF4G. Asterisk indicates unspecified proteins. 3C and its precursors are indicated on the top of the figure and the molecular mass of protein standards are shown on the right.

eIF4G is not cleaved in HAV-infected cells.

eIF4G is a major component of the translation initiation complex interacting with several proteins. It has been shown that complexed eIF4G found in vivo is folded differently than the protein in isolation with a concomitant change in its susceptibility to proteinases (Ohlmann et al., 1997). To test whether eIF4G in its natural condition might be cleaved by HAV 3C, mock- and HAV-infected Huh-7 cells (**Fig. 34**, lanes 3 and 4) were compared. No eIF4G cleavage products were detected. Similarly, eIF4G in cells over-expressing HAV 3C with the help of vaccinia virus was unaffected (lane 2). In contrast, we detected eIF4G cleavage products when the Huh-7 S10 cell extract was treated with CVB 3C. Taken together, we conclude that eIF4G does not serve as substrate for the HAV proteinase or its precursors in infected Huh-7 cells. This result directly supports the observation of others that showed that HAV translation needs intact eIF4G and is thus similar to host mRNA translation (Borman et al., 2001). Obviously other cellular proteins might be involved in the switch from translation to replication.

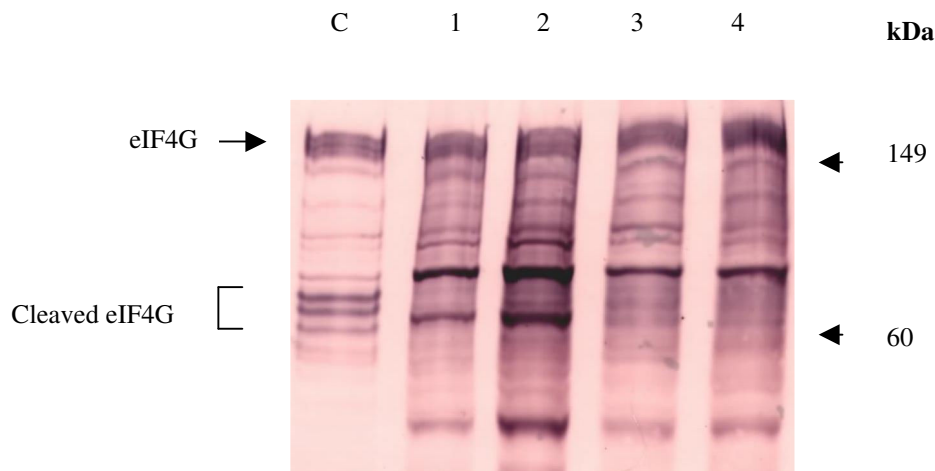


Fig. 34. No eIF4G cleavage in HAV-infected cells. Lane C shows the Huh-7 S10 extract treated in vitro with CVB 3C. Lanes 1 and 2 show extracts of mock and 3C transfected Huh-7 cells. Lanes 3 and 4 show mock- and HAV-infected cells. eIF4G and its cleavage products were detected by anti-eIF4G. The molecular masses of protein standards are shown on the right.

6. Discussion

HAV replicates in a highly protracted and asynchronous fashion in cells without either shutting off host protein synthesis or diverting the host's synthetic machinery for its own use. HAV replication in cultured cells results in a persistent and noncytopathic infection with low yields of viral progeny. In a recent report from our laboratory, it was shown that HAV replication was enhanced, when the host cell was metabolically active and cell division was allowed (Kusov et al., 2005). Various molecular properties of HAV have been proposed to limit the extent and rate of viral gene expression and replication (e.g. inefficient translation initiation and polyprotein processing, low activity of the viral polymerase). Viruses that establish persistent infections have to cope with the cellular antiviral response system and HAV has developed mechanisms to prevent or reduce the cellular antiviral response (Brack et al., 2002). This report showed that HAV inhibits double-stranded (dsRNA)-induced beta interferon (IFN- β) gene expression. However, the inhibitory effect of HAV on the cellular defense mechanisms appears not to be sufficient to completely prevent the antiviral reactions. At a later stage of infection, HAV possibly counteracts this situation by down regulation of its own replication. Combined these results are a sign of the unique and tight interdependence of HAV and its host cell. In order to improve understanding of the molecular mechanisms and of host and viral factors involved in HAV RNA translation and replication, an optimized host cell system was developed here. Various cell lines were compared for their ability to support HAV infection, replicon replication, for their content of essential host factors and finally their use as cell-free system.

6.1 Role of the host cell and template switching during HAV replication.

The data presented in **Fig. 5** and **Fig. 7** clearly show that HAV infection and genome expression, respectively, was more efficient in Huh-T7 cells than in Huh-7 cell confirming the notion that the host cell exerts a dominant role on HAV replication. Not only the complete HAV life cycle, but also genome replication as determined with the HAV replicon was noticeably dependent on the type of host cell confirming a recent observation that not all HAV-susceptible cells were suitable for HAV replicon replication (Yi and Lemon, 2002). The reporter gene kinetics of the replication-competent and replication-deficient replicon clearly demonstrated that after a 24 h phase when the transfected replicon RNA was exclusively translated a stage followed where the reporter gene activity declined resulting either in a complete loss or a stagnation of luciferase

activity (**Fig. 6** and **Fig. 7 B**, respectively). After translation of input RNA and its cessation (here 24 to 48 h pt), a next phase was evident only for the replication-competent replicon in which an increase in reporter gene activity was due to the translation of newly synthesized RNA produced by the RC). The decline of luciferase activity at 48 h pt was surprising and is in contrast to the luciferase activity profile of the active PV replicon (not shown here, see (Herold and Andino, 2000)). Whereas replication-dependent luciferase activity of the PV replicon initiates about 2 – 5 h pt when translation still seems to continue, initiation of the HAV replication activity is retarded until 48 pt when translation of input RNA had already ceased. From the kinetic profile of the HAV replicon it appears that the input RNA can only serve as replication template, after the translating ribosomes have been completely freed from all templates. The data described here strongly support the notion that template switching on the HAV RNA (translation to replication) is very inefficient and/or protracted. Further evidence obtained in independent systems will be needed to better understand the limiting factor involved in HAV template switching.

6.2 RNA secondary structures involved in HAV translation and replication – *cis*-acting elements in the HAV genome

In the picornaviral genome various *cis*-acting elements are presented that map to the non-coding terminal domains and within the ORF. Owing to their secondary structure and binding to *trans*-acting factors, these domains exert their effect on translation and replication in *cis*, i.e. on the same molecule. During this study, the role and binding properties of the HAV 5'CL, the IRES, the intragenomic CRE, and the 3'NTR with the poly (A) tail were assessed.

6.2.1 The 5'CL and the role of the authentic 5'end of the HAV genome for replication

The HAV 5'CL folds into three stem-loops (see **Fig. 3**) that were shown to interact specifically with HAV proteins 3C and 3ABC (Kusov et al., 1997; Peters et al., 2005). Host cell proteins interacting with the HAV 5'CL have been described elsewhere and it has been suggested for PV that a multi-protein complex is formed around the 5'CL that might be important for plus and minus strand RNA synthesis (Shaffer et al., 1994; Graff et al., 1998). RNA circularization through a protein bridge composed of host and viral polypeptides has been postulated for PV RNA synthesis (Herold and Andino, 2001). The specific interaction of the HAV 5'CL with PCBP2 was shown here (**Fig. 17**) confirming an earlier report (Graff et al., 1998). Furthermore, binding of PABP to the HAV 5'CL was found to be negative (see **Fig. 16**). However when both

proteins were incubated with the HAV 5'CL (**Fig. 18**), PABP interaction was enhanced possibly indicating a co-operative effect that might involve a conformational change of either protein due to protein-protein interaction (here PCBP2 or PABP). A similar enhancement of RNA interaction was found when PCBP2 and 3C were incubated with the HAV 5'CL in suboptimal amounts preventing binding by themselves (**Fig. 20**). In this context it is interesting to note that direct interaction of PABP with PCBP was detected using the yeast two hybrid system and a pull-down assay (Wang et al., 1999). Taken together the RNA binding data indirectly point to the participation of the HAV 5'CL in RNA circularization through protein-protein bridge.

To fold into a stable CL-like structure and to ensure efficient RNA synthesis it was experimentally shown that no additional nucleotides are tolerated at the 5' end of the PV genome (Herold and Andino, 2001). Following the same cloning strategy, the hammerhead ribozyme was added to the 5' end of the HAV genome to test whether the authentic 5' end is important for efficient HAV replication. From the data shown in **Fig. 11**, it was concluded that the infectivity of HAV was mostly unaffected by the presence of an active or inactive ribozyme at the 5' end of the HAV genome. This was mostly confirmed when the replication capability of two replicons were compared that contained or did not contain an active ribozyme at their 5' end (**Fig. 12**). It still remains unresolved why in the replicon assay in contrast to the full-length genome the RNA with the inactive ribozyme was completely replication-defective.

6.2.2 The HAV IRES

In contrast to most cellular capped mRNAs, picornaviral translation is initiated from an IRES that is located in the 5' NTR. In general, mammalian cells possess the machinery required for IRES-directed translation, although some IRESes are not active in all cell types, and tissue-specific activity profiles have been described for some IRESes (Borman and Kean, 1997; Creancier et al., 2000). The HAV IRES exhibits considerable structural and functional divergence and is distinct from all other picornaviral IRESes, as intact eIF4G is required for HAV IRES-driven translation (see introduction). High concentrations of cap-analogue can significantly reduce HAV IRES-driven translation, but not EMCV or PV IRES-driven translation confirming the competition of HAV with host protein translation (Bergamini et al., 2000). In addition, the presence of both eIF4E and PABP is required for optimal HAV IRES activity (Borman et al., 2001). Moreover opposing effects of GAPDH and PTB on the HAV IRES function have been reported (Yi, 2000). Unlike capped mRNA, HAV translation however does not require eIF1 and eIF1A, and the role of eIF3A for HAV translation is still debated. Here we show that HAV 3C does not cleave eIF4GI (**Fig. 32**) in vivo or in vitro, providing direct support

for the general idea that the requirements for HAV translation are very similar to that of host mRNA. In this context, it is interesting that the proteasomal cleavage of eIF4G and/or eIF3A inhibits translation initiation of HAV and cellular mRNA, but not of HCV RNA (Baugh and Pilipenko, 2004). Combined these observations strengthen the notion that HAV translation competes with host mRNA translation.

6.2.3 The putative HAV CRE

Internally located, *cis*-acting RNA replication elements, termed CREs, are essential for replication of the genomes of picornaviruses (McKnight and Lemon, 1996; Rieder et al., 2000; Mason et al., 2002). The CREs template uridylylation of the protein primer, VPg, by the viral polymerase 3D during positive strand RNA synthesis (Rieder et al., 2000). Their role in negative strand RNA synthesis is still debated (Morasco et al., 2003; Murray and Barton, 2003). Preliminary computational data obtained in collaboration with Dr. D. Evans (University of Glasgow) have suggested as the putative HAV CRE a stem-loop structure with a loop formed by nucleotides **CAAACGCUUUUUAGAAA** (position 6005 – 6022 of HAV strain 18f, located at the 5' end of gene 3D (**Fig. 35**)). In order to abolish the stem-loop structure, 8 nucleotide exchanges (underlined) were introduced such that the wild type sequence:

```
ACUCAGUGUCAAUGAAUGUGGUCUCCCAAACGCUUUUUAGAAAAGAGUCCCAUU  
UAUCAUCACAUUGAUAAAACCAUGAUUAAUUUUCCU
```

was changed to:

```
ACUCAGUGUCAAUGAAACGUUGUAUCCAAGACGCUUUUUAGAAAAUCUCCAAUU  
UAUCAUCACAUUGAUAAAACCAUGAUUAAUUUUCCU.
```

The mutated nucleotides (underlined) encode an unaltered amino acid sequences, however it folds into an altered secondary structure where the **CAAAC** motif is no longer part of the loop (**Fig. 35**, indicated by bracket). Evidence for the role of this putative CRE structure was provided by the expression kinetics of the wild type (18f-Luc-A60) and the mutated HAV replicon (18f-Luc-A60-cre). Whereas translation of the mutated replicon (18f-Luc-A60-cre) was similar to the wild type replicon (18f-Luc-A60), no increase in luciferase activity caused by replication was observed 48 h pt (see **Fig. 8**). When the corresponding full-length HAV genome with the CRE mutation was tested, it was obvious that its infectivity was lost (data not shown). Overall these data implicate that HAV genome replication is controlled by an intragenomic RNA structure, which forms a stem-loop structure at the 5' end of gene 3D and might serve as template for uridylylation of the protein primer VPg.

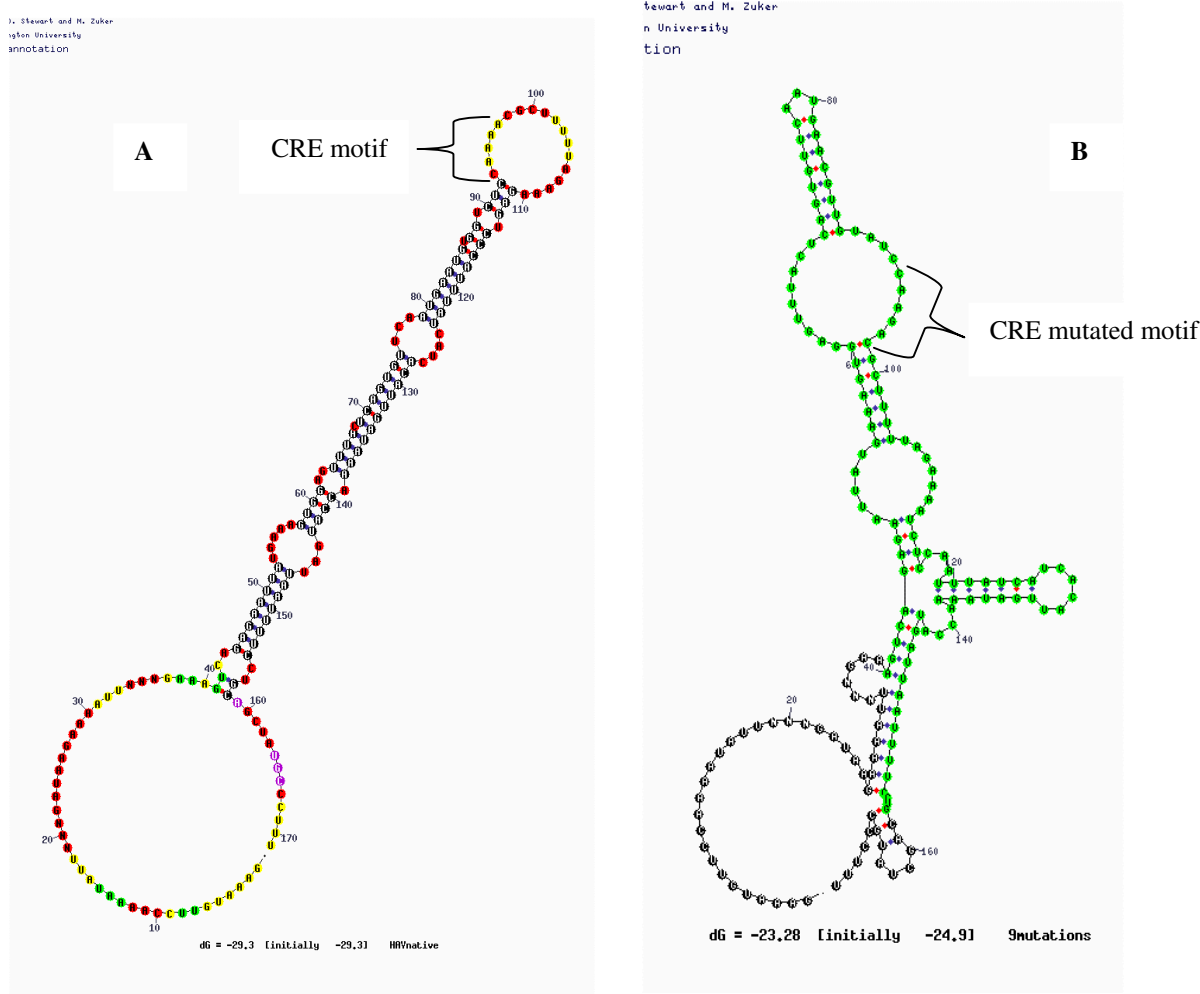


Fig. 35. Predicted RNA secondary structures of the wild type (A) and mutant HAV CRE motif (B) located at the 5'end of 3D. The CAAAAC motif is indicated by brackets.

6.2.4 The HAV 3'NTR and poly (A) tail

Similar to host mRNA, the picornaviral genome contains a 3' poly (A) tail that might stabilize the RNA by its interaction with PABP. The poly (A) tail is preceded by the 3'NTR, for which a pseudoknot structure has been proposed (Kusov et al., 1996) and binding to GAPDH was noted (Dollenmaier and Weitz, 2003). For PV and HAV it was shown that the poly (A) is an important *cis*-acting element for minus strand RNA synthesis. The removal or shortening of poly (A) tail results in a defect in RNA replication (Barton et al., 1996; Kusov, Gosert, and Gauss-Muller, 2005). Purified PV 3D uses the poly (A) tail as template to uridylate VPg (the putative primer for RNA synthesis) (Paul et al., 1998). However as all cellular mRNAs contain a poly (A) tail at their 3'end, this sequence cannot be the exclusive only *cis*-acting element that specifies replication of the viral RNA (Herold and Andino, 2001). Here it is shown that PABP binding to the HAV 3' NTR depended on the presence of the poly (A) tail and its length (**Fig. 15**) and that

PABP enhanced the interaction of PCBP with the HAV 5'CL. Combined these data suggest that PABP and the poly (A) might bridge the 5' and 3' ends of the viral genome. This cross-talk of the genomic ends might thus play a regulatory role in both translation initiation and viral RNA synthesis.

6.3 Trans-acting host proteins

6.3.1 eIF4G

In the last years the hypothesis has been put forward that efficiently translated mRNA must be circular rather than linear, with various canonical and non-canonical translation factors bridging the 5' and 3' ends. Among the various eIFs, eIF4G, a scaffold linker molecule in the translation initiation complex, is cleaved by different picornaviral proteinases (enteroviral 2A, aphthoviral Lb) in such a way that the PABP and eIF4E binding sites are removed from the part of the molecule that fixes the eIF3 complex and brings the 40S ribosomal subunit into contact with the mRNA. As a consequence of eIF4G cleavage, cap-dependent host translation initiation can no longer occur while enteroviral IRES-dependent translation can continue. Interestingly, eIF4G cleavage results also in a loss of poly (A)-mediated stimulation of the IRES activity. It has been proposed that the closed loop model is only active early in enteroviral infection whereas at later stages of the viral life cycle when host cell translation is shut off, the closed loop might no longer be formed and necessary (Kean, 2003).

These regulatory conditions appear to be inactive in HAV-infected cells where eIF4G remains uncleaved (see **Fig. 34**) and intact eIF4G is required for HAV translation (Borman and Kean, 1997). From the data reported here and elsewhere, it is striking that HAV translation requires the same pool of initiation factors as capped host mRNA and is thus locked in a constant competition situation. However, HAV replication in vivo leads to partial PABP cleavage (see **Fig. 25**) without affecting host mRNA translation. It is tempting to speculate that the limiting effects exerted by HAV might ensure that host and HAV mRNA differently regulate their translation initiation, in spite of the large number of host proteins engaged in both processes (for PABP, see below).

6.3.2 PABP and its function in host and viral translation

A wealth of data has accumulated in the past years describing the specific properties and functions of PABP (see Introduction and for review (Kuhn and Wahle, 2004; Mangus, et al., 2003)). PABP is a representative of a large family of eukaryotic RNA-binding proteins. The primary sequence of PABP is highly conserved among the *Xenopus*, mouse, and human species.

The N-terminal of PABP consists of four highly conserved RNA recognition motifs (RRMs) that are composed of approximately 90 amino acids, with highly conserved hydrophobic cores (Nagai et al., 1995). The C-terminal domain (CTD) is a less conserved proline-rich domain, which mediates PABP homodimerization on RNA and creates higher-order PABP-poly (A) structures. The footprint of PABP occupies about 25 nucleotides, and multiple PABP molecules are oligomerized on poly (A) tails longer than 50 nucleotides (up to eight or nine on poly (A) RNA of 200 nt) (Smith et al., 1997; Kuyumcu-Martinez et al., 2002). Translation initiation is stimulated by the poly (A) tail-PABP complex through interaction between PABP and eIF4GI, giving rise to the "closed-loop" model for translation initiation. PABP as a non-canonical translation initiation factor is therefore a key player in the promotion of the mRNA closed loop. mRNA circularization has been directly demonstrated in vitro by using recombinant yeast eIF4E, eIF4G, and PABP and is thought to increase the efficiency of translation by promoting de novo initiation of new ribosomes and also by promoting reinitiation of terminating ribosomes on the same RNA. This complex has been reconstituted in vitro using purified components and visualized by atomic force microscopy (Sachs et al., 1997; Wells et al., 1998). In higher eukaryotes, PABP also appears to indirectly stimulate translation initiation through its interaction with the translation factor Paip-1. Paip-1 interacts with eIF4A, and over expression of Paip-1 increases the rate of translation initiation (Craig et al., 1998). The CTD of PABP binds to various proteins involved in translation regulation, such as the translation initiation factor eIF4B (a cofactor of RNA helicase eIF4A) (Bushell et al., 1999), Paip-2 (Khaleghpour et al., 2001), and the eukaryotic release factor 3 (eRF3) indicating its distinct role in translation initiation (see **Fig. 36**). Interestingly, RRM 4 of PABP interacts with PCBP ((Wang and Kiledjian, 2000), see below).

Both PV and CVB proteinases 2A and 3C cleave PABP during viral infection (Joachims, et al., 1999; Kuyumcu-Martinez et al., 2002; Kuyumcu-Martinez et al., 2004). In kinetic experiments PABP cleavage correlated with host translation inhibition. PABP cleavage by PV 3C specifically inhibited poly (A)-dependent translation (Kuyumcu-Martinez et al., 2004). The eIF4GI-PABP interaction was not disrupted during PV infection after cleavage of eIF4GI and PABP, as their N-terminal cleavage products can still potentially interact via intact binding domains (Kuyumcu-Martinez et al., 2004).

Here data are presented for the first time showing that also the only HAV proteinase 3C catalyses PABP cleavage in vivo and in vitro (**Fig. 21, Fig. 23, Fig. 24**). Compared to PV or CVB-infected cells, the proportion of PABP cleaved in vivo was smaller in HAV-infected cells. Less than 10% of the total PABP was cleaved in HAV-infected cells, whereas up to 25 - 35 % in

PV-infected cells (Kuyumcu-Martinez et al., 2002). As already concluded by Kuyumcu-Martinez, PABP cleavage alone was not sufficient for PV-induced host shut-off, but might contribute to this effect in combination with eIF4G cleavage.

Identification of HAV 3C cleavage sites

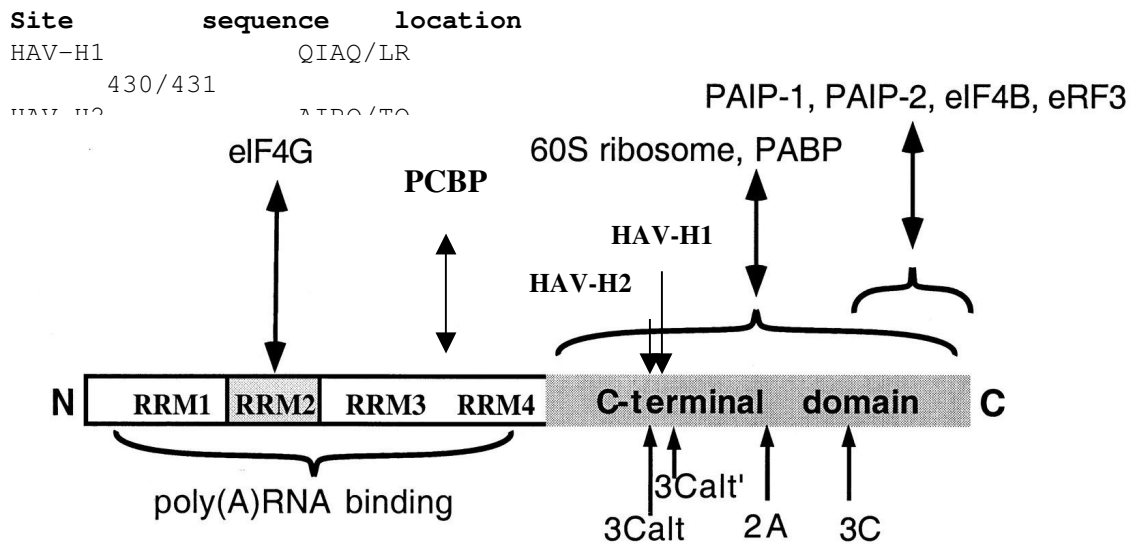


Fig. 36. Identification of 3C cleavage sites in PABP (modified after (Kuyumcu-Martinez et al.,2002)). Supposed sequences and locations of HAV cleavage sites in PABP are indicated above the figure. The HAV 3C sites (HAV-H1 and HAV-H2) were deduced based on gel migration of products and matching with the HAV 3C cleavage site consensus sequence at the appropriate location in the PABP amino acid sequence. PV 3C, 3Calt sites and known binding protein for N-terminal or C-terminal domains of PABP are taken from (Kuyumcu-Martinez et al., 2002) except the PCBP binding site (Wang and Kiledjian, 2000).

Comparison of the PABP cleavage products of CBV and HAV 3C (**Fig. 26**, lanes 5 and 6) revealed that the HAV 3C cleavage products had similar, yet distinctly different molecular masses than the two small cleavage products of CBV 3C. Based on their electrophoretic mobility and the known PABP amino acid sequence (gene bank NP_002559), HAV 3C might cleave PABP at amino acid positions 430 (QIAQ/LR) and 415 (AIPQ/TQ) (**Fig. 36**). The second site might be the same as that cleaved by CBV 3C and listed in **Fig. 36**. Both cleavage site match the consensus sequence proposed for HAV 3C and make cleavage at this site likely. PABP cleavage at these sites separates the CTD from the N-terminal 4 RRM, in a way similar to PV 3C. Although unproven, it can be speculated that CTD removal might destabilize the RNA circle and thus abolish reinitiation of ribosomes at the viral IRES and/or the host's mRNA.

As no host shut-off is observed in HAV-infected cells, the low level of PABP cleavage might be without consequence for host mRNA translation, but might affect the viral synthetic processes.

The following hypothesis for the role of PABP cleavage in HAV-infected cells is proposed. PABP cleavage products arise late in HAV infection and might therefore not affect viral translation initiation, but rather play a regulatory role in viral RNA synthesis, a step downstream of viral translation. HAV 3C-mediated separation of the N- or C-terminal parts of PABP and thus obstruction of its ability to circularize the viral RNA by interacting with PCBP might result in inhibition of HAV genome translation and thus allow initiation of viral minus strand RNA synthesis. For picornaviral minus strand RNA synthesis to occur, it is generally assumed that the RNA template has to be free of ribosomes. It will be interesting to test whether cleaved PABP can still bind to the poly (A) tail and to PCBP. Will the viral RC formed at the 3' end of the plus strand RNA template need a PABP fragment for its activity in minus RNA synthesis? What role might PCBP binding to the 5'CL play at this step? Since HAV 3C-mediated PABP cleavage does not grossly affect host translation, the PABP cleavage product(s) might specifically interfere with viral translation, with a beneficial effect on viral RNA synthesis. It is conceivable that in the presence of large amounts of uncleaved PABP cellular mRNA translation continues, and that limiting amounts of PABP fragments are sufficient to allow viral RNA synthesis and thus to switch template function from translation to replication.

6.3.3 PCBP: RNA binding and function in translation

PCBP2 that is essential for both PV IRES-driven translation and RNA synthesis was identified in RSW of HeLa cells by RNA affinity chromatography using stem-loop IV RNA of the PV IRES (Blyn et al., 1996; Blyn et al., 1997). PCBP2 binds also to sequences in the 5'CL structure (stem-loop I) of PV RNA and has been implicated in PV RNA replication (Gamarnik and Andino, 1997; Parsley et al., 1997). PCBP binding to the PV 5'CL greatly enhanced viral translation, while the binding of the viral polymerase precursor, 3CD, repressed viral translation and promoted the synthesis of negative-strand RNA. It is thought that these competing RNA-protein interactions determine the switch from translation to RNA replication (Gamarnik and Andino, 1998). Graff and Ehrenfeld clearly demonstrated the interaction of PCBP2 with the first 157 nucleotides of the HAV 5'CL, including the 5'-terminal pyrimidine-rich tract. They conclude that PCBP plays a role in HAV translation (Graff et al., 1998). Experiments using the yeast two hybrid system and pull-down assays have shown that PCBP interacts with PABP and the interaction was RNA-dependent, which was confirmed here (see **Fig. 18**). The binding site seemed to be within or after RRM3 of PABP and the interaction between PABP and PCBP can increase the stability of mRNA with poly (A) (Wang et al., 1999).

Here it is shown that PCBP2 directly binds to the HAV 5'CL formed by the first 148 nucleotides (see **Fig. 17**). This interaction was confirmed using the yeast three hybrid system (R. Zell, unpublished observation). In this study, it was also demonstrated that the first 42 5' terminal nucleotides of the HAV CL were not involved in PCBP interaction and that PCBP with a mutation in KH domain 3 interacted less efficiently with the HAV 5'CL. In addition to RNA binding, the data presented clearly here show that PCBP2 is cleaved by HAV 3C in vitro. After co-expression of PCBP with HAV 3C in vivo, intact PCBP disappeared compared with the control (**Fig. 29** A, lane 4, 11 and 5, 12). However, PCBP cleavage products and a loss of intact PCBP were not detectable in HAV-infected cells. Possibly, PCBP2 cleavage occurs at such low levels in HAV-infected cells, that the methods used here were not sensitive enough to detect specific cleavage products. According to the apparent molecular weight of the PCBP cleavage product, the 3C cleavage site lies within the PCBP C terminus, roughly around amino acid position 250 - 280. PCBP contains three KH domains with KH3 comprising amino acids 285 - 358. It seems that 3C removes domain KH3. It was demonstrated that KH1 is the major RNA binding determinant of PCBP2. The integrity of this KH module is absolutely essential for translation initiation on the PV IRES element and for replication of PV RNA (Silvera, et al., 1999; Walter et al., 2002). An intact KH3 was essential for efficient translation initiation on the PV IRES element, but not for replication of PV RNA (Walter et al., 2002). In this context and based on the observation with PV, we hypothesize that the HAV 3C-catalysed removal of PCBP KH3 might reduce HAV translation, but not affect HAV replication. Combined, PCBP cleavage may contribute to template switching from translation to replication. In this respect, HAV 3C with or without other viral proteins might play a key regulatory role in the viral life cycle. Combined with the observations of others and the results on PABP and PCBP cleavages reported here, HAV RNA circularization mediated by PCBP and PABP seems to be essential both viral translation and replication and both cellular and viral proteins play important regulatory roles during these two processes.

In conclusion, evidence was presented here showing that the interplay of the HAV RNA (secondary structures) *cis*-acting elements with transacting host factors is distinct from that of other picornaviruses. Although HAV RNA is endowed with RNA structural elements that might allow its efficient competition with host cell translation, this unusual picornavirus is “locked” into a perpetual, persistent expression situation. As this is common among the hepatitis viruses, it will be intriguing to identify the liver-specific factors.

7. Summary

HAV is a unique picornavirus that does not grossly affect the host cell metabolism, but still effectively competes with host cell translation, implying a complex balance of the viral and host metabolism. In this study, the human liver cell line Huh-T7 was found to optimally support persistent viral replication as well as genome translation and replication of the HAV replicon. Using mutants of the HAV replicon, a putative intragenomic *cis*-acting replication element (CRE) was identified and the role of the authentic viral 5' end was assessed. Using Huh-T7 cells, a cell-free system allowing the identification of host and viral factors directly involved in HAV translation/replication was developed. In analogy to poliovirus, poly (A) and poly (C) binding proteins (PABP and PCBP) were studied for their capacity to interact with the terminal viral RNA structures, in particular to the 5' cloverleaf (CL) and the 3' nontranslated region (NTR) with the poly (A) tail. Whereas PCBP efficiently interacted with the HAV 5'CL, the poly (A) tail was required for PABP-binding to the 3'NTR. The interaction of PCBP with the 5'CL was enhanced when either PABP or the viral proteinase 3C was part of the RNA-protein complex, suggesting a cooperative binding effect and possibly the cross-talk of the 5' and 3' ends of the viral genome through a protein bridge. PABP and PCBP were specifically cleaved *in vivo* and *in vitro* by HAV proteinase 3C implying that protein-mediated RNA circularization might be regulated by the viral proteinase. eIF4G was not cleaved by the HAV proteinase, confirming the notion that HAV RNA has to compete with cellular mRNA during translation.

In conclusion, indirect experimental evidence is presented strengthening the notion that PABP and/or PCBP are necessary translation initiation factors, yet that their cleavages might be involved in viral RNA template switching from translation to replication.

8. References

- Ali, I. K., McKendrick, L., Morley, S. J., and Jackson, R. J. (2001). Activity of the hepatitis A virus IRES requires association between the cap-binding translation initiation factor (eIF4E) and eIF4G. *J Virol* **75**(17), 7854-63.
- Anderson, D. A., Ross, B. C., and Locarnini, S. A. (1988). Restricted replication of hepatitis A virus in cell culture: encapsidation of viral RNA depletes the pool of RNA available for replication. *J Virol* **62**(11), 4201-6.
- Andino, R., Rieckhof, G. E., Achacoso, P. L., and Baltimore, D. (1993). Poliovirus RNA synthesis utilizes an RNP complex formed around the 5'-end of viral RNA. *Embo J* **12**(9), 3587-98.
- Back, S. H., Kim, Y. K., Kim, W. J., Cho, S., Oh, H. R., Kim, J. E., and Jang, S. K. (2002). Translation of polioviral mRNA is inhibited by cleavage of polypyrimidine tract-binding proteins executed by polioviral 3C(pro). *J Virol* **76**(5), 2529-42.
- Barton, D. J., Morasco, B. J., and Flanagan, J. B. (1996). Assays for poliovirus polymerase, 3D(Pol), and authentic RNA replication in HeLa S10 extracts. *Methods Enzymol* **275**, 35-57.
- Barton, D. J., Morasco, B. J., and Flanagan, J. B. (1999). Translating ribosomes inhibit poliovirus negative-strand RNA synthesis. *J Virol* **73**(12), 10104-12.
- Baugh, J. M., and Pilipenko, E. V. (2004). 20S proteasome differentially alters translation of different mRNAs via the cleavage of eIF4F and eIF3. *Mol Cell* **16**(4), 575-86.
- Bergamini, G., Preiss, T., and Hentze, M. W. (2000). Picornavirus IRESes and the poly(A) tail jointly promote cap-independent translation in a mammalian cell-free system. *Rna* **6**(12), 1781-90.
- Binn, L. N., Lemon, S. M., Marchwicki, R. H., Redfield, R. R., Gates, N. L., and Bancroft, W. H. (1984). Primary isolation and serial passage of hepatitis A virus strains in primate cell cultures. *J Clin Microbiol* **20**(1), 28-33.
- Blyn, L. B., Swiderek, K. M., Richards, O., Stahl, D. C., Semler, B. L., and Ehrenfeld, E. (1996). Poly(rC) binding protein 2 binds to stem-loop IV of the poliovirus RNA 5' noncoding region: identification by automated liquid chromatography-tandem mass spectrometry. *Proc Natl Acad Sci U S A* **93**(20), 11115-20.
- Blyn, L. B., Towner, J. S., Semler, B. L., and Ehrenfeld, E. (1997). Requirement of poly(rC) binding protein 2 for translation of poliovirus RNA. *J Virol* **71**(8), 6243-6.
- Borman, A. M., Bailly, J. L., Girard, M., and Kean, K. M. (1995). Picornavirus internal ribosome entry segments: comparison of translation efficiency and the requirements for optimal internal initiation of translation in vitro. *Nucleic Acids Res* **23**(18), 3656-63.
- Borman, A. M., and Kean, K. M. (1997). Intact eukaryotic initiation factor 4G is required for hepatitis A virus internal initiation of translation. *Virology* **237**(1), 129-36.
- Borman, A. M., Kirchweger, R., Ziegler, E., Rhoads, R. E., Skern, T., and Kean, K. M. (1997). eIF4G and its proteolytic cleavage products: effect on initiation of protein synthesis from capped, uncapped, and IRES-containing mRNAs. *Rna* **3**(2), 186-96.
- Borman, A. M., Michel, Y. M., and Kean, K. M. (2001). Detailed analysis of the requirements of hepatitis A virus internal ribosome entry segment for the eukaryotic initiation factor complex eIF4F. *J Virol* **75**(17), 7864-71.
- Boyer, J. C., and Haenni, A. L. (1994). Infectious transcripts and cDNA clones of RNA viruses. *Virology* **198**(2), 415-26.
- Brack, K., Berk, I., Magulski, T., Lederer, J., Dotzauer, A., and Vallbracht, A. (2002). Hepatitis A virus inhibits cellular antiviral defense mechanisms induced by double-stranded RNA. *J Virol* **76**(23), 11920-30.
- Brown, C. E., and Sachs, A. B. (1998). Poly(A) tail length control in *Saccharomyces cerevisiae* occurs by message-specific deadenylation. *Mol Cell Biol* **18**(11), 6548-59.
- Brown, E. A., Day, S. P., Jansen, R. W., and Lemon, S. M. (1991). The 5' nontranslated region of hepatitis A virus RNA: secondary structure and elements required for translation in vitro. *J Virol* **65**(11), 5828-38.
- Brown, E. A., Zajac, A. J., and Lemon, S. M. (1994). In vitro characterization of an internal ribosomal entry site (IRES) present within the 5' nontranslated region of hepatitis A virus RNA: comparison with the IRES of encephalomyocarditis virus. *J Virol* **68**(2), 1066-74.
- Bushell, M., McKendrick, L., Janicke, R. U., Clemens, M. J., and Morley, S. J. (1999). Caspase-3 is necessary and sufficient for cleavage of protein synthesis eukaryotic initiation factor 4G during apoptosis. *FEBS Lett* **451**(3), 332-6.
- Chang, K. H., Brown, E. A., and Lemon, S. M. (1993). Cell type-specific proteins which interact with the 5' nontranslated region of hepatitis A virus RNA. *J Virol* **67**(11), 6716-25.
- Clark, M. E., Lieberman, P. M., Berk, A. J., and Dasgupta, A. (1993). Direct cleavage of human TATA-binding protein by poliovirus protease 3C in vivo and in vitro. *Mol Cell Biol* **13**(2), 1232-7.

- Craig, A. W., Haghighat, A., Yu, A. T., and Sonenberg, N. (1998). Interaction of polyadenylate-binding protein with the eIF4G homologue PAIP enhances translation. *Nature* **392**(6675), 520-3.
- Creancier, L., Morello, D., Mercier, P., and Prats, A. C. (2000). Fibroblast growth factor 2 internal ribosome entry site (IRES) activity ex vivo and in transgenic mice reveals a stringent tissue-specific regulation. *J Cell Biol* **150**(1), 275-81.
- Daemer, R. J., Feinstone, S. M., Gust, I. D., and Purcell, R. H. (1981). Propagation of human hepatitis A virus in African green monkey kidney cell culture: primary isolation and serial passage. *Infect Immun* **32**(1), 388-93.
- Das, S., and Dasgupta, A. (1993). Identification of the cleavage site and determinants required for poliovirus 3CPro-catalyzed cleavage of human TATA-binding transcription factor TBP. *J Virol* **67**(6), 3326-31.
- Dehlin, E., Wormington, M., Korner, C. G., and Wahle, E. (2000). Cap-dependent deadenylation of mRNA. *Embo J* **19**(5), 1079-86.
- Dollenmaier, G., and Weitz, M. (2003). Interaction of glyceraldehyde-3-phosphate dehydrogenase with secondary and tertiary RNA structural elements of the hepatitis A virus 3' translated and non-translated regions. *J Gen Virol* **84**(Pt 2), 403-14.
- Flehmg, B. (1980). Hepatitis A-virus in cell culture: I. propagation of different hepatitis A-virus isolates in a fetal rhesus monkey kidney cell line (Frhk-4). *Med Microbiol Immunol (Berl)* **168**(4), 239-48.
- Fuerst, T. R., Niles, E. G., Studier, F. W., and Moss, B. (1986). Eukaryotic transient-expression system based on recombinant vaccinia virus that synthesizes bacteriophage T7 RNA polymerase. *Proc Natl Acad Sci U S A* **83**(21), 8122-6.
- Funkhouser, A. W., Schultz, D. E., Lemon, S. M., Purcell, R. H., and Emerson, S. U. (1999). Hepatitis A virus translation is rate-limiting for virus replication in MRC-5 cells. *Virology* **254**(2), 268-78.
- Gamarnik, A. V., and Andino, R. (1997). Two functional complexes formed by KH domain containing proteins with the 5' noncoding region of poliovirus RNA. *Rna* **3**(8), 882-92.
- Gamarnik, A. V., and Andino, R. (1998). Switch from translation to RNA replication in a positive-stranded RNA virus. *Genes Dev* **12**(15), 2293-304.
- Gao, M., Fritz, D. T., Ford, L. P., and Wilusz, J. (2000). Interaction between a poly(A)-specific ribonuclease and the 5'Cap influences mRNA deadenylation rates in vitro. *Mol Cell* **5**(3), 479-88.
- Gauss-Muller, V., and Deinhardt, F. (1984). Effect of hepatitis A virus infection on cell metabolism in vitro. *Proc Soc Exp Biol Med* **175**(1), 10-5.
- Gauss-Muller, V., and Kusov, Y. Y. (2002). Replication of a hepatitis A virus replicon detected by genetic recombination in vivo. *J Gen Virol* **83**(Pt 9), 2183-92.
- Gauss-Muller, V., von der Helm, K., and Deinhardt, F. (1984). Translation in vitro of hepatitis A virus RNA. *Virology* **137**(1), 182-4.
- Gerber, K., Wimmer, E., and Paul, A. V. (2001). Biochemical and genetic studies of the initiation of human rhinovirus 2 RNA replication: identification of a cis-replicating element in the coding sequence of 2A(pro). *J Virol* **75**(22), 10979-90.
- Glass, M. J., Jia, X. Y., and Summers, D. F. (1993). Identification of the hepatitis A virus internal ribosome entry site: in vivo and in vitro analysis of bicistronic RNAs containing the HAV 5' noncoding region. *Virology* **193**(2), 842-52.
- Goodfellow, I., Chaudhry, Y., Richardson, A., Meredith, J., Almond, J. W., Barclay, W., and Evans, D. J. (2000). Identification of a cis-acting replication element within the poliovirus coding region. *J Virol* **74**(10), 4590-600.
- Goodfellow, I. G., Kerrigan, D., and Evans, D. J. (2003). Structure and function analysis of the poliovirus cis-acting replication element (CRE). *Rna* **9**(1), 124-37.
- Gorlach, M., Burd, C. G., and Dreyfuss, G. (1994). The mRNA poly(A)-binding protein: localization, abundance, and RNA-binding specificity. *Exp Cell Res* **211**(2), 400-7.
- Graff, J., Cha, J., Blyn, L. B., and Ehrenfeld, E. (1998). Interaction of poly(rC) binding protein 2 with the 5' noncoding region of hepatitis A virus RNA and its effects on translation. *J Virol* **72**(12), 9668-75.
- Herold, J., and Andino, R. (2000). Poliovirus requires a precise 5'end for efficient positive-strand RNA synthesis. *J Virol* **74**(14), 6394-400.
- Herold, J., and Andino, R. (2001). Poliovirus RNA replication requires genome circularization through a protein-protein bridge. *Mol Cell* **7**(3), 581-91.
- Holcik, M., and Lieber, S. A. (1997). Four highly stable eukaryotic mRNAs assemble 3' untranslated region RNA-protein complexes sharing cis and trans components. *Proc Natl Acad Sci U S A* **94**(6), 2410-4.
- Huang, P., and Lai, M. M. (2001). Heterogeneous nuclear ribonucleoprotein a1 binds to the 3'-untranslated region and mediates potential 5'-3'-end cross talks of mouse hepatitis virus RNA. *J Virol* **75**(11), 5009-17.
- Iizuka, N., and Sarnow, P. (1997). Translation-competent extracts from *Saccharomyces cerevisiae*: effects of L-A RNA, 5'Cap, and 3' poly(A) tail on translational efficiency of mRNAs. *Methods* **11**(4), 353-60.
- Joachims, M., Harris, K. S., and Etchison, D. (1995). Poliovirus protease 3C mediates cleavage of microtubule-associated protein 4. *Virology* **211**(2), 451-61.

- Joachims, M., Van Breugel, P. C., and Lloyd, R. E. (1999). Cleavage of poly(A)-binding protein by enterovirus proteases concurrent with inhibition of translation in vitro. *J Virol* **73**(1), 718-27.
- Kanda, T., Zhang, B., Kusov, Y., Yokosuka, O., and Gauss-Muller, V. (2005). Suppression of hepatitis A virus genome translation and replication by siRNAs targeting the internal ribosomal entry site. *Biochem Biophys Res Commun* **330**(4), 1217-23.
- Kean, K. M. (2003). The role of mRNA 5'-noncoding and 3'-end sequences on 40S ribosomal subunit recruitment, and how RNA viruses successfully compete with cellular mRNAs to ensure their own protein synthesis. *Biol Cell* **95**(3-4), 129-39.
- Kerekatte, V., Keiper, B. D., Badorff, C., Cai, A., Knowlton, K. U., and Rhoads, R. E. (1999). Cleavage of Poly(A)-binding protein by coxsackievirus 2A protease in vitro and in vivo: another mechanism for host protein synthesis shutoff? *J Virol* **73**(1), 709-17.
- Khaleghpour, K., Svitkin, Y. V., Craig, A. W., DeMaria, C. T., Deo, R. C., Burley, S. K., and Sonenberg, N. (2001). Translational repression by a novel partner of human poly(A) binding protein, Paip2. *Mol Cell* **7**(1), 205-16.
- Kiledjian, M., Wang, X., and Liebhaber, S. A. (1995). Identification of two KH domain proteins in the alpha-globin mRNP stability complex. *Embo J* **14**(17), 4357-64.
- Kuhn, U., and Wahle, E. (2004). Structure and function of poly(A) binding proteins. *Biochim Biophys Acta* **1678**(2-3), 67-84.
- Kusov, Y., and Gauss-Muller, V. (1999). Improving proteolytic cleavage at the 3A/3B site of the hepatitis A virus polyprotein impairs processing and particle formation, and the impairment can be complemented in trans by 3AB and 3ABC. *J Virol* **73**(12), 9867-78.
- Kusov, Y., Weitz, M., Dollenmeier, G., Gauss-Muller, V., and Siegl, G. (1996). RNA-protein interactions at the 3' end of the hepatitis A virus RNA. *J Virol* **70**(3), 1890-7.
- Kusov, Y. Y., and Gauss-Muller, V. (1997). In vitro RNA binding of the hepatitis A virus proteinase 3C (HAV 3Cpro) to secondary structure elements within the 5' terminus of the HAV genome. *Rna* **3**(3), 291-302.
- Kusov, Y. Y., Gosert, R., and Gauss-Muller, V. (2005). Replication and in vivo repair of the hepatitis A virus genome lacking the poly(A) tail. *J Gen Virol* **86**(Pt 5), 1363-8.
- Kusov, Y. Y., Morace, G., Probst, C., and Gauss-Muller, V. (1997). Interaction of hepatitis A virus (HAV) precursor proteins 3AB and 3ABC with the 5' and 3' termini of the HAV RNA. *Virus Res* **51**(2), 151-7.
- Kuyumcu-Martinez, M., Belliot, G., Sosnovtsev, S. V., Chang, K. O., Green, K. Y., and Lloyd, R. E. (2004). Calicivirus 3C-like proteinase inhibits cellular translation by cleavage of poly(A)-binding protein. *J Virol* **78**(15), 8172-82.
- Kuyumcu-Martinez, N. M., Joachims, M., and Lloyd, R. E. (2002). Efficient cleavage of ribosome-associated poly(A)-binding protein by enterovirus 3C protease. *J Virol* **76**(5), 2062-74.
- Kuyumcu-Martinez, N. M., Van Eden, M. E., Younan, P., and Lloyd, R. E. (2004). Cleavage of poly(A)-binding protein by poliovirus 3C protease inhibits host cell translation: a novel mechanism for host translation shutoff. *Mol Cell Biol* **24**(4), 1779-90.
- Lamphear, B. J., Kirchweger, R., Skern, T., and Rhoads, R. E. (1995). Mapping of functional domains in eukaryotic protein synthesis initiation factor 4G (eIF4G) with picornaviral proteases. Implications for cap-dependent and cap-independent translational initiation. *J Biol Chem* **270**(37), 21975-83.
- Le, S. Y., Chen, J. H., Sonenberg, N., and Maizel, J. V., Jr. (1993). Conserved tertiary structural elements in the 5' nontranslated region of cardiovirus, aphthovirus and hepatitis A virus RNAs. *Nucleic Acids Res* **21**(10), 2445-51.
- Lemon, S. M., Murphy, P. C., Shields, P. A., Ping, L. H., Feinstone, S. M., Cromeans, T., and Jansen, R. W. (1991). Antigenic and genetic variation in cytopathic hepatitis A virus variants arising during persistent infection: evidence for genetic recombination. *J Virol* **65**(4), 2056-65.
- Liebig, H. D., Ziegler, E., Yan, R., Hartmuth, K., Klump, H., Kowalski, H., Blaas, D., Sommergruber, W., Frasel, L., Lamphear, B., and et al. (1993). Purification of two picornaviral 2A proteinases: interaction with eIF-4 gamma and influence on in vitro translation. *Biochemistry* **32**(29), 7581-8.
- Lobert, P. E., Escriou, N., Ruelle, J., and Michiels, T. (1999). A coding RNA sequence acts as a replication signal in cardioviruses. *Proc Natl Acad Sci U S A* **96**(20), 11560-5.
- Lohmann, V., Korner, F., Koch, J., Herian, U., Theilmann, L., and Bartenschlager, R. (1999). Replication of subgenomic hepatitis C virus RNAs in a hepatoma cell line. *Science* **285**(5424), 110-3.
- Makeyev, A. V., and Liebhaber, S. A. (2002). The poly(C)-binding proteins: a multiplicity of functions and a search for mechanisms. *Rna* **8**(3), 265-78.
- Mangus, D. A., Evans, M. C., and Jacobson, A. (2003). Poly(A)-binding proteins: multifunctional scaffolds for the post-transcriptional control of gene expression. *Genome Biol* **4**(7), 223.
- Mason, P. W., Bezborodova, S. V., and Henry, T. M. (2002). Identification and characterization of a cis-acting replication element (cre) adjacent to the internal ribosome entry site of foot-and-mouth disease virus. *J Virol* **76**(19), 9686-94.

- McKnight, K. L., and Lemon, S. M. (1996). Capsid coding sequence is required for efficient replication of human rhinovirus 14 RNA. *J Virol* **70**(3), 1941-52.
- Michel, Y. M., Borman, A. M., Paulous, S., and Kean, K. M. (2001). Eukaryotic initiation factor 4G-poly(A) binding protein interaction is required for poly(A) tail-mediated stimulation of picornavirus internal ribosome entry segment-driven translation but not for X-mediated stimulation of hepatitis C virus translation. *Mol Cell Biol* **21**(13), 4097-109.
- Michel, Y. M., Poncet, D., Piron, M., Kean, K. M., and Borman, A. M. (2000). Cap-Poly(A) synergy in mammalian cell-free extracts. Investigation of the requirements for poly(A)-mediated stimulation of translation initiation. *J Biol Chem* **275**(41), 32268-76.
- Morasco, B. J., Sharma, N., Parilla, J., and Flanagan, J. B. (2003). Poliovirus cre(2C)-dependent synthesis of VPgUpU is required for positive- but not negative-strand RNA synthesis. *J Virol* **77**(9), 5136-44.
- Morley, S. J., Curtis, P. S., and Pain, V. M. (1997). eIF4G: translation's mystery factor begins to yield its secrets. *Rna* **3**(10), 1085-104.
- Murray, K. E., and Barton, D. J. (2003). Poliovirus CRE-dependent VPg uridylylation is required for positive-strand RNA synthesis but not for negative-strand RNA synthesis. *J Virol* **77**(8), 4739-50.
- Nagai, K., Oubridge, C., Ito, N., Avis, J., and Evans, P. (1995). The RNP domain: a sequence-specific RNA-binding domain involved in processing and transport of RNA. *Trends Biochem Sci* **20**(6), 235-40.
- Nakabayashi, H., Taketa, K., Miyano, K., Yamane, T., and Sato, J. (1982). Growth of human hepatoma cells lines with differentiated functions in chemically defined medium. *Cancer Res* **42**(9), 3858-63.
- Nietfeld, W., Mentzel, H., and Pieler, T. (1990). The *Xenopus laevis* poly(A) binding protein is composed of multiple functionally independent RNA binding domains. *Embo J* **9**(11), 3699-705.
- Ohlmann, T., Pain, V. M., Wood, W., Rau, M., and Morley, S. J. (1997). The proteolytic cleavage of eukaryotic initiation factor (eIF) 4G is prevented by eIF4E binding protein (PHAS-I; 4E-BP1) in the reticulocyte lysate. *Embo J* **16**(4), 844-55.
- Ohlmann, T., Rau, M., Pain, V. M., and Morley, S. J. (1996). The C-terminal domain of eukaryotic protein synthesis initiation factor (eIF) 4G is sufficient to support cap-independent translation in the absence of eIF4E. *Embo J* **15**(6), 1371-82.
- Ostareck-Lederer, A., Ostareck, D. H., and Hentze, M. W. (1998). Cytoplasmic regulatory functions of the KH-domain proteins hnRNPs K and E1/E2. *Trends Biochem Sci* **23**(11), 409-11.
- Parsley, T. B., Towner, J. S., Blyn, L. B., Ehrenfeld, E., and Semler, B. L. (1997). Poly (rC) binding protein 2 forms a ternary complex with the 5'-terminal sequences of poliovirus RNA and the viral 3CD proteinase. *Rna* **3**(10), 1124-34.
- Paul, A. V., van Boom, J. H., Filippov, D., and Wimmer, E. (1998). Protein-primed RNA synthesis by purified poliovirus RNA polymerase. *Nature* **393**(6682), 280-4.
- Percy, N., Barclay, W. S., Sullivan, M., and Almond, J. W. (1992). A poliovirus replicon containing the chloramphenicol acetyltransferase gene can be used to study the replication and encapsidation of poliovirus RNA. *J Virol* **66**(8), 5040-6.
- Peters, H., Kusov, Y. Y., Meyer, S., Benie, A. J., Bauml, E., Wolff, M., Rademacher, C., Peters, T., and Gauss-Muller, V. (2005). Hepatitis A virus proteinase 3C binding to viral RNA: correlation with substrate binding and enzyme dimerization. *Biochem J* **385**(Pt 2), 363-70.
- Pilipenko, E. V., Poperechny, K. V., Maslova, S. V., Melchers, W. J., Slot, H. J., and Agol, V. I. (1996). Cis-element, oriR, involved in the initiation of (-) strand poliovirus RNA: a quasi-globular multi-domain RNA structure maintained by tertiary ('kissing') interactions. *Embo J* **15**(19), 5428-36.
- Probst, C., Jecht, M., and Gauss-Muller, V. (1997). Proteinase 3C-mediated processing of VP1-2A of two hepatitis A virus strains: in vivo evidence for cleavage at amino acid position 273/274 of VP1. *J Virol* **71**(4), 3288-92.
- Probst, C., Jecht, M., and Gauss-Muller, V. (1998). Processing of proteinase precursors and their effect on hepatitis A virus particle formation. *J Virol* **72**(10), 8013-20.
- Rieder, E., Paul, A. V., Kim, D. W., van Boom, J. H., and Wimmer, E. (2000). Genetic and biochemical studies of poliovirus cis-acting replication element cre in relation to VPg uridylylation. *J Virol* **74**(22), 10371-80.
- Sachs, A. B., and Davis, R. W. (1989). The poly(A) binding protein is required for poly(A) shortening and 60S ribosomal subunit-dependent translation initiation. *Cell* **58**(5), 857-67.
- Sachs, A. B., Sarnow, P., and Hentze, M. W. (1997). Starting at the beginning, middle, and end: translation initiation in eukaryotes. *Cell* **89**(6), 831-8.
- Schultheiss, T., Sommergruber, W., Kusov, Y., and Gauss-Muller, V. (1995). Cleavage specificity of purified recombinant hepatitis A virus 3C proteinase on natural substrates. *J Virol* **69**(3), 1727-33.
- Schultz, D. E., Hardin, C. C., and Lemon, S. M. (1996). Specific interaction of glyceraldehyde 3-phosphate dehydrogenase with the 5'-nontranslated RNA of hepatitis A virus. *J Biol Chem* **271**(24), 14134-42.

- Schultz, D. E., Honda, M., Whetter, L. E., McKnight, K. L., and Lemon, S. M. (1996). Mutations within the 5' nontranslated RNA of cell culture-adapted hepatitis A virus which enhance cap-independent translation in cultured African green monkey kidney cells. *J Virol* **70**(2), 1041-9.
- Shaffer, D. R., Brown, E. A., and Lemon, S. M. (1994). Large deletion mutations involving the first pyrimidine-rich tract of the 5' nontranslated RNA of human hepatitis A virus define two adjacent domains associated with distinct replication phenotypes. *J Virol* **68**(9), 5568-78.
- Shiroki, K., Isoyama, T., Kuge, S., Ishii, T., Ohmi, S., Hata, S., Suzuki, K., Takasaki, Y., and Nomoto, A. (1999). Intracellular redistribution of truncated La protein produced by poliovirus 3Cpro-mediated cleavage. *J Virol* **73**(3), 2193-200.
- Silvera, D., Gamarnik, A. V., and Andino, R. (1999). The N-terminal K homology domain of the poly(rC)-binding protein is a major determinant for binding to the poliovirus 5'-untranslated region and acts as an inhibitor of viral translation. *J Biol Chem* **274**(53), 38163-70.
- Sladic, R. T., Lagnado, C. A., Bagley, C. J., and Goodall, G. J. (2004). Human PABP binds AU-rich RNA via RNA-binding domains 3 and 4. *Eur J Biochem* **271**(2), 450-7.
- Smith, B. L., Gallie, D. R., Le, H., and Hansma, P. K. (1997). Visualization of poly(A)-binding protein complex formation with poly(A) RNA using atomic force microscopy. *J Struct Biol* **119**(2), 109-17.
- Svitkin, Y. V., Imataka, H., Khaleghpour, K., Kahvejian, A., Liebig, H. D., and Sonenberg, N. (2001). Poly(A)-binding protein interaction with eIF4G stimulates picornavirus IRES-dependent translation. *Rna* **7**(12), 1743-52.
- Svitkin, Y. V., and Sonenberg, N. (2003). Cell-free synthesis of encephalomyocarditis virus. *J Virol* **77**(11), 6551-5.
- Tarun, S. Z., Jr., and Sachs, A. B. (1995). A common function for mRNA 5' and 3' ends in translation initiation in yeast. *Genes Dev* **9**(23), 2997-3007.
- Tarun, S. Z., Jr., Wells, S. E., Deardorff, J. A., and Sachs, A. B. (1997). Translation initiation factor eIF4G mediates in vitro poly(A) tail-dependent translation. *Proc Natl Acad Sci U S A* **94**(17), 9046-51.
- Todd, S., Towner, J. S., Brown, D. M., and Semler, B. L. (1997). Replication-competent picornaviruses with complete genomic RNA 3' noncoding region deletions. *J Virol* **71**(11), 8868-74.
- Vallbracht, A., Hofmann, L., Wurster, K. G., and Flehmig, B. (1984). Persistent infection of human fibroblasts by hepatitis A virus. *J Gen Virol* **65** (Pt 3), 609-15.
- Walter, B. L., Parsley, T. B., Ehrenfeld, E., and Semler, B. L. (2002). Distinct poly(rC) binding protein KH domain determinants for poliovirus translation initiation and viral RNA replication. *J Virol* **76**(23), 12008-22.
- Wang, Z., Day, N., Trifillis, P., and Kiledjian, M. (1999). An mRNA stability complex functions with poly(A)-binding protein to stabilize mRNA in vitro. *Mol Cell Biol* **19**(7), 4552-60.
- Wang, Z., and Kiledjian, M. (2000). The poly(A)-binding protein and an mRNA stability protein jointly regulate an endoribonuclease activity. *Mol Cell Biol* **20**(17), 6334-41.
- Wei, C. C., Balasta, M. L., Ren, J., and Goss, D. J. (1998). Wheat germ poly(A) binding protein enhances the binding affinity of eukaryotic initiation factor 4F and (iso)4F for cap analogues. *Biochemistry* **37**(7), 1910-6.
- Wells, S. E., Hillner, P. E., Vale, R. D., and Sachs, A. B. (1998). Circularization of mRNA by eukaryotic translation initiation factors. *Mol Cell* **2**(1), 135-40.
- Wheeler, C. M., Fields, H. A., Schable, C. A., Meinke, W. J., and Maynard, J. E. (1986). Adsorption, purification, and growth characteristics of hepatitis A virus strain HAS-15 propagated in fetal rhesus monkey kidney cells. *J Clin Microbiol* **23**(3), 434-40.
- Whetter, L. E., Day, S. P., Elroy-Stein, O., Brown, E. A., and Lemon, S. M. (1994). Low efficiency of the 5' nontranslated region of hepatitis A virus RNA in directing cap-independent translation in permissive monkey kidney cells. *J Virol* **68**(8), 5253-63.
- Willcocks, M. M., Carter, M. J., and Roberts, L. O. (2004). Cleavage of eukaryotic initiation factor eIF4G and inhibition of host-cell protein synthesis during feline calicivirus infection. *J Gen Virol* **85**(Pt 5), 1125-30.
- Wormington, M., Searfoss, A. M., and Hurney, C. A. (1996). Overexpression of poly(A) binding protein prevents maturation-specific deadenylation and translational inactivation in *Xenopus* oocytes. *Embo J* **15**(4), 900-9.
- Yalamanchili, P., Datta, U., and Dasgupta, A. (1997). Inhibition of host cell transcription by poliovirus: cleavage of transcription factor CREB by poliovirus-encoded protease 3Cpro. *J Virol* **71**(2), 1220-6.
- Yalamanchili, P., Weidman, K., and Dasgupta, A. (1997). Cleavage of transcriptional activator Oct-1 by poliovirus encoded protease 3Cpro. *Virology* **239**(1), 176-85.
- Yi, M., and Lemon, S. M. (2002). Replication of subgenomic hepatitis A virus RNAs expressing firefly luciferase is enhanced by mutations associated with adaptation of virus to growth in cultured cells. *J Virol* **76**(3), 1171-80.
- Yi, M., Schultz, D. E., and Lemon, S. M. (2000). Functional significance of the interaction of hepatitis A virus RNA with glyceraldehyde 3-phosphate dehydrogenase (GAPDH): opposing effects of GAPDH and polypyrimidine tract binding protein on internal ribosome entry site function. *J Virol* **74**(14), 6459-68.

- Zhang, H., Chao, S. F., Ping, L. H., Grace, K., Clarke, B., and Lemon, S. M. (1995). An infectious cDNA clone of a cytopathic hepatitis A virus: genomic regions associated with rapid replication and cytopathic effect. *Virology* **212**(2), 686-97.
- Ziegler, E., Borman, A. M., Deliat, F. G., Liebig, H. D., Jugovic, D., Kean, K. M., Skern, T., and Kuechler, E. (1995). Picornavirus 2A proteinase-mediated stimulation of internal initiation of translation is dependent on enzymatic activity and the cleavage products of cellular proteins. *Virology* **213**(2), 549-57.

9. Appendix

- Figure list presented in this thesis.

Fig. 1. The proportion of HAV infection among all viral hepatitis cases.....	8
Fig. 2. Structure of the HAV genome (A) and replicon (B). Primary cleavages by 3C are indicated by arrows.	9
Fig. 3. Proposed secondary structure of the HAV HM175/wt 5'NTR	11
Fig. 4. The flow chart of the hammerhead ribozyme cloning.	30
Fig. 5. HAV particle formation in infected Huh-7 and Huh-T7 cells.....	37
Fig. 6. HAV replicon expression in Huh-T7 cells with and without Gu-HCl (5 mM).....	39
Fig. 7. Comparison of replicon replication in Huh-7 (A) and Huh-T7 cells (B).	40
Fig. 8. Luciferase activity of the HAV replicon carrying mutations in the putative CRE.	41
Fig. 9. Replicon replication in HuhT7 cells after cell passage.	42
Fig. 10. HAV-specific <i>cis</i> -acting hammerhead ribozyme at the 5'end of the genome.....	44
Fig. 11. Particle formation of HAV full-length RNA transcripts with and without a 5'terminal ribozyme...45	
Fig. 12. Luciferase activity of the HAV replicon with and without the ribozyme.....	46
Fig. 13. HAV replicon expression in a Huh-7 S10 extract in short time (A) and long time (B) kinetics.	46
Fig. 14. Translation comparison of the HAV replicon (A) and the PV replicon RNA (B) in the Huh-T7 S10 extract.....	47
Fig. 15. PABP binds to the poly (A) tail of the HAV 3'NTR.....	49
Fig. 16. PABP does not interact with the HAV 5'CL.	49
Fig. 17. PCBP2 directly interacts with the HAV 5'CL.....	50
Fig. 18. PABP enhanced PCBP interaction with the HAV 5'CL.....	51
Fig. 19. PABP enhanced PCBP interaction with the HAV 5'CL.....	51
Fig. 20. The mobility of the HAV 5'CL is altered in the presence of PCBP together with 3C	52
Fig. 21. Cleavage of purified recombinant PABP by HAV 3C	53
Fig. 22. Concentration dependence of PABP cleavage by HAV 3C.	54
Fig. 23. Cleavage of endogenous PABP by HAV 3C in vitro	55
Fig. 24. Recombinant PABP cleavage by 3C and its precursors in vivo.	56
Fig. 25. PABP cleavage of HAV-infected Huh-7 cells.....	58
Fig. 26. Endogenous PABP cleavage by HAV and CVB 3C in various cell extracts.	58
Fig. 27. PCBP2 cleavage by HAV and CVB 3C.	60
Fig. 28. Concentration dependence of PCBP2 cleavage by HAV 3C.	60
Fig. 29. PCBP2 cleavage by 3C and its precursors in vivo.....	61
Fig. 30. Cleavage of endogenous PCBP in HAV-infected Huh-7 cells is not detectable.	63
Fig. 31. Amounts and cleavage of constitutive PCBP in different cell lines.	63
Fig. 32. PABP (A) and eIF4G (B) cleavage by HAV and CVB 3C in Huh-7 S10 extract.....	64
Fig. 33. PABP (A) and eIF4G (B) cleavage by recombinant HAV 3C and its precursors in vTF7-3 Huh-7 cells.	65
Fig. 34. No eIF4G cleavage in HAV-infected cells.	66
Fig. 35. Predicted RNA secondary structures of the wild type (A) and mutant HAV CRE motif (B) at the 5'end of 3D.	71
Fig. 36. Identification of 3C cleavage sites in PABP	74

CURRICULUM VITAE

FIRST NAME: Bo
LAST NAME: Zhang
SEX: Male
DATE OF BIRTH: February 4, 1977
NATIONALITY: Chinese

EDUCATION AND WORKING EXPERIENCE:

2002.6-present: PhD student, Department of Medical Molecular Biology, University of Luebeck, Luebeck, Germany
2001.8-2002.5: Researcher, Beijing Genomics Institute, Beijing, China
1998.9-2001.6: Master of Science, specialized in Microbiology, Shandong University, Jinan, Shandong Province, China
1994.9-1998.6: Bachelor of Science, specialized in Microbiology, Shandong University, Jinan, Shandong Province, China

PUBLICATIONS:

1. **Zhang Bo**, Li Shu-Qin, Chen Guan-Jun, Huang Cui-Fen, Zhang Zhao-Shan. Expression of Clonization Factor Antigen of Enterotoxigenic *Esherichia coli* in *Shigella flexneri* 2a T32. ACTA Biochimica et Biophysica SINICA (2001), 33 (3):277-280
2. **Zhang Bo**, Chen Guan-Jun, Zhang Zhao-Shan. Bacterial carrier for Vaccine. Prog Microbiol Immunol (2002), 30 (2):86-90
3. Kanda T, **Zhang B**, Kusov Y, Yokosuka O, Gauss-Muller V. Suppression of hepatitis A virus genome translation and replication by siRNAs targeting the internal ribosomal entry site. Biochem Biophys Res Commun. 2005 May 20; 330 (4):1217-23.

POSTER PRESENTATION

- **Bo Zhang**, Yuri Kusov and Verena Gauss-Müller. Host protein cleavage during HAV infection. Poster for Europic 2005

AWARD

- Award from FEMS Young Scientist Meeting Grant for attending the meeting Europic 2005 (European Study Group on Molecular Biology of Picornaviruses)